Sede Amministrativa: Università degli Studi di Padova

DIPARTIMENTO: SCIENZE MEDICO-DIAGNOSTICHE E TERAPIE SPECIALI

SCUOLA DI DOTTORATO DI RICERCA IN : SCIENZE MEDICHE, CLINICHE E SPERIMENTALI

INDIRIZZO: SCIENZE CARDIOVASCOLARI

CICLO: 23°

CARDIAC MAGNETIC RESONANCE IMAGING IN DILATED AND ARRHYTHMOGENIC CARDIOMYOPATHIES: AN INSIGHT INTO CLINICAL AND PATHOLOGICAL SIGNIFICANCE OF LATE GADOLINIUM ENHANCEMENT

Direttore della Scuola : Ch.mo Prof. Gaetano Thiene

Coordinatore d'indirizzo: Ch.mo Prof. Gaetano Thiene

Supervisore : Ch.mo Prof. Sabino Iliceto, Ch.ma Prof.ssa Cristina Basso

Dottorando : Dott.ssa Martina Perazzolo Marra

INDEX

A mio marito, alla sua pazienza ed ai suoi sorrisi

ABBREVIATIONS

ARVC = arrhythmogenic right ventricular cardiomyoapathy

CAD = coronary artery disease

CMR = cardiac magnetic resonance

EF = ejection fraction

EMB = endomyocardial biopsy

EVM = endocardial voltage mapping

EAS = electro-anatomic scar

DCM = dilated cardiomyopathy

HF = heart failure

ICD = Implantable Cardioverter Defibrillator

LGE = late gadolinium enhancement

LV = left ventricular

NYHA= New York Heart Association

RBBB = right bundle branch block

LBBB = left bundle branch block

RV = right ventricular

RVOT = right ventricular outflow-tract

SAECG = signal average ECG

VF = ventricular fibrillation

VT = ventricular tachycardia

SUMMARY

Background: Cardiomyopathies are an important and heterogeneous group of diseases of the heart muscle in which tissue characterization has been extensively studied only ex-vivo so far. Cardiac magnetic resonance (CMR) can provide in vivo the detection of post-contrast deposition (so called Late Gadolinium Enhancement, LGE). The role of LGE in the differential diagnosis of cardiac diseases has advanced through the years, in particular thanks to its capability to differentiate post-ischemic scar (with subendocardial or transmural coronary artery-related deposition) versus non-ischemic scar of different aetiologies. Among cardiomyopathies, the prognostic significance of LGE pattern is not well established, with the exception of hypertrophic cardiomyopathy. Detection in vivo of LGE in different cardiomyopathies has been used as a surrogate of fibrosis, even if the real basis of contrast deposition is not well understood. To this regard, dilated cardiomyopathy (DCM) is characterized by diffuse interstitial fibrosis with or without replacement-type fibrosis, which are associated with worse prognosis. Another myocardial disease in which CMR offers the capability of a non-invasive tissue characterization is Arrhythmogenic Right Ventricular Cardiomyopathy (ARVC), an inherited heart muscle disease with progressive loss of myocardium and replacement by fibrofatty tissue. The extensively application of CMR to these cardiomyopathies and its comparison with traditional invasive and non-invasive techniques for diagnostic and prognostic purposes has been limited so far.

Aim: in order to assess the clinical significance of LGE in DCM and ARVC, the following lines were pursued:

1) in patients with DCM the diagnostic and the prognostic value of LGE, in particular evaluating the possible different significance of various LGE patterns, total amount of LGE against survival, heart failure and ventricular arrhythmias;

2) in patients with ARVC the comparison between CMR findings and: 1a) traditional electrocardiographic features; 1b) scar detction by endocardial voltage mapping (EVM), and 1c) the prognostic significance of LGE;

3) the significance of CMR tissue abnormalities by comparing LGE and specimen heart and/or endomyocardial biopsy (EMB) findings in DCM and ARVC.

Material and Methods: Between January 2007 and December 2010 we prospectively evaluated two different groups of patients referred to our Tertiary Referral Centre for a complete invasive and non-invasive evaluation for unexplained left ventricle (LV) dilatation (DCM Group, A) and for suspected ARVC (ARVC Group, B). DCM Group (A): we prospectively evaluated 210 patients referred for unexplained LV dilatation with subacute-chronic onset (≥ 1 month), with or without previous history of heart failure, who underwent during the same hospitalization to a complete screening including CMR with LGE, angiography and EMB. ARVC group (B): we prospectively evaluated 52 patients who were referred to our Tertiary Centre for susptected ARVC and in which the diagnosis was reached according to 1994 Task Force Criteria and 2010 Modified Criteria. Data on clinical history, ECG, ECG Holter monitoring, echocardiography, CMR and EMB in selected cases were collected. In a subgroup of patients an electrophysiological study with EVM was performed. For each subject enrolled, a clinical, ECG and echocardiographic follow-up was obtained.

Results: Group A. On the basis of coronary angiography, patients were divided into two groups: ischemic (99 patients) and DCM (111 patients). Ischemic group patients were then excluded from the analysis. Compared to angiography, CMR showed an excellent accuracy (96.5%) for the identification of non-ischemic versus ischemic aetiology for LV dilatation. In the DCM group (111 patients) LGE was present (with a non-ischemic pattern) in 67 cases (60.4%) and absent in 44 (39.6%); no differences between RV and LV volumes and ejection fraction (EF) were found between the two groups. Out of 67 patients with positive LGE, a “gray” pattern was present in 12 patients (17.9%), a midwall/subepicardial stria in 49 (73.1%), a septal junction pattern (anterior and/or posterior) either isolated in 4 (5.9%) or associated with other patterns in 25 patients (37.3%) and finally a spotty (“patchy”) pattern in 2 (2.9%). Among patients with positive LGE, the extent of LGE was 6.3%±8.8% of LV mass. Fifty-eight patients underwent to EMB: 33/58 patients (56.9%) showed replacement-type fibrosis, of this subgroup 23 patients (69.7%) showed LGE on CMR. Out of 13/58 patients (22%) without replacement-type fibrosis on EMB, LGE was present in 9/13 (69.2%) patients: in this subgroup the most frequent LGE pattern was midwall/subepicardial stria (n=8/9; 89%) and one patient (11%) showed a “patchy” LGE pattern . Compared to EMB, CMR showed a low accuracy for fibrosis detection. The range of follow-up in LGE group was 8 years-1 month. Kaplan-Meier curves for composite end-point and ventricular arrhythmias showed a significant differences between patients with and without LGE on CMR (Wilcoxon-Breslow: $p < 0.05$). The amount of LGE%, by univariate analysis, was

strongly associated with ventricular arrhythmias (HR 1.05, 95% CI 1.02 to 1.08; p<0.0001). This association was unchanged in multivariate analysis adjusted for a EF<30% (model 5): HR 1.067, 95% CI 1.034 to 1.1; p<0.0001.With an associated HR of 2.5, the presence of LGE was among the strongest multivariate predictors for the combined end point, surpassed only by age < 49 years. ROC curve analysis revealed a LGE percentage of 3.5 as optimal discriminator for the occurrence of ventricular arrhythmic events with an associated HR of 4.11 (95% CI 1.3 to 12.7; p<0.001).

Group B: On the basis of clinical and CMR evaluation, 24 patients (46%) were defined as "classic ARVC phenotype"; 14 (27%) as "left dominant phenotype", and finally 14 (27%) as "biventricular ARVC phenotype". Comparison between ECG and CMR showed that ECG indexes of LV dilatation are ST-segment elevation and T-wave inversion beyond V3 (p<0.05); among tissue characterization parameters, only LV LGE has an identifiable ECG abnormality, i.e. ST segment elevation (p<0.05). On EVM, endocardial voltages of RV was abnormal in 21/23 (91%) patients, with a total of 45 electroanatomic scars (EAS). RV LGE was found in 9/23 (39%) patients, with a total of 23 RV LGE scars: there was a mismatch in 24 RV scars, with 22 EAS not confirmed by LGE. In 9/12 (75%) patients with abnormal RV EVM/normal RV LGE, ≥1 LGE were identified in the LV. The patients of ARVC group enrolled for the follow-up were 52 (34 males; mean age 33±15 years). The mean LV ejection fraction was 57±8%; the mean fractional area change of RV was 39±10%. The mean follow-up was 25.6 months (range 38±4 months). Considering only the major events (aborted sudden death/ ventricular fibrillation; sudden death; non sudden death/heart transplantation) these occurred in 12 (7 in the LGE group, 5 in the non-LGE group).Kaplan-Meier curves did not show difference between LGE presence/absence for all events and major events. Kaplan-Meier curves did not show difference between three phenotypes detected by CMR both for all events and major events.

Conclusions: CMR can provide a wide range of information in DCM and ARVC, beyond traditional imaging modalities. In the setting of DCM, CMR shows high accuracy in the detection of non-ischemic aetiology compared with angiography. LGE identifies the patients with increased risk of ventricular arrhythmic events. Compared to EMB, CMR with LGE imaging shows low accuracy for fibrosis detection, probably due to resolution power of CMR. However, an integrated approach with CMR and EMB may be useful in cases with negative

EMB/positive LGE to identify epicardial lesion, which are not caught by EMB due to its endocardial approach.

In the setting of ARVC, CMR confirms its superiority in assessing the full spectrum of morpho-functional and tissue abnormalities of a disease that should be as a biventricular cardiomyopathy. The ECG indexes able to identify LV dilatation are ST-segment elevation and T-wave inversion beyond V3; as far as tissue characterization parameters are concerned, LV LGE was associated to ST segment elevation. The correlation between EVM and CMR confirms that EVM allows an accurate identification of RV EAS in patients with ARVC and supports its clinical use for substrate-based mapping and catheter ablation of RV tachycardias as well as for imaging-guided EMB. Currently available LGE CMR appears to visualize unsatisfactorily RV scars and this limits its usefulness in ARVC diagnosis and guiding interventional RV procedures. However, the high prevalence of LV involvement in ARVC patients is in keeping with the current perspective of biventricular disease and points out the diagnostic relevance of LV scar detection by LGE CMR.

RIASSUNTO

Introduzione: Le cardiomiopatie rappresentano un gruppo eterogeneo di malattie del muscolo cardiaco la cui caratterizzazione tissutale finora è stata eseguita prevalentemente mediante analisi ex vivo. La risonanza magnetica cardiaca (RMC), grazie all'utilizzo di apposite sequenze e all'impiego di un mezzo di contrasto (gadolinio, visibile come Late Gadolinium Enhancement, LGE), rende possibile una caratterizzazione tissutale in vivo. L'analisi della sede ed estensione dell'LGE permette di differenziare la cicatrice miocardica post-infartuale (LGE sub endocardico o trans murale) rispetto ad altre cicatrici di tipo non ischemico. Nelle diverse cardiomiopatie, il significato prognostico dei depositi di LGE non è del tutto chiarito, se non in parte per la cardiomiopatia ipertrofica. In generale la presenza di LGE nel contesto di una cardiomiopatia viene identificato con la presenza di fibrosi miocardica, nonostante il meccanismo di deposito del gadolinio non sia uguale nelle diverse eziologie di cardiomiopatie, non necessariamente associate a fibrosi miocardica. Nell'ambito delle cardiomiopatie, la cardiomiopatia dilatativa (non dovuta ad una eziologia ischemica) (CMD) si caratterizza da un punto di vista istologico per la presenza di fibrosi interstiziale, con o senza fibrosi sostitutiva, entrambe associate ad una prognosi infausta. Una diversa patologia miocardica in cui la RMC offre una eccezionale capacità di caratterizzazione tissutale è la Cardiomiopatia Aritmogena del Ventricolo Destro (CAVD), una miocardiopatia dovuta ad una progressiva atrofia miocardica con successiva sostituzione fibroadiposa. Benché la RMC stia consolidando il suo ruolo nella pratica clinica, non è stata ancora eseguita una applicazione estensiva della RMC in queste due differenti cardiomiopatie a scopo diagnostico e prognostico, ed ancor più manca una analisi sistematica delle correlazioni tra i diversi quadri radiologici ed i tradizionali parametri invasivi e non-invasivi di queste cardiomiopatie.

Scopo dello Studio: al fine di valutare il significato clinico e prognostico dell'LGE nelle CMD e nella CAVD sono state perseguite le seguenti linee di ricerca:

1) nei pazienti affetti da CMD il significato prognostico dell'LGE nelle DCM, con particolare riferimento ad un end-point di eventi combinati ed all'outcome aritmico;

2) nei pazienti affetti da CAVD il confronto tra i diversi aspetti alla RMC ed 1a) i quadri elettrocardiografici; 1b) il confronto con dati ottenuti dal mappaggio endocavitario del ventricolo destro ("Endocardial Voltage Mapping", EVM); 1c) il significato prognostico dell'LGE;
3) il significato della alterazioni di caratterizzazione tissutale alla RMC confrontati con i dati istologici dei pazienti con biopsia endomiocardica (BEM) o che sono andati incontro a decesso/trapianto cardiaco nei due gruppi.

Materiali e Metodi: tra il Gennaio 2007 e il Dicembre 2010 sono stati arruolati prospetticamente i pazienti riferiti presso il nostro Centro per una valutazione invasiva per il riscontro di una dilatazione del ventricolo sinistro (Gruppo CMD, A) o per sospetta CAVD (Gruppo CAVD, B). Gruppo CMD (A): sono stati valutati 210 riferiti per riscontro di dilatazione ventricolare con esordio subacuto-cronico (≥ 1 mese), con o senza pregressa storia di scompenso cardiaco, che durante la stessa ospedalizzazione sono stati sottoposti a coronarografia, RMC con contrasto e BEM. Gruppo CAVD (B): 52 soggetti riferiti presso il nostro Centro per sospetta CAVD e la cui diagnosi è stata raggiunta in accordo con i correnti criteri clinico-strumentali recentemente modificati. Durante la stessa ospedalizzazione sono stati sottoposti RMC con contrasto e studio elettrofisiologico con EVM e BEM in casi selezionati. Ogni paziente appartenente ad entrambi i gruppi è stato sottoposto ad un follow-up clinico-strumentale.

Resultati: Gruppo A. Sulla base dei risultati della coronarografia i pazienti sono stati suddivisi in due gruppi in base alla presenza o meno di coronaropatia: in 99 è stato definita una eziologia ischemica alla base della disfunzione ventricolare, 111 non mostravano alcuna coronaropatia (gruppo CMD). Il gruppo dei soggetti ischemici è stato escluso dalla successive analisi. Rispetto all'angiografia coronarica, la RMC ha dimostrato un'ottima accuratezza diagnostica (96.5%) nell'escludere una eziologia ischemica. Nel gruppo A la presenza di un LGE di tipo non-ischemico è stata riscontrata in 67 casi (60.4%) mentre era assente in 44 (39.6%). Nessuna differenza nei volumi ventricolari e funzione sistolica è stata riscontrata nei due sottogruppi. Nei 67 pazienti con LGE era presente un pattern di tipo "gray" in 12, tipo stria "midural"/epicardica in 49 (73.1%), alla giunzione settale tra ventricolo destro e sinistro isolatamente in 4 (5.9%), associato ad altri pattern in 25 (37.3%), ed infine tipo "patchy" in 2 casi (2.9%). Nei pazienti con LGE, l'estensione media era pari al 6.3%±8.8% della massa del ventricolo sinistro. In 58 casi è stata eseguita la BEM: 33/58 pazienti (56.9%) mostravano aspetti di fibrosi sostitutiva; di questi, 23/33 (69.7%) mostravano anche LGE alla RMC. In 13/58 casi (22%) si riscontrava una BEM negativa: in questo sottogruppo di soggetti era presente un LGE in 9/13 (69.2%): nella

maggioranza dei casi (8/9 pari all'89%) l'LGE era tipo stria "midmural"/epicardica, in uno solo (11%) tipo "patchy". Nel gruppo A il range del follow-up è 8 anni-1 mese. Le curve di sopravvivenza Kaplan-Meier per eventi combinati ed aritmie ventricolari maggiori hanno mostrato una differenza significativa tra i due gruppi di pazienti con una prognosi peggiore nel gruppo con LGE (Wilcoxon-Breslow: $p< 0.05$). La quantità totale di LGE si è dimostrata associata alle aritmie ventricolari (HR 1.05, 95% CI 1.02-1.08; $p<0.0001$); tale correlazione rimaneva anche all'analisi multivariata aggiustata per una frazione d'eiezione inferiore al 30% (HR 1.067, 95% CI 1.034-1.1; $p<0.0001$).I pazienti con LGE mostravano un rischio di 2.5 per la comparsa di aritmie ventricolari e mediante l'analisi della curva ROC la percentuale di LGE pari a 3.5% è risultato il miglior valore predittivo di eventi aritmici (HR 4.11 (95% CI 1.3-12.7; $p<0.001$).

Gruppo B. Sulla base dei risultati della RMC, 24 soggetti (46%) sono stati definiti affetti da un forma "classica", 14 (27%) "dominante sinistra", e 14 (27%) "biventricolare". Analizzando la correlazione tra ECG e RMC, gli unici predittori della dilatazione del ventricolo sinistro sono risultati la presenza di un sopraslivellamento del tratto ST e le T invertite oltre V3 ($p<0.05$); nelle sequenze per la caratterizzazione tissutale la presenza di LGE a carico del ventricolo sinistro era associata ad un sopraslivellamento del tratto ST. Dall'analisi di confronto tra mappaggio endocavitario (EVM) e LGE è emerso che in 21/23 (91%) si dimostrava la presenza di un voltaggio ridotto, per un totale di 45 cicatrici elettroanatomiche. La presenza di LGE a carico del ventricolo destro si è riscontrata in 9/23 (39%) casi, per un totale di 23 cicatrici alla RMC: in 24 casi vi è stato un mismatch tra le due metodiche nel riconoscere le cicatrici di sostituzione fibro-adiposa. In 9/12 (75%) dei soggetti con EVM patologico/RMC normale, sono state riscontrate aree di LGE in almeno una regione del ventricolo sinistro. Il follow-up medio dei pazienti con CAVD arruolati nel follow-up (52; 34 maschi; età media 33 ± 15 anni) è stato di 25.6 mesi (38 ± 4 mesi). Considerando come eventi maggiori la morte cardiaca (abortita o meno), la fibrillazione/tachicardia ventricolare, morte/trapianto cardiaco gli eventi combinati sono stati 12 (7 nel gruppo con LGE e 5 in quelli senza LGE). Non si è dimostrata alcuna differenza in termini di tempo libero da eventi nei tre gruppi.

Conclusioni: La RMC nell'ambito dello studio della CMD e della CAVD offre delle capacità diagnostiche al di là delle tradizionali metodiche di imaging. Nella CMD presenta un'ottima accuratezza diagnostica, rispetto alla ventricolo-coronarografia, nell'escludere una eziologia

ischemica alla base della dilatazione e disfunzione ventricolare. La presenza di LGE nella DCM è in grado inoltre di individuare i paziente a maggior rischio aritmico. Tuttavia se confrontata con la BEM, l'accuratezza diagnostica della RMC rimane bassa, probabilmente a causa del suo potere di risoluzione spaziale che limita il riconoscimento di piccole aree di fibrosi miocardica. D'altra parte, la RMC è in grado di vedere lesioni epicardiche che non sono raggiunte dalla BEM supportando così l'importanza di una valutazione combinata delle due metodiche nelle CMD.

Nei soggetti con CAVD, la RMC si conferma tecnica di imaging capace di esplorare l'intero spettro di alterazioni morfo-funzionali e tissutali della CAVD, che spesso è una malattia bi ventricolare e non può essere esclusiva del ventricolo destro. Il confronto tra ECG e RMC indica la presenza di un sopraslivellamento del tratto ST e l'inversione delle onde T come predittori della dilatazione del ventricolo sinistro; la presenza di LGE a carico del ventricolo sinistro è associato ad un sopraslivellamento del tratto ST. Analizzando i dati relativi al mappaggio elettronatomico, emerge come quest'ultimo riconosca più cicatrici di quanto non riesca a fare la RMC, probabilmente per la difficoltà di riconoscere un LGE a carico della parete assai assottigliata del ventricolo destro. Tuttavia la capacità della RMC di riconoscere le lesioni anche a carico del ventricolo sinistro, laddove il mappaggio elettroanatomico non viene applicato, suggerisce un sinergismo diagnostico tra le due metodiche. Probabilmente il breve tempo di follow-up nel quale si è indagato il significato prognostico dell'LGE a carico del ventricolo sinistro ha reso non significativa la differenza in termini di tempo libero da eventi nei tre gruppi. Studi futuri su casistiche più numerose, tipizzate dal punto di vista genetico e con RMC seriate, delucideranno meglio il significato prognostico di un coinvolgimento precoce del ventricolo sinistro.

BACKGROUND

Classification of Cardiomyopathies

Introduction

Cardiomyopathies are an important and heterogeneous group of heart muscle diseases in which the rapid evolution of molecular genetics in cardiology recently allow the identification of new entities needing an update of previous acknowledgement. The current definition of "cardiomyopathy" takes into account both morphology and function, either mechanical and electrical. According to 2006 American Heart Association (AHA) consensus panel "*cardiomyopathies are a heterogeneous group of diseases of the myocardium associated with mechanical and/or electrical dysfunction that usually (but not invariably) exhibit inappropriate ventricular hypertrophy or dilatation and are due to a variety of causes that frequently are genetic. Cardiomyopathies either are confined to the heart or are part of generalized systemic disorders, often leading to cardiovascular death or progressive heart failure–related disability"* (1).This current definition represents the result of a classification incorporating both the concepts of previous classifications and the new idea of ion channelopathies as primary cardiomyopathies, recognized only few years ago by the application of molecular genetics in cardiology.

Before 2006 AHA Classification several systematic classifications of cardiomyopathies have been advanced through the years, designed for physicians and basic scientists, and based on different taxonomic criteria, including origin, anatomy, physiology, symptoms, therapy, diagnosis, and histopathology.

In 1968, the WHO defined cardiomyopathies as "diseases of different and often unknown aetiology in which the dominant feature is cardiomegaly and heart failure"; subsequently in 1980 the WHO reported a classification in which cardiomyopathies were defined as "heart muscle diseases of unknown cause," reflecting a general lack of information available about etiopathogenesis and basic disease mechanisms (2). In this 1980 WHO classification three forms of cardiomyopathies were recognized: dilated, hypertrophic and restrictive (due to endocardial disease). More recently, in 1995, the WHO updated the previous classification by including two newly recognized entities i.e. ARVC and the primary restrictive cardiomyopathy (3).

Through the years, the advent of cardiac transplantation and the renewed interest on sudden cardiac death have arisen exciting opportunities in the clinico-pathologic study of cardiomyopathies, as to allow the discovery of new entities (4) The availability of sophisticated methods of investigation like molecular biology techniques, other than the traditional tools in morphology, opened extraordinary avenues in the understanding the causes, other than the substrates of cardiomyopathies. Moreover, the increasing systematic use of non-invasive imaging techniques emphasized that, from the functional viewpoint, some cardiomyopathies do not have always the same static phenotype, buy may dynamically evolve, as a consequence of remodelling, from one category to another during their natural clinical course. On this basis, the 2006 AHA recognizing the rapid evolution of molecular genetics in cardiology, as well as the introduction of several recently described diseases, updated the previous classification and incorporated ion channelopathies as a primary cardiomyopathy.

The major difference from prior efforts (1980 and 1995 WHO Classifications) is the genomic and molecular orientation of this proposed cardiomyopathy classification. It is based upon the hypothesis that causative mutations in genes encoding proteins regulating the transport of ions ("channelopathies") across the cell membrane are responsible for electrical dysfunction that triggers primary life-threatening ventricular tachyarrhythmias. They ultimately may evolve in a structural disease. However, the authors themselves admit that it is probably still premature and inadvisable to formulate a classification that is entirely dependent on genomics. The molecular genetics of myocardial disease is not yet completely developed, and more complex genotype–phenotype relationships will continue to emerge for these diseases. For example, several sarcomeric gene mutations are now known to cause both dilated and hypertrophic cardiomyopathies. Furthermore, troponin I mutations have been found to underlie both hypertrophic and restrictive cardiomyopathy. On the basis of the 2006 AHA Classification the cardiomyopathies are now divided into 2 major groups based on predominant organ involvement. *Primary cardiomyopathies* were defined as those solely or predominantly confined to heart muscle. This group was subdivided into genetic, mixed (genetic and nongenetic), and acquired forms (Figure 1).

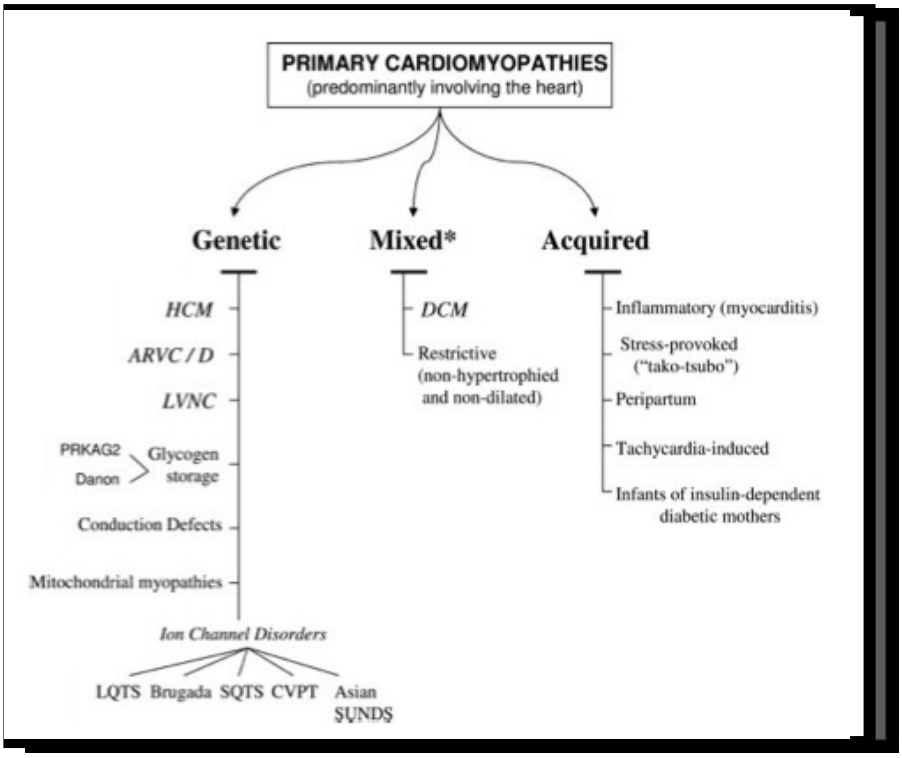

Figure 1. AHA 2006 Classification. Primary cardiomyopathies in which the clinically relevant disease processes solely or predominantly involve the myocardium. The conditions have been segregated according to their genetic or non-genetic etiologies. *Predominantly non-genetic are defined those familial cardiomiopathies in which a genetic origin has been reported in a minority of cases. (From Maron et al 1).

Secondary cardiomyopathies present myocardial involvement as part of a large number and variety of generalized systemic (multiorgan) disorders (Figure 2). In the WHO 1980 and 1995 classifications, these systemic diseases associated with secondary forms of cardiomyopathies have been referred to as "specific cardiomyopathies" or "specific heart muscle diseases", respectively.

An important goal of the 2006 AHA document is that pathological myocardial dysfunction directly consequence of other cardiovascular abnormalities, such as valvular heart disease, systemic hypertension, congenital heart disease, andatherosclerotic coronary artery disease, have not been considered anymore as cardiomyopathies.

These systemic diseases associated with secondary forms of cardiomyopathies had previously been referred to as "specific cardiomyopathies" or "specific heart muscle diseases" in prior classifications, abandoned here. The frequency and degree of secondary myocardial involvement vary considerably among these diseases, some of which are exceedingly uncommon and for

which the evidence of myocardial pathology may be sparse and reported in only a few patients. Because many cardiomyopathies may predominantly involve the heart but are not necessarily confined to that organ, some of the distinctions between primary and secondary cardiomyopathy are necessarily arbitrary and inevitably rely on judgment about the clinical importance and consequences of the myocardial process.

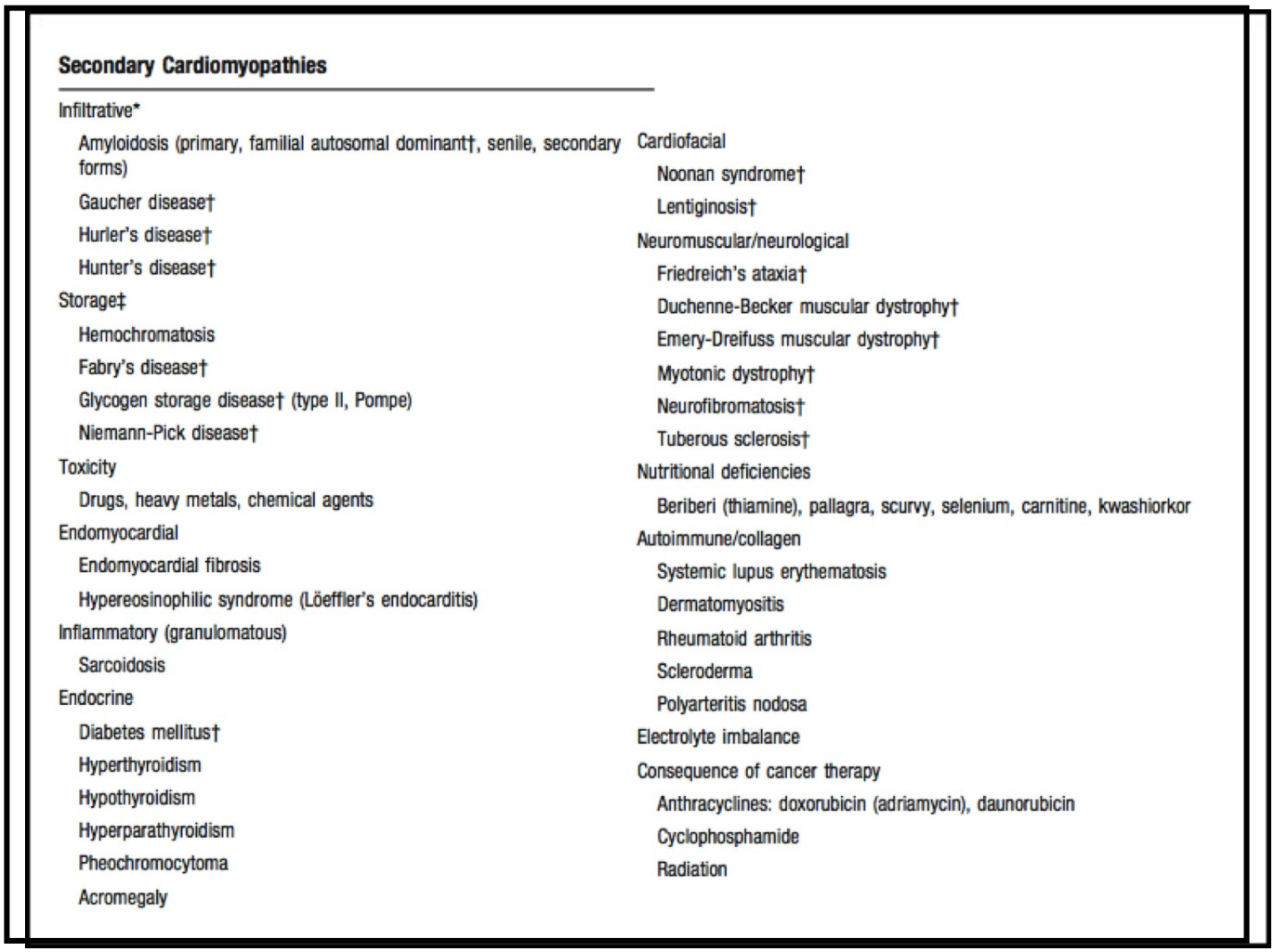

Secondary Cardiomyopathies

Infiltrative*
- Amyloidosis (primary, familial autosomal dominant†, senile, secondary forms)
- Gaucher disease†
- Hurler's disease†
- Hunter's disease†

Storage‡
- Hemochromatosis
- Fabry's disease†
- Glycogen storage disease† (type II, Pompe)
- Niemann-Pick disease†

Toxicity
- Drugs, heavy metals, chemical agents

Endomyocardial
- Endomyocardial fibrosis
- Hypereosinophilic syndrome (Löeffler's endocarditis)

Inflammatory (granulomatous)
- Sarcoidosis

Endocrine
- Diabetes mellitus†
- Hyperthyroidism
- Hypothyroidism
- Hyperparathyroidism
- Pheochromocytoma
- Acromegaly

Cardiofacial
- Noonan syndrome†
- Lentiginosis†

Neuromuscular/neurological
- Friedreich's ataxia†
- Duchenne-Becker muscular dystrophy†
- Emery-Dreifuss muscular dystrophy†
- Myotonic dystrophy†
- Neurofibromatosis†
- Tuberous sclerosis†

Nutritional deficiencies
- Beriberi (thiamine), pallagra, scurvy, selenium, carnitine, kwashiorkor

Autoimmune/collagen
- Systemic lupus erythematosis
- Dermatomyositis
- Rheumatoid arthritis
- Scleroderma
- Polyarteritis nodosa

Electrolyte imbalance

Consequence of cancer therapy
- Anthracyclines: doxorubicin (adriamycin), daunorubicin
- Cyclophosphamide
- Radiation

Figure 2. AHA 2006 Classification. Secondary cardiomyopathies in which the clinically relevant disease processes is a generalized (multiorgan) disorder with a secondary involvement of the myocardium. (Modified from Maron et al 1).

An update of the 1995 WHO/ISFC classification has also beenproposed as a position statement of the ESC Working Group onMyocardial and Pericardial diseases in 2008 on the basis of a "clinically oriented classification system" in which heart muscle disorders were grouped on

the basis of ventricular morphology and function (5). According to this Position Paper, cardiomyopathyhas been defined '*a myocardial disorder in which heart muscle is structurallyand functionally abnormal in the absence of coronary arterydisease, hypertension, valvular disease, and congenital heartdiseases*'. While accepting and reinforcing the idea advanced by the AHA statement to divide cardiomyopathies into familial/genetic and non-familial/non-genetic, the traditional division of primary and secondary (specific) cardiomyopathies was abolished, probably with the erroneous belief that primary means idiopathic and secondary means of known aetiology. Moreover, the concept of pure electrical dysfunction was denied, thus ruling out ion channel and conduction system diseases from the umbrella of cardiomyopathies.

Basically, five types of cardiomyopathies are recognized according to the morpho-functional phenotype (hypertrophic, dilated, arrhythmogenic, restrictive, and unclassified), either familial or non-familial, whether or not the heart is the only target of the disease (Figure 2). Only cardiomyopathies with structural deformities were included, renewing the purely morpho-functional approach, without considering the problem of possible evolution of a disease phenotype into another during the natural history and leaving electrical disorders without a taxonomic location.

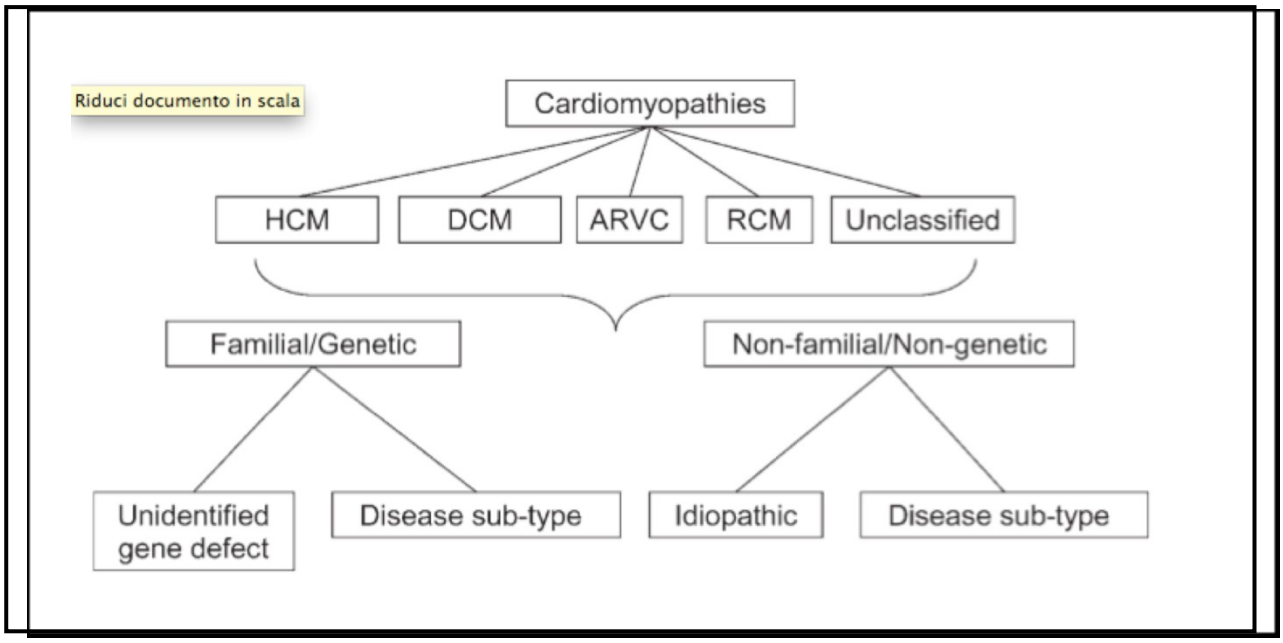

Figure 2. Summary of ESC proposed classification system. ARVC, arrhythmogenic right ventricular cardiomyopathy; DCM, dilated cardiomyopathy; HCM, hypertrophic cardiomyopathy; RCM, restrictive cardiomyopathy. (Modified from Elliott et al 5).

This approach is certainly a simplification of a complex nosographic puzzle, but does not yet fully answer the question raised by emerging evidence (5). While removal of specific cardiomyopathies such as ischemic, hypertensive, and valvular should be greeted with cheers, as the AHA document first did in 2006, it is notconvincing at all why myocarditis should be grouped ‘tout court’ among dilated cardiomyopathies. Moreover, the AHA position statement abolished the so-called non-classified cardiomyopathies, whereas the ESC position statement still regardsforms such as non-compaction and TakoTsubo in search of a room.

Clinico-Pathological Issues of Dilated Cardiomyopathies

Dilated cardiomyopathy (DCM) is characterized by ventricular chamber enlargement and systolic dysfunction with normal left ventricular (LV) wall thickness. DCM leads to progressive heart failure and a decline in LV contractile function, ventricular and supraventricular arrhythmias, conduction system abnormalities, thrombo-embolism, and sudden or heart failure-related death. Indeed, DCM is a common and largely irreversible form of heart muscle disease with an estimated prevalence of 1:2500 and an incidenceof 7 per 100 000/year (7) it is the third

most common cause of heart failure and the most frequent cause of heart transplantation. The DCM may be a primary cardiomyopathy in which the heart is the solely or predominantly involved organ. On the contrary, in the secondary DCM, this morpho-functional phenotype may derive from a particularly broad range causes: infectious agents (viruses, such as coxsackievirus, adenovirus, parvovirus, HIV; bacterial; fungal rickettsial; myobacterial; and parasitic). Other non-infective causes include toxins; alcohol; chemo-therapeutic agents, metals, autoimmune and systemic disorders pheochromocytoma; neuromuscular disorders, mitochondrial, metabolic, endocrine, and nutritional disorders.

About 20% to 35% of DCM cases have been reported as familial, although with incomplete and age-dependent penetrance, and linked to a diverse group of more than 20 loci and causative genes. Although genetically heterogeneous, the predominant mode of inheritance for DCM is autosomal dominant, with X-linked autosomal recessive and mitochondrial inheritance less frequent. DCM is mostly caused by a number of mutations in genes encoding cytoskeletal/sarcolemmal, nuclear envelope, and transcriptional co-activator proteins. The most common of these probably is the lamin A/C gene, also associated with conduction system disease, which encodes a nuclear envelope intermediate filament protein. Mutations in this gene also cause Emery-Dreifuss muscular dystrophy. The X-linked gene responsible for Emery-Dreifuss muscular dystrophy, emerin (another nuclear lamin protein), also causes similar clinical features. Other DCM genes of this category include desmin, caveolin, and α- and β-sarcoglycan, as well as the mitochondrial respiratory chain gene. X-linked DCM is caused by the Duchenne muscular dystrophy (dystrophin) gene, whereas G 4.5 (tafazzin), a mitochondrial protein of unknown function, causes Barth syndrome, which is an X-linked cardio-skeletal myopathy in infants. Several of the mutant genes linked to autosomal dominant DCM encode the same contractile sarcomeric proteins that are responsible for HCM, including α-cardiac actin; α-tropomyosin; cardiac troponin T, I. Research carried out in the past few decades have confirmed that genetic factors are the underlying cause of several forms of previously called “idiopathic” and that careful examination of the relatives of an index case often reveals other affected family members and a familiar pattern of disease. Systematic studies of idiopathic and familial cases have shown that DCMs may either confined to the heart with ventricular enlargement and systolic dysfunction, or it may occur in the setting of extracardiac features, such as skeletal myopathy and elevated serum creatine kinase levels. DCM may manifest clinically at a wide range of ages (most commonly in the third fourth decade but also in children). In family

screening by echocardiography, asymptomatic or mildly symptomatic relatives may be identified and the incidence of DCM is increasing also due to advances in diagnostic tools and awareness among physicians.

The phenotype of DCM is mainly defined by cardiac enlargement and impaired systolic function (8), easily detectable by echocardiography. Similar features can be recognized by contrast ventriculography or nuclear imaging. For instance, DCM may be diagnosed in patients whose symptoms are initially ascribed to ischemic heart disease in whom stress nuclear scintigraphy then shows a dilated, hypocontractile left ventricle without ischemia. Variability in cut-off values for abnormal chamber size across different imaging modalities, age, sex, and indices of body size should be taken into account when assessing for cardiac enlargement. Recognizing abnormal myocardial relaxation by mitral inflow and tissue Doppler velocities is particularly important, because some genetic variants of DCM, such as lamin A/C cardiomyopathy, predominantly affect diastolic function in the initial stages of the disease. Although many other conditions (such as hypertensive heart disease) may also manifest as diastolic dysfunction, these echo Doppler findings warrant consideration of potential genetic aetiologies when recognized in the context of a family history of cardiomyopathy or high risk clinical markers (eg, malignant ventricular arrhythmias and conduction disturbance). Whereas a more precise etiologic determination may be limited, echo Doppler provides valuable information on the degree of pulmonary hypertension and LV filling pressures, with prognostic implications (9).

From a macroscopic point of view, DCM is characterized by an increase in myocardial mass and a reduction in ventricular wall thickness “eccentric” hypertrophy. The heart assumes a globular shape and there is pronounced ventricular chamber dilatation, diffuse endocardial thickening, and atrial enlargement often with endocavitary thrombi in the appendages. The histological changes associated with DCM are frequently non-specific and not all features may be present. These include myocyte abnormalities with or without fibrosis. Myocyte diameter is variable with usually myocyte hypertrophy and features of myocyte attenuation and vacuolization due to sarcolysis, nuclear dysmetry, and pleomorphism, perinuclear halo (10). Increased interstitial fibrosis has been described in DCM and associated with an adverse prognosis and impaired response to therapeutic interventions in selected groups of patients with DCM (11,12). Fibrotic changes in hearts of patients with DCM can be classified into either *interstitial* or *replacement-type* fibrosis (13,14,15). The mechanisms believed to contribute to the development of myocardial fibrosis are multiple and include inflammation, neurohumoral changes and

microvascular ischaemia (15,16). Interstitial and replacement-type fibrosis have been described in as many as 57% of patients (17), and grossly visible scars have been noted in 23% (18).
An ex-vivo transplanted heart pathological study, addressed the distribution of fibrosis and cellular hypertrophy in nine hearts of patients with DCM, compared with six controlsubjects. Section taken from RV, LV and septum (divided into epicardium and endocardium) showed a greater percentage of fibrosis in patients with DCM. Associated to fibrosis, a myocardial cell diameter was greater in the DCM group (19). A frequent findings is the presence of T lymphocytes as well as macrophages associated with myocyte death.

The annual mortality rate is 11-13% and is related to the phase of the disease (20). In the subset of patients with advanced DMC, progression of heart failure is the main cause (56%) of cardiac death. On the contrary in the lower functional classes (defined by New York Heart Association, NYHA class I-II and III) cardiac death is mainly due to arrhythmic events (21) The anatomical substrates of arrhythmias in DCM include ventricular remodelling with histopathologic abnormalities and subsequently inhomogeneity of electrophysiological proprieties (including the duration of depolarization), remodelling of ion cannel and finally abnormalities of autonomic nervous system. In the post-ischemic “dilated” cardiomiopathy, the re-entry ventricular arrhythmias, due to the post-infarction scar, represent the most frequent mechanism.On the contrary, in DCM ventricular arrhythmias are due to repolarisation abnormalities (22).
The prognostic indexes for the arrhythmic stratification of patients affected by DCM include: a) the grade of systolic dysfunction of LV; b) frequent ventricular premature beats and sustained ventricular tachycardia; c) increased duration of QRS, QT dispersion and the T-wave alternance; and finally d) the heart rate variability (expression of the degree of autonomic disease). Several clinical trial, including MADIT I (23) and II (24), COMPANION (25) indicated that a reduced ejection fraction (EF) (< 35%) represents the most important risk factor for cardiac sudden death in patient with “ischemic dilated” cardiomyopathy. However, data on the role of the prevention of sudden death by Implantable Cardioverter Defibrillator (ICD) in patients with non-ischemic DCM are more limited (26).The SCD-HeFT trial (27) enrolled patients with both ischemicand non-ischemic DCM and showed a 23% reduction in mortality. A meta-analysis of trials enrolling only “non-ischaemic” DCM patients showed a 25% reduction in mortality in the group of patients receiving an ICD ($p = 0.003$) (28). These data suggest that the aetiology of heart failure may not justify a different approach for the primary prevention of sudden cardiac death.

Current European Guidelines for the treatment of heart failure recommend the ICD therapy for primary prevention to reduce mortality in patients with non-ischemic cardiomyopathy with an left ventricular ejection fraction≤35%, in NYHA functional class II or III, receiving optimal medical therapy, and who have a reasonable expectation of survival with good functional status for >1 year (Class IB) (26).

Clinico-Pathological Issues of Arrhythmogenic Right Ventricular Cardiomyopathy

Arrhythmogenic Right Ventricular Cardiomyopathy (ARVC) is an uncommon form of inheritable heart muscle disease (estimated prevalence 1:2000-1:5000). ARVC involves predominantly the right ventricle (RV) with progressive loss of myocytes and fatty or fibrofatty tissue replacement, resulting in regional (segmental) or global abnormalities. The replacement of the RV myocardium by fibrofatty tissue is progressive, starting from the epicardium or mid-myocardium and then extending to become transmural. Progression then leads to wall thinning and aneurysms, typically located at the inferior, apical, and infundibular walls (so-called triangle of dysplasia), the hallmark of ARVC (29-31). The fibrofatty replacement interferes with electrical impulse conduction, and is the key cause of epsilon waves, right bundle branch block, late potentials, and re-entrant ventricular arrhythmias. ARVC has a broad clinical spectrum, usually presenting clinically with ventricular tachyarrhythmias (eg, monomorphic ventricular tachycardia) (32). A recognized cause of sudden cardiac death in the young, it is also regarded as the most common cause of sudden death in competitive athletes in Italy. Non-invasive clinical diagnosis may be confounding, and since no single test is definitively diagnostic (“gold standard”), the diagnosis generally requires an integrated assessment of electrical, functional, and anatomic abnormalities.

The discovery of gene mutations involved in the pathogenesis of ARVC has offered the potential to identify genetically affected individuals by DNA characterization before the disease phenotype occurs. The first chromosomal locus (14q23-q24) for autosomal dominant ARVC was published in 1994 after clinical evaluation of a large Venetian family. Subsequently, linkage analysis provided evidence for genetic heterogeneity with sequential discovery of several ARVC loci on chromosomes1, 2, 3, 6, 10, 12, 14, and 18. Actually, the mutations identifies thus far in the autosomal dominant ARVC are in 12 genes (33). ARVC/D is heredo-familial in nearly 50%

of cases, thus the ongoing myocardial atrophy may be genetically determined. Three different groups of genes have been found to be linked to ARVC: the ryanodine receptor-2 gene (RyR2), the gene encoding for the growth facto TGFbeta 3 and genes encoding for intercellular junction proteins (plakoglobin, desmoplakin, plakophillin-2, desmoglein-2, and desmocollin-2). The candidate genes were first searched for in those coding cytoskeleton or sarcomeric proteins, however ARVC revealed to be neither a cytoskeleton disease, like dilated cardiomyopathy, nor a sarcomeric disease, like hypertrophic cardiomyopathy. The key for interpretation came from a recessive form of ARVC, the so-called Naxos disease, a cardiocutaneous syndrome featured by palmoplantar keratosis, woolly hair and heart muscle disease (34,48). Noteworthy, epidermic cells and myocytes share similar mechanical junctional apparatus, i.e. desmosomes and fascia adherens, which provides continuous cell-to-cell connection. This explains why genes coding proteins of the intercellular junction became candidate genes. Thus, ARVC was found to be a cell junction disease also in the dominant form, with the plakophilin-2 as the most frequent disease gene. Genotype-phenotype correlations revealed that the desmoplakin mutation is associated with a high occurrence of sudden death and frequent LV involvement (49). In contrast, the plakophilin mutation results in a more extensive disease manifestation with life-threatening ventricular arrhythmias. Plakoglobin and plakophilin mutations leads to similar cardiac phenotypes with RV preponderance (34) .

Non-invasive tests used to diagnose ARVC, in addition to personal and family history, include 12-lead ECG, echocardiography, right ventricular angiography, cardiac magnetic resonance (CMR) imaging, and computerized tomography. Major and minor diagnostic criteria have been proposed that encompass structural, electrophysiologic, and histopathologic variables (35,36). Identification of abnormalities in RV structure and function constitutes an important part of the diagnosis of ARVC and accounts for a major or minor criterion based on the severity of the abnormality. The Task Force criteria, initially proposed in 1994, were recently revised to include quantitative parameters for RV functional evaluation, reassessing the evaluation of wall motion abnormalities, underscoring the importance of a thorough assessment of the RV in cases ofsuspected ARVC. Thismodification of Task Force Criteria has been mainly proposed to allow detection of ARVC in first degree relatives with early or incomplete phenotype during family screening of probands with clinically or pathologically proven ARVC, to increase sensibility by maintaining specificity.

The assessment of structural and functional abnormalities of the RV is the most challenging aspect of diagnosis. Initially angiography has been used extensively and seemed to have a high diagnostic specificity (more than 90%) for detecting akinetic or dyskinetic bulging in the infundibulum, apical, and subtricuspid regions ("triangle of dysplasia") (37). Echocardiography is a widely available non-invasive imaging tool and is often the first imaging modality used to assess cardiac structure and function in cases of known or suspected ARVC. Inherent limitations imposed by the acoustic window with ultrasound-based cardiac imaging may preclude in some patients the visualization of the segmental RV abnormalities that constitute the phenotypic hallmarks of ARVC. Recently. The modified ARVC Task Force Criteria provide detailed cut-offs regarding abnormal RV size and wall motion (36).

Another important issue of the diagnostic work-up is the analysis of ECG and ventricular arrhythmias. The ECG depolarisation abnormalities result from delayed RV activation and include right bundle-branch block (RBBB), prolongation of right precordial QRS duration (110 ms or more), and epsilon waves, defined as small amplitude potentials occurring after the QRS complex and before the onset of the T waves (38, 39). A more sensitive method of detecting delayed RV depolarisation is to record late potentials by signal-averaged ECG (40-42). Brugada syndrome–like RBBB and right precordial ST-segment elevation accompanied by polymorphic ventricular tachycardia (VT) also have been reported in a small subpopulation of ARVC patients (43).T-wave inversion in the right precordial leads (V1–V3) is the most common repolarisation abnormality. An S wave duration of more than 55 ms in V1–V3 is also a marker of the disease. (44,45). Ventricular arrhythmias range from premature ventricular complexes to sustained VT or ventricular fibrillation (VF) leading to cardiac arrest (45). The distinctive QRS morphology of ventricular arrhythmias is left bundle branch block (LBBB), which indicates an origin from the right ventricle. Moreover, the mean QRS axis suggests the site of origin, i.e., inferior axis from the right ventricular outflow tract and superior axis from the right ventricular inferior wall or the apex. Patients with widespread ARVC can show several morphologies of VT.

VF is the mechanism of instantaneous sudden death in young people and athletes with ARVC, who are often previously asymptomatic. In this subset of patients, VF is most likely related to a phase of disease progression, due to acute myocyte death and reactive inflammation (31).VF seems to be rare in older patients with a long-lasting ARVC, who more often have scar-related, haemodynamically stable VT (33).

Evidence of LV involvement with fibrofatty replacement, chamber enlargement, and myocarditis

is reported in up to 75% of patients (31; 46). EMB from the RV free wall is a sensitive diagnostic marker when fibrofatty infiltration is associated with surviving strands of myocytes. Histological examination reveals islands of surviving myocytes interspersed with fibrous and fatty tissue (47) . Fatty infiltration of the right ventricle alone is not considered a sufficient morphological hallmark of ARVC as recently defined in the modified Task Force criteria (36). Clusters of myocytes can also be seen to be dying at histology, providing evidence of the acquired nature of myocardial atrophy. Current criteria indicate a residual myocytes<60% by morphometric analysis (or <50% if estimated), with fibrous replacement of the RV free wall myocardium in ≥1 sample, with or without fatty replacement of tissue on endomyocardial biopsy (major criteria); a residual myocytes 60% to 75% by morphometric analysis (or 50% to 65% if estimated), with fibrous replacement of the RV free wall myocardium in ≥1 sample, with or without fatty replacement of tissue on EMB represents a minor criteria (36). These changes are frequently associated with inflammatory infiltrates, which probably play a major part in triggering life-threatening arrhythmias (31).Whether the inflammatory cells are a reaction to cell death (either necrosis or apoptosis) or the consequence of infective or immune mechanisms is not known (48). Cardiotropic viruses have been reported in the myocardium of patients with ARVC, thus supporting an infective pathogenesis, even though viruses might not play a part or the dystrophic myocardium favours viral settlement (superimposed myocarditis). Similar pathological features have been described in spontaneous animal models, with a clinical picture dominated by right heart failure and ventricular arrhythmias with the risk of sudden death.

Recently, it has been emphasized that these histological findings are not exclusive of the RV disease. In fact phenotypes with early and predominant LV involvement have been recognized. Bauce et (49) in a clinico-pathologic study described ina patient suddenly died without evidence of coronary artery and valve disease, an ‘infarct-like’ band of acute–subacute myocytes necrosis associated with inflammation in the outer mid–subepicardial layer of the postero-septal and postero-lateral walls of the LV.

Including CMR as a surrogate for in-vivo pathology three distinct patterns of ARVC have been identified by clinico-genetic characterization of families (50): *RV phenotype*, either isolated or associated with some LV involvement; *left dominant phenotype*, with early and prominent LV manifestations; and *biventricular phenotype*, characterized by equal involvement of both ventricles. Arrhythmias of RV or LV origin, or both, and inferolateral ECG abnormalities are seen in the last two patterns, which might be misdiagnosed as DCM, although ECG

abnormalities and arrhythmic symptoms predominate.

Prevention of sudden death is the most important management strategy of ARVC. Treatment with ICD is indicated in patients with cardiac arrest, syncope, or haemodynamically poorly-tolerated VT despite anti-arrhythmic therapy. In this high-risk group, the ICD intervention rate is around 10% per year, and appropriate shocks have been shown to provide life-saving protection by terminating potentially lethal tachyarrhythmias. Prophylactic ICD implantation in asymptomatic patients, with no or minimal manifestations of the disease, or in healthy gene carriers is currently not recommended. An exception is a patient with early and severe RV dysfunction or advanced disease with biventricular involvement, which probably carries an increased risk of sudden death irrespective of warning arrhythmic events. ICD implantation for primary prevention of sudden death in patients with multiple risk factors, family history of sudden death, or VT/VF inducibility at programmed ventricular stimulation is controversial and needs individual clinical decision perhaps guided to new clinical and imaging parameters.

Cardiac Magnetic Resonance Imaging

Technical Issues

Since from its discovery in 1946 and the real fruition in the mid 1990s, magnetic resonance, because of its unique versatility and non-invasive nature, has become an attracting diagnostic modality in cardiovascular medicine, being a non-invasive comprehensive and reproducible imaging modality to asses function, morphology an tissue characterization.

Magnetic resonance imaging views the water and fat in the human body by observing the

hydrogen nuclei in these molecules (51). Magnetic resonance is sensitive to any nucleus that possesses a net “spin”. Nuclear spin is a fundamental property of atomic nuclei that depends on the numbers of neutrons and protons it contains, and so nuclei either have it. Nuclei possessing net spin will behave as tiny radiofrequency receivers and transmitters when placed in a strong magnetic field. Both the frequency and the strength of the transmitter increase with increasing magnetic field strength. One feature of magnetic resonance is that the frequency at which signals are received and re-emitted (known as the resonant frequency) is exquisitely sensitive to the exact magnetic field, for example hydrogen nuclei (lone protons) resonate at 42.575 Hz/Tesla. So, if we have two regions where the magnetic field is different by a small amount (e.g. at 1.000 Tesla and 1.001 Tesla), then the protons in one region will transmit at 42.575 MHz (the Larmor frequency for protons), and the protons from the other region will transmit at 42.575±0.042 MHz. If we sample this transmitted signal, it is possible to determine these two different frequencies. Numerically this transformation from a sampled signal to the component frequencies is known as a Fourier transform. By modifying the frequency of the RF pulse, and by playing out the gradient pulses on more than one axis simultaneously we can move the slice of interest freely. We are not limited to axial planes, since that we can acquire data with oblique or doubly oblique axes with complete flexibility too. The term “pulse sequence” or “imaging sequence” describes the way in which the scanner plays out RF pulse and gradient fields and how it acquires and reconstructs the resultant data to form an image.

The basic imaging sequences used in CMR are the following (52):

- FLASH (Fast Low Angle SHot). This plays out a small excitation RF pulse which is followed by a rapid read-out and then spoiling (or removing) of the residual signal to prevent it appearing as an artefact in subsequent acquisitions. The process is repeated, yielding a single phase-encode line per acquisition.
- TrueFISP (Balanced FFE (Balanced Fast Field Echo). This sequence is similar to FLASH but instead of spoiling the magnetization at the end of each acquisition it re-uses that signal. Compared to FLASH the benefit of this approach is that the images are of higher signal-to-noise ratio, with natural contrast between cavity and myocardium; the disadvantages being increased sensitivity to artefacts, increased RF power deposition, and contrast that is more complex to interpret.
- FSE (Fast Spin Echo, TSE (Turbo Spin Echo). This sequence acquires a number of phase-encode lines per acquisition by playing out a series of refocusing pulses after the

initial excitation pulse. These refocusing pulses are a phenomenon of MR, which allow us to hold into the signal created by the excitation pulse for longer so that we can sample it multiple times. The optimum excitation pulse can be used, which maximises the available signal, and it is possible with this sequence to obtain T2 contrast without the undesirable effects of T2*. It is possible to acquire all the phase encodes in FSE in a single acquisition, which has some advantages, although this is likely to result in low temporal resolution.

Additional modules can be included with the above sequences to modify the image contrast, for example:

- Black-blood pulses can be applied to effectively remove all the signal from material that moves quickly (i.e. blood). This is usually performed using double inversion, which requires a delay prior to acquisition so is most compatible with FSE-based sequences.
- Inversion recovery is a pre-pulse method that allows to introduce T1 contrast into an image. An inversion time that completely removes the signal from materials with a certain T1 can be chosen. In practice this is often used to better define small changes in T1 in late enhancement type sequences.
- Fat suppression (or water suppression) can be used to remove all the signal from either of these tissues, which may improve the delineation of the structures of interest.

Tissue characterization of myocardium is provided by CMR combining the different previously described sequences, in particular comparing cine images with T1 and T2 sequences with and without fat saturation. However, the most robust application comes from initial experiences of CMR application to the field of myocardial infarction. In 1984 the first application of post-contrast sequences for the evaluation of an experimental canine model of acute myocardial infarctionwas described (53). Injured myocardium demonstrates significantly greater T1 shortening after contrast. These initial studies were hampered, however, by insufficient image contrast between normal and injured myocardium due to technical (e.g. gradients, phased array etc.) and sequence limitations. In recent years, a number of studies have demonstrated the effectiveness of a segmented inversion recovery fast gradient echo (segmented IR-GE) sequence for differentiating irreversible injured from normal myocardium with signal intensity differences of nearly 500% (54). This technique of delayed enhancement imaging also called Late

Gadolinium Enhancement (LGE) from the contrast agent used (gadolinium), pioneered by Simonetti, Kim and Judd, has been shown in animal and human studies, to identify the presence, location, and extent of acute and chronic myocardial irreversible injury (54-57). LGE allows assessment of the transmural extent of irreversible injury, and is superior to single-positron-emission-computed-tomography for the identification of subendocardial myocardial infarction (58,59). LGE imaging can be performed in a single brief examination, requiring only a peripheral intravenous line. It does not require pharmacological or physiological stress. Initially cine images are obtained to provide a matched assessment of left ventricular morphology and contractile function. A bolus of 0.10–0.20 mmol/kg intravenous gadolinium is then given by hand injection. After a 10–15 min delay, high spatial resolution LGE images of the heart are obtained at the same imaging planes as the cine images using the segmented IR-FGE pulse sequence. Each LGE image is acquired during a 10–14 s breath-hold, and the imaging time for the entire examination (including cine imaging) is generally 30–40 min.

The timing diagram for the segmented IR-GE pulse sequence is shown in Figure 4.

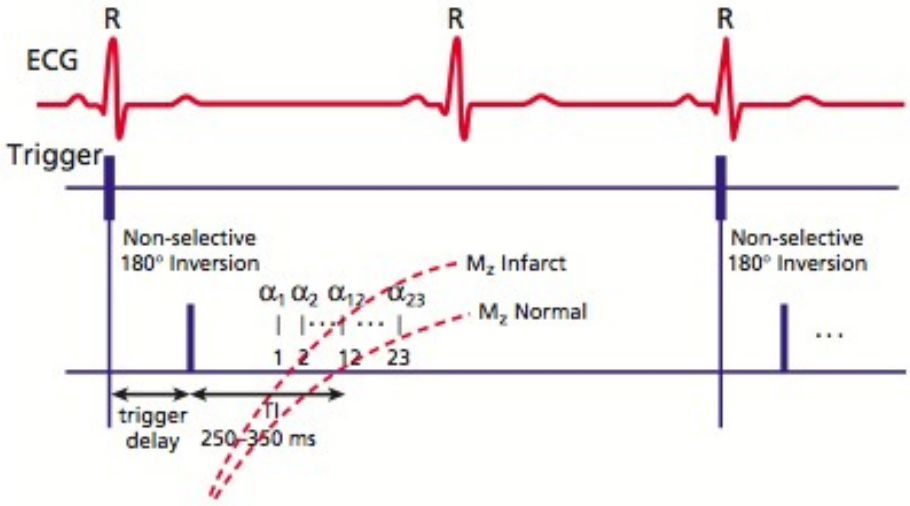

Figure 4. Timing diagram of two-dimensional segmented inversion-recovery fast gradient echo pulse sequence. ECG = electrocardiogram, TI = inversion time delay, α´ = shallow flip angle excitation. Ref. 54.

Immediately after the onset of the R wave trigger, there is a delay period before a non-selective 180° inversion pulse is applied. Following this inversion pulse, a second variable wait period (usually referred to as the inversion time or TI), occurs corresponding to the time between the inversion pulse and the centre of acquisition of k-space lines. The flip angle used for radiofrequency excitation for each k-space line is shallow (20°–30°) to retain regional

differences in magnetization that result from the inversion pulse and TI delay.

The following factors need to be considered when performing contrast CMR:

Dose: The dose of gadolinium given is usually 0.1– 0.2 mmol/kg. Early validation studies used doses as high as 0.3 mmol/kg in animal models (55) and 0.2 mmol/kg in patients (60). More recent studies have found that using 0.1–0.15 mmol/kg still provides excellent image contrast between injured and normal myocardium with the added advantage that the time required to wait after contrast administration is reduced (61). It is necessary to allow the blood pool signal in the LV cavity to decline and provide discernment between LV cavity and hyperenhanced myocardium.

Gating factor: Image contrast is also optimized by applying the inversion pulse every other heart beat in order to allow for adequate longitudinal relaxation between successive 180° inversion pulses. If there are limitations related to breath-hold duration and/or bradycardia, every heart beat imaging may have to be performed. In this situation there may be incomplete relaxation of normal myocardium. Incomplete relaxation will result in not only an artificially shorter "effective" TI needed to null normal myocardium, but may also lead to a reduction in the image intensity differences between abnormal and normal myocardium.

Inversion time (TI): This is defined as the time between the 180° pulse and the center of acquisition of the k-space lines. Selecting the appropriate TI is probably the most important element in obtaining accurate imaging results. The TI is chosen to "null" normal myocardium, the time at which the magnetization of normal myocardium reaches the zero crossing. If the TI is too short, normal myocardium will be below the zero crossing and will have a negative magnetization vector at the time of k-space data acquisition. Since the image intensity corresponds to the magnitude of the magnetization vector, the image intensity of normal myocardium will increase as the TI becomes shorter and shorter, whereas the image intensity of infarcted myocardium will decrease until it reaches its own zero crossing. At the other extreme, if the TI is set too long, the magnetization of normal myocardium will be above zero and will appear gray. Usually only one or two "test" images need to be acquired as with experience one can estimate the optimal TI based on the amount of contrast agent that is administered and the time after contrast agent administration. As the gadolinium concentration within normal myocardium gradually washes out with time the TI will need to be adjusted upwards (e.g.

10 ms every 3 –4 images) to provide optimal image quality with multiple time-point imaging. Recently available automated TI finding sequences (Lock-Looker) can also help in

establishing the optimal inversion time.

Contrast agent: Gadolinium

Addition of even small amounts of certain molecules, called CMR contrast agents, can massively change relaxation rates (i.e. T1, T2 and T2*) within the patient, which results in major changes in the appearance of an CMR image (62). There are two types of contrast agents:

- T1 contrast agents, which by interaction with the nuclear spins, shorten the T1 of the sample. For this to operate there needs to be intimate contact between the agent and the protons;
- T2 and T2* contrast agents. In this case the contrast agents will shorten the T2 and T2* of the sample. These effects do not need close interactions between the nuclei and the agent as they occur over much larger distances.

In each case the contrast agents are based upon molecules or ions that are magnetically active. Paramagnetic moieties (typically, Fe, Dy, Gd but also O2) are used because these demonstrate the greatest effects. The most commonly used nucleus is gadolinium, chelated with diethylenetriaminepentaacetate (DTPA) so as to render it non-toxic and safe for injection. Gadolinium compounds act predominantly as T1 contrast agents in the blood and myocardium, although where the contrast cannot freely mix with the observed water (i.e. in the brain because of the blood-brain barrier), their small T2 and T2* effects can also be observed. Iron- oxide particles predominantly affect the T2 and T2* of the sample.

About the safety of CMR as an emerging problem, numerous reports describing the development of nephrogenic systemic sclerosis have been published. This is a systemic disease involving fibrosis of multiple organs, particularly the skin, that has been linked to gadolinium exposure in patients with renal insufficiency (63). There have been numerous reports describing the development of nephrogenic systemic sclerosis in small numbers of patients with renal failure exposed to CMR contrast agents. The prevailing theory is that gadolinium dissociates from its carrier molecule and accumulates in the tissue of patients with renal failure because it is not cleared. The European Society of Urogenital Radiology released guidelines regarding the use of gadolinium-containing CMR contrast agents (64), suggesting that these agents are contraindicated for patients with a glomerular filtration rate <30 ml/min and recommending caution for patients with a glomerular filtration rate of 30 to 60 ml/min. However, the patients at risk of developing this disease are not only those with acute or chronic severe renal insufficiency,

but also those with renal dysfunction caused by the hepatorenal syndrome or in the perioperative liver transplantation period (65). In the latter two conditions, the risk applies to any severity of renal dysfunction.

Magnetic Resonance and Cardiomyopathies

Functional assessment

Cardiac functional evaluation is an important pillar of the assessment of myocardial disease. Unlike echocardiography, CMR has the ability to image in any desired plane and with a nearly unrestricted field of view, allowing unprecedented flexibility to evaluate abnormal cardiac and extracardiac structures. The functional information derived from cine CMR includes global LV and RV volumes and mass, without the need to make any geometrical assumptions, and therefore applies to ventricles of all sizes and shapes, even to those that have been extensively remodelled (66). Moreover, the inherent 3-dimensional nature of CMR makes it particularly well suited to studying the RV, which is difficult to assess with echocardiography because of its complex and variable morphology. With regard to regional ventricular function, CMR enables the accurate identification of even subtle regional wall motion abnormalities with the use of steady-state free-precession sequences, which provide excellent delineation of the blood–myocardium interface (67).

Applied to DCM, functional studies by CMR reveal increased end-diastolic and end-systolic LV volumes, reduced EF in one or both ventricles associated or not with cine abnormalities. Although segmental wall motion abnormalities are not uncommon in DCM, they are still more characteristic of ischemic heart disease, whereas diffuse global dysfunction is more typical of DCM. Cardiac imaging techniques are used also to detect the repercussion of the LV dilatation on valvular function and on morphology of LV trabeculae, an important issue to avoid a pitfalls diagnosis with LV non-compaction (68). In fact, while in normal subjects, LV trabeculae are small, in subjects with DCM these trabecuale are larger, very different to the trabeculae of post-infarctual LV dilatation in which those are scarce and the inner sides of the myocardium become very smooth.

In the field of ARVC, CMR can provide a detailed analysis of regional ventricular function, wall motion, as well as wall thickening, and accurate quantification of global RV function, allowing the impact of the fibrofatty myocardial replacement on RV and, eventually also LV function. The dysfunctional areas are typically located in the RV free wall, the apex and in the inflow and outflow tracts, and range from segmental areas to a more uniform and extensive involvement that correlate well with areas of abnormally low amplitude on endocardial voltage mapping (69). Of note, recent Modified Task Force criteria (36) cancelled the hypokinesia as a criterion for ARVC diagnosis and the cut-offs of RV dilation and dysfunction evaluated by CMR were also reported. Currently, a *major* criteria are represented by the presence on CMR of a regional RV akinesia or dyskinesia or dyssynchronous RV contraction and 1 of the following: a) ratio of RV end-diastolic volume to BSA ≥110 mL/m2 (male) or b) ≥100 mL/ m2 (female) or c) RV ejection fraction ≤40%. *Minor* criteria are the presence on CMR of a regional RV akinesia or dyskinesia or dyssynchronous RV contraction and 1 of the following: a) a ratio of RV end-diastolic volume to BSA ≥100 to <110 mL/m2 (male) or b) ≥90 to <100 mL/m2 (female) or c) RV ejection fraction >40% to ≤45%.

Tissue characterization of Dilated Cardiomyopathy

Post-contrast sequences are the essential CMR technique for myocardial characterization in DCM: LGE imaging leverages contrast-induced T1 shortening to distinguish between necrotic/fibrotic and normal myocardium. Although findings such as mid-myocardial fibrosis may be nonspecific, they reliably distinguish DCM from infiltrative and ischemic cardiomyopathies. In fact, post-infarction LGE typically proceeds from the endocardium as to become transmural, accordingly with the “wave-front phenomenon” of myocardial ischemia. On the opposite, in DCM, the typical LGE pattern may be, besides the absence of contrast deposition, a mid-wall stria, an epicardial stria, and patchy (spot) LGE (Figure 5) (70).

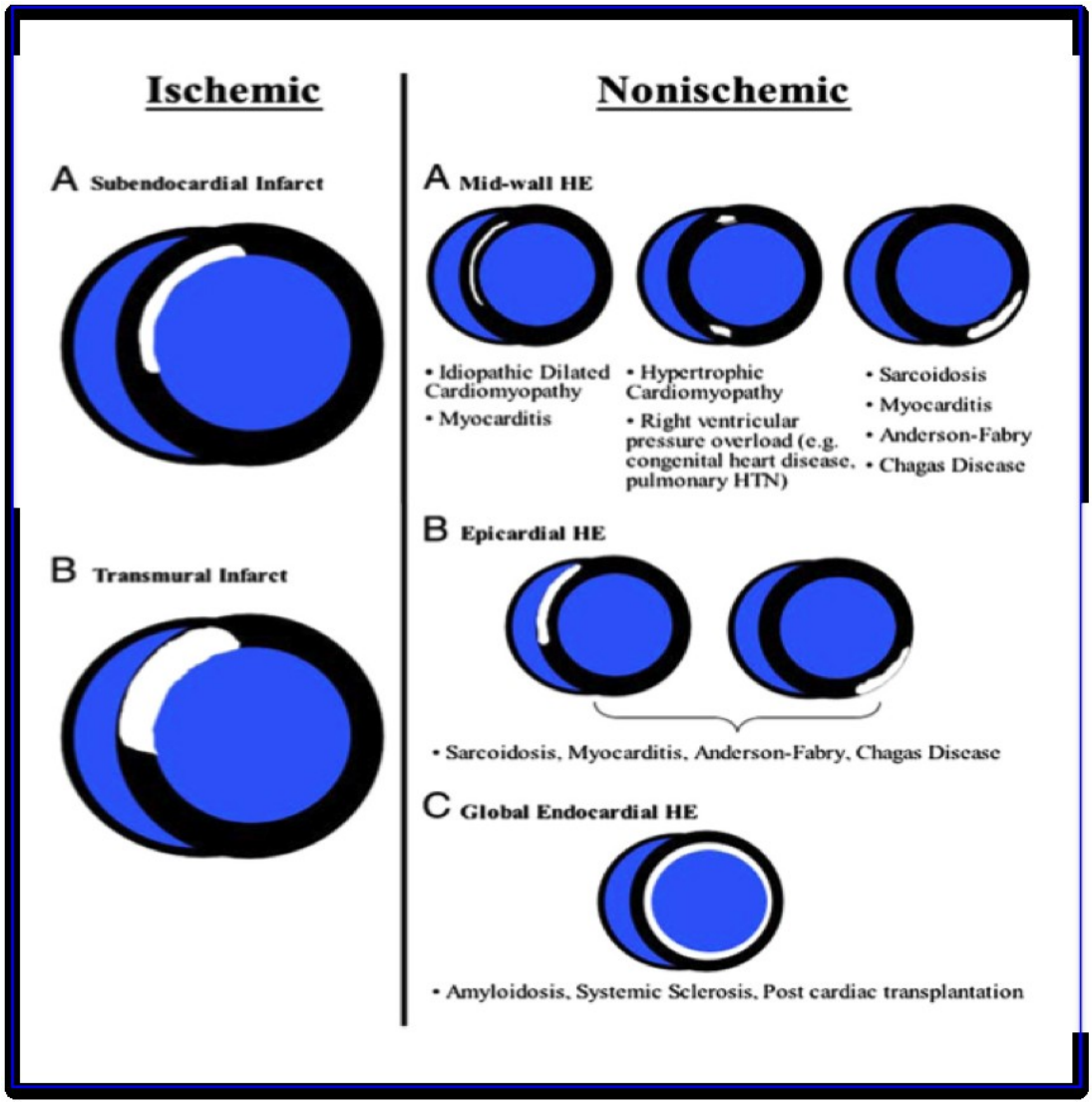

Figure 5. Late Gadolinum Enhancement pattern in dilated cardiomyopathy and ischemic heart diseases. A schematic representation of hyperenhancement patterns that are characteristic for ischemic and nonischemic disorders. Note that the area of LGE in ischemic cardiomyopathy always involves the subendocardium. In contrast, midwall or epicardial LGE strongly suggests a nonischemic aetiology (From Karamitsos et al Ref 70).

Sometimes LGE findings of non ischemic DCM may coexist with infarct scar, which should prompt the interpreting team to consider non ischemic cardiomyopathy superimposed on ischemic heart disease. McCrohon et al. (71) reported that 41% of patients with DCM showed LGE areas in the myocardial walls. This 41% consisted of 13% with a pattern (subendocardial and transmural) that cannot be distinguished from the typical ischemic pattern, and of 28% with a midmural distribution of LGE areas. Therefore, the distinction of these 2 subgroups may be

fundamental in the therapeutic and prognostic approach to the patients.

By evaluating the different LGE patterns reproduced in Figure 5, it is important to note that similar contrast distribution correspond to different diseases, leading to a low specifity of CMR. In myocarditis, the subepicardium is usually affected with varying degrees of progression toward the midmyocardial wall and typical sparing of the subendocardium, and the lateral and inferolateral walls are frequently involved (72). A single center-experience showed a different pattern of midwall septal LGE associated with human herpesvirus 6 or combined herpesvirus 6/Parvo B19 myocarditis (73). During time-of-course of myocarditis, it has been demonstrated that focal areas of LGE become diffuse over a period of days to weeks, then decrease during healing, and because of shrinking, may disappear after recovery (74). Alternatively, large areas of scarring may still be visible after healing, causing distinctive linear midwall striae of LGE, a pattern similar to that seen in DCM patients (75).

Myocardial involvement occurs in at least 25% of patients with sarcoidosis at autopsy. The LGE in these patients usually shows a non-ischemic pattern with LGE of the mid-myocardial wall or the epicardium in an unpredictable distribution (76). The anteroseptal and inferolateral walls are also frequently involved, although LGE is seen in other territories, including the RV and the basal septum (77). Even in the Anderson-Fabry disease the LGE pattern typically spares the subendocardium and shows a typical deposition in basal inferolateral LV region (78). Finally, there is an overlap for LV infero-lateral region even with Chagas disease, since the LV apex and inferolateral regions are the sites where fibrosis is most commonly seen (79). Moreover, in this condition there is an overlap of reported LGE patterns with both ischemic (subendocardial or transmural) and nonischemic patterns (subepicardial, midwall).

CMR with LGE sequences seems to have a role also in the evaluation of the degree of fibrosis and of its prognostic significance in patients with DCM. Testing the hypothesis that fibrosis in DCM might predict outcome, Assomull et al. (80) used LGE CMR to study a group of patients with DCM and found that 35% of these patients had midwall myocardial fibrosis, which was a predictor of the combined end point of all-cause mortality and cardiovascular hospitalization, and also of sudden cardiac death and ventricular tachycardia. These results perhaps suggest that CMR has a potential role in risk stratification of patients with dilated DCM.

Tissue characterization of Arrhythmogenic Right Ventricular Cardiomyopathy

In the diagnostic work-up of ARVC, CMR is now considered an important tool for myocardial tissue characterization. One of the main advantages of CMR is the combination of cine images with sequences to detect fatty replacement and fibrosis.

Black-blood imaging may demonstrate replacement of ventricular myocardium with a hyperintense fat signal, which infrequently appears as a signal void on a corresponding fat-suppressed image (81). In the Literature, the incidence of fat infiltration in ARVC has been reported to range from 60% to 100%, likely related to differences in patient selection (82). However, identification of fatty infiltration has high interobserver variability and can occur as a normal variant (83). A combination off fat-suppressed and non-fat-suppressed techniques increases the interobserver agreement and confidence in the diagnosis (84). Fat infiltration often affects the basal RV, RV outflow tract, and the RV anterior wall close to the tricuspid inlet. However, relying on intramyocardial fat visualization to make the diagnosis is problematic, owing to the often-abundant epicardial fat and underscoring the need to carefully distinguish between abnormal fat infiltrating the RV myocardium and fat in the atrio-ventricular groove. By rule of thumb, the presence or absence of myocardial fat and other morphological abnormalities should always be regarded and interpreted in combination with segmental RV function and LGE in the same location to reduce the number of false-positive imaging-based diagnoses (85). Recent evidence suggests that ARVC is a biventricular cardiomyopathy; the extent and severity of LV involvement may be related to the underlying genotype. Detection of fatty replacement has been studied even for LV myocardium, showing that in PKP2-related ARVC (the most common mutation in the Unites States) LV fat infiltration is present up to 25% and most commonly affects the posterolateral LV epicardium (86,87).

Since myocardial inflammatory infiltration and fibrosis are two main features of ARVC, the complete CMR protocol in these patients has to include the detection of myocardial fibrosis. Several groups have recently evaluated the application of IR post-contrast sequences (previosly applied for post-infartual scar detection) to LGE in suspected ARVC. Tandri et al. (88) have found a good agreement between the presence of the fibrosis on EMB evaluation and LGE on CMR in patients with ARVC; none of the patients without the diagnosis of ARVC showed LGE. However, there are many controversies on this topic because LGE imaging is not always detectable in the RV walls due to the very thin wall and partial volume effects (89).

However, LGE has the potential to identify myocardial fibrous changes in both RV and LV in ARVC. The London group (50) showed recently cases of early and/or predominant LV involvement in ARVC, confirming previous post-mortem and clinical studies in which LV involvement was demonstrated not only as an end-stage complication of progressive RV dilatation and dysfunction in ARVC (31,46,49). The typical LGE pattern in LV dominant ARVC is a midmural and subepicardial LGE, mostly located in the inferior and infero-lateral LV walls, which may be seen also in DCM. This location arises important controversies about the specificity of this pattern, taking also into account that the same region is often involved in sarcoidosis, a disease mimicking ARVC for its arrhythmic profile.

AIM

In order to assess the clinical significance of Late Gadolinium Enhancement (LGE) in dilated and arrhythmogenic ventricular cardiomyopathies, the following lines of investigation of my PhD thesis were pursued:

1. Dilated Cardiomyopathy (DCM):

- The prognostic value of LGE in patients with non-ischemic dilated cardiomyopathy, with special reference to the possible different significance of various LGE patterns and of the total amount of LGE against survival, heart failure and ventricular arrhythmias;

2. Arrhythmogenic Right Ventricular Cardiomyopathy (ARVC):

- The comparison between CMR findings (in terms of tissue characterization) and traditional electrocardiographic features of ARVC;

- The comparison between electroanatomic scar detected by endocardial voltage mapping (EVM) and LGE scars on CMR examination;

- The prognostic significance of LGE in ARVC, with special reference to left ventricular involvement on arrhythmic events or disease progression.

3. DCM and ARVC:

- The pathological basis of CMR tissue abnormalities were evaluated by comparing LGE CMR and heart specimen (autopsy, cardiac transplantation) and/or EMB findings.

METHODS

Between January 2007 and December 2010 we prospectively evaluated two different groups of patients referred to our Tertiary Referral Centre for a complete non-invasive and invasive evaluation for unexplained LV dilatation (DCM Group) and for suspected ARVC (ARVC Group). For each subject were evaluated the traditional clinical and instrumental findings to reach the final diagnosis.

- DCM Group (Group A): we prospectively evaluated 210 patients referred for unexplained LV dilatation, with or without heart failure with onset ≥ 1 month (subacute-chronic), who were hospitalized and underwent to a complete evaluation including: clinical history, electrocardiography (ECG), transthoracic echocardiography, CMR including LGE, coronary angiography, right side catheterization, endomyocardial biopsy (EMB) in non-ischemic disease. After the complete evaluation, the ischemic forms were used only for the evaluation of the accuracy of CMR to distinguish the different aetiologies and were not included in the clinical follow up.

  Inclusion criteria were: echocardiographic LV end-diastolic volume (LV EDV) >70 ml/m2, and coronary angiography performed, based on clinical indications, during the same hospitalization. All patients provided their informed consent to undergo both coronary angiography and CMR.

  Exclusion criteria were: recent onset of heart failure (<1 month), myocarditis proven by EMB; diagnosis of hypertrophic cardiomyopathy, restrictive cardiomyopathy, ARVC, suspected infiltrative heart disease or other specific cardiomyopathies; severe valvular diseases; previous coronary artery bypass graft; hemodynamic unstable conditions and contraindication to CMR (claustrophobia, pacemaker, ICD, metallic clips, atrial fibrillation, severe obesity preventing the patient from entering the scanner bore; pregnancy); chronic renal failure with an estimated glomerular filtration rate < 30 ml/min. All patients had coronary angiography and were classified as “non ischemic” if they had no history of myocardial infarction or revascularization and no evidence of

coronary artery stenosis >50% of two or more epicardial vessels or left main or proximal left anterior descending coronary artery stenosis >50% (90). All patients gave their informed consent.

- ARVC group (Group B): we prospectively evaluated 52 patients who were referred to our Tertiary Centre for susptected ARVC and in which the diagnosis was reached in according with 1994 Task Force Criteria (35) and Modified 2010 Criteria (36). Collected data included clinical history (in particular history of sudden death, ARVC, syncope), ECG, signal averaged ECG (SAECG), ECG Holter monitoring, transthoracic echocardiography, CMR including LGE, angiography, right side catheterization and EMB in selected cases. In a subgroup of patients an electrophysiological study and the Endocardial Voltage Mapping (EVM) by C.A.R.T.O. System was performed. For each subject enrolled, a clinical, ECG and echocardiographic follow-up was obtained.

Clinical/Family History

Clinical data such as age, gender, New York Heart Association (NYHA) functional class, history of prior myocardial infarction and/or heart failure were recorded for each patient. For all patients, data regarding family history of sudden death and/or ARVC and DCM were also collected. Patients were diagnosed with ARVC independently of the results of endocardial voltage mapping (EVM) and CMR.

Electrocardiographic Data Analysis

Twelve-leads ECG

Electrocardiographic data were collected for each patient of both Groups (DCM group and ARVC group). ECGs at rest were evaluated using digital calibers on standard-speed paper (25 mm/s, 10 mm/mV). For the DCM group, the presence of LBBB, presence and location of Q waves assessed by criteria of Minnesota codes 1-1-1 to1-2-7) were also collected (91-93). The ECG parameters considered for ARVC group were: (1) type of rhythm; (2) QRS duration in leads V1 to V3 (normal <110 ms); (3) presence of epsilon wave (defined as a distinct wave of low amplitude localized immediately after the QRS complex); (4) differences in QRS duration between leads V1 to V3 and V6 (defined as parietal block when ≥25 ms); (5) complete right

branch bundle block (RBBB) (QRS duration <120 ms with notched R waves in V1/V2 and wide deep S waves in V5/V6); ST-segment elevation (defined as maximal displacement of the ST segment ≥ 0.15 to 0.2 mV from the isoelectric line); (6) presence of pathologic Q waves (Q-wave duration ≥40 ms and amplitude ≥2⁄3 of QRS complex); (7) R/S wave ratio in V1 and V2; (18) r wave progression through V1 to V3; (8) prolonged corrected QT interval (calculated using Bazett's formula); (9) T-wave inversions in the precordial, inferior and lateral leads, considering pathologic T-wave inversion beyond V1 without the presence of complete RBBB; and (10) measurement of QRS voltages in precordial leads, calculated summing the amplitude of the different QRS components in each precordial lead (the final voltage was calculated using the sum of QRS voltages in all leads).

Signal Averaged ECG (SAECG)

SAECGs were obtained using a MAC15 system (Marquette Inc., Milwaukee, Illinois). The parameters for each filter evaluated, accordingly with the previously described criteria (41, 40,42), were: filtered QRS duration (fQRSD), high-frequency low-amplitude signal duration in the terminal portion of the filtered QRS with voltage amplitude <40 µV (or <20 µV for only the 80- to 250-Hz filter) (HFLA), and root mean square of the voltage in the last 40 ms of the filtered QRS (root mean square). The normal values established in a population of 146 healthy subjects of our Laboratory for the 25- to 250-Hz filter were fQRSD <120 ms, HFLA <40 ms, and root mean square >25 µV; for the 40- to 250-Hz filter were fQRSD <118 ms, HFLA <40 ms, and root mean square >20 µV; and for the 80- to 250-Hz filter were fQRS <106 ms, HFLA <34 ms, and root mean square >12 µV. SAECGs were considered positive when ≥2 parameters were abnormal in 1 filter.

All ECG measurements were performed independently by 2 observers blinded to clinical and procedural characteristics and subsequently by 1 observer 1 week later. Discrepancies were resolved by consensus.

Holter ECG

On 24-h Holter ECG the recorded ventricular arrhythmias were: (1) ventricular fibrillation (VF); (2) sustained ventricular tachycardia (VT) (when lasting more than 30 s); (3) non-sustained VT; and (4) frequent premature ventricular complexes (PVCs) (>30/h).

Transthoracic Echocardiography

Echocardiograms were obtained using a 2.5- to 4-MHz transducer (Hewlett Packard model 5500, Andover, Massachusetts) and included M-mode, 2-dimensional, and Doppler examinations. Parasternal, apical, and subcostal views were performed and the presence of wall motion abnormalities were carefully analyzed. Left ventricular end-diastolic volume was calculated using an ellipsoid biplane area-length model derived from LV images in the apical 4-chamber view. Left ventricular ejection fraction was calculated using the formula end-diastolic volume minus end-systolic volume divided by end-diastolic volume. Right ventricular end-diastolic and end-systolic volumes were calculated using an area-length method derived from orthogonal planes (apical 4-chamber and short-axis subcostal views), and RV ejection fraction was calculated from these 2 values. Right ventricular end-diastolic area, RV end-systolic area, and RV fractional area change were calculated from the apical 4-chamber view. The right ventricular dilatation and dysfunction were defined accordingly with the cut-off proposed by modified Task Force criteria (36): Parasternal long axis view RV outflow tract (RVOT) (PLAX) ≥ 29; corrected for body size (PLAX/BSA) ≥ 16 mm/m2i. Parasternal short axis view RVOT (PSAX): ≥ 32; corrected for body size (PSAX/BSA) ≥ 18 mm/m2i. Fractional area change ≤40%.

Cardiac Magnetic Resonance

Data Analysis

Cardiac magnetic resonance was performed on a 1.5-Tesla scanner (Magnetom Avanto, Siemens Medical Solutions, Erlangen, Germany) using a comprehensive dedicated protocol (94).

Sequences views. All patients underwent detailed CMR study protocol including post-contrast sequences. Images were acquired using a 1) steady-state free precession sequence (true FISP) cine loops in sequential short axis (slice thickness 8 mm, gap 2 mm) views and transverse long-

axis views of RVOT to diaphragm; 2) T1-weighted turbo spin echo images in the axial and short-axis planes; 3) T2-weighted STIR for fat suppression.

Imaging parameters for cine images were: Repetition Time 2.5 to 3.8; Echo Time 1.1 to 1.6 , average in-plane resolution 1.5x2.4 mm, flip angle 45° to 60°, temporal resolution 40 to 45 ms.

Imaging parameters for the evaluation of fat infiltration: fast spin echo with field of view 40 cm, matrix of 256 x 256, flip angle 90°, Repetition Time/Echo Time of 1,791/41.5. Fast spin echo images were also reacquired using a fat saturation pulse to selectively null signals from fat.

After intravenous administration of contrast agent (gadobenate dimeglumine, Multihance, Bracco, 0.2 mmol/kg of body weight) 2-dimensional segmented fast low-angle shot inversion recovery sequence after at least 10 minutes were acquired in the same views of cine images, covering the entire RV and LV. Considering the T1 relaxation times of the tissues and the wash-in and wash-out kinetics of extracellular interstitial contrast agents (95), the optimized T1 nullifies the signal from normal myocardium in the images acquired 10 min after contrast medium injection, allowing a clear visualization of the LGE areas, defined as a signal intensity at least 400% higher than the signal from normal (remote) myocardium or skeletal muscle (54). Inversion time adjusted to null normal myocardium was typically 220-300 msec. Imaging parameters for post-contrast T1 inversion recovery sequences were: Repetition Time 5.4 to 8.3 ms, Echo Time 1.3 to 3.9 ms, average in-plane spatial resolution 1.4 to 1.5 x 2.2 to 2.4 mm, 8-mm slice thickness, 2-mm gap, and flip angle 20° to 25°.

Definitions

Image Analysis. Global ventricular volumes were calculated from the short-axis cine images using a summation of disks methods (“Simpson’s Rule”), with integration over the image slices using the standard software provided by the manufacturer. RV and LV volumes and systolic function were evaluated comparing the values with references ranges reported elsewhere (96,97,36) and were normalized to body surface area. Wall motion and trabeculation were evaluated by a subjective assessment and localized aneurysms were defined as akinetic or dyskinetic regions of the ventricular wall showing bulging during diastole. Thinning of the RV wall was defined under a cut-off of 4 mm. The normal epicardial fat was distinguished from fibrofatty myocardial replacement by comparing corresponding slices on T1 spin echo

(with/without fat saturation) and post-contrast IR sequences and by showing that fatty tissue and DCE images did not overlap (85). Sections within 1 cm of the atrio-ventricular groove were excluded in the analysis because of the difficulty to distinguish between normal epicardial fat and fibrofatty myocardial infiltration in basal images. Two observers blinded to the clinical outcome independently determined the dichotomous presence or absence of LGE by reviewing all short- and long-axis contrast-enhanced images; regions of elevated signal intensity had to be confirmed in 2 spatial orientations.If CMR LGE was present, the quantitative extent of hyperenhancement was defined as regions with abnormally increased signal intensity greater than peak remote (98). For each short-axis cross section, after the endocardial and epicardial borders were traced, a region of interest averaging 50 $mm^2$was defined within the normal remote myocardium in an area with uniform myocardial suppression free of artefacts. The peak signal intensity (SI) within the remote region of interest was then determined. Total myocardial LGE was defined as abnormal myocardium with SI above peak remote SI and areas were measured by manual planimetry and expressed as a percent of total LV mass. Despite LGE quantification, the LGE pattern was defined as “stria” (both epicardial and midmural), “spot” (patchy, not including LV-RV junctions), “junctional” (across LV-RV junctions at septum levels), “gray”. A “gray” pattern was defined as the presence of myocardium with SI > peak remote SI but < 50% of maximal SI within the LGE region (99) in at least 2 LV walls. The topographic location of LGE stria pattern was subsequently defined as multiregional presence: interventricular septum (IVS), lateral (L) wall, IVS+L wall, IVS+ L wall+anterior (A) wall. Patients initially diagnosed as having DCM displaying a subendocardial or transmural pattern of LGE suggestive of myocardial infarction were excluded from the final analysis and included in the “Ischemic” DCM. Patients with a normal LV EF on CMR (>55%) were also excluded.

For RV scars analysis, the following RV regions were defined: the infero-basal region, the antero-lateral region, the RVOT and the apex. For regional analysis of LV LGE, a 17-segment model was used (100). For the RV the presence of LGE was evaluated as previously reported (88). The images of RV-EVM and CMR were analyzed independently by two observers blinded to clinical and procedural characteristics. *Control Group*. Eighteen healthy volunteers (asymptomatic, with negative family history and no clinical evidence of heart disease) underwent CMR according to the same protocol and served as control subjects.

Endocardial Voltage Mapping

Endocardial Voltage Mapping (EVM) and electrophysiological study were performed only in selected ARVC patients. Endocardial voltage mapping by the CARTO system (Biosense-Webster) was performed during sinus rhythm, as previously reported (101,102). In brief, a 7-F Navi-Star (Biosense-Webster) catheter, with a 4-mm distal tip electrode and a 2-mm ring electrode with an interelectrode distance of 1 mm, was introduced into the RV under fluoroscopic guidance and used as the mapping/ablation catheter. The catheter was placed at multiple sites on the endocardial surface to record bipolar electrograms from RV inflow, anterior free wall, apex, and RVOT. Bipolar electrogram signals (filtered at 10 to 400 Hz and displayed at 100 mm/s speeds on the CARTO system) were analyzed with regard to amplitude, duration, relation to the surface QRS, and presence of multiple components. A recording was accepted and integrated into the map when the variability in cycle length, local activation time stability, and maximum beat-to-beat difference of the location of the catheter were <2%, <3 ms, and <4 mm, respectively. These parameters, combined with impedance measurements, were used to exclude signals with low amplitude due to poor endocardial catheter contact. In addition, adequate catheter contact was confirmed by concordant catheter tip motion with the cardiac silhouettes on fluoroscopy. Bipolar voltage reference for normal and abnormal myocardium was based on values validated by intraoperative and catheter mapping (103,104) and used in previous voltage mapping studies (101, 104, 105-109).

The colour display for depicting normal and abnormal voltage myocardium ranged from red representing “Electroanatomic Scar” (“EAS”) (amplitude <0.5 mV) to purple representing electroanatomical “normal tissue” (amplitude ≥1.5 mV). Intermediate colors represented the electroanatomical “border zone” (signal amplitudes between 0.5 and 1.5 mV). Complete endocardial maps were obtained in all patients to ensure reconstruction of a 3-dimensional geometry of the RV chamber and to identify scar regions. Regions showing low-amplitude electrograms were mapped with greater point density to delineate the extent and borders of EAS areas.

Bipolar voltage reference for normal and abnormal myocardium was based on values validated by intraoperative and catheter mapping (103,104), and used in previous voltage mapping studies (101,105,106,108). In particular, to avoid low voltage recordings due to poor contact, the following tools were used: 1) the signal had to satisfy 3 stability criteria automatically detected by CARTO system in terms of cycle length, local activation time and beat-to-beat difference of the location of the catheter (<2%, <3ms, and <4 mm, respectively); 2) both bipolar and unipolar signals were simultaneously acquired to confirm true catheter contact through the analysis of local electrocardiogram (in particular the shape of the unipolar electrocardiogram); 3) in the presence of a low voltage area, at least 3 additional points were acquired in the same site to confirm the reproducibility of the voltage measurement (101). Finally perivalvular regions were excluded by the analysis.

Control Group. In 19 patients (asymptomatic, with negative family history and no clinical evidence of heart disease), who underwent electrophysiological study for evaluation of supraventricular tachycardia, the same EVM protocol was used. These data served as control group.

Electrophysiological study and ventricular tachycardia mapping/ablation

All antiarrhythmic drugs were discontinued 5 half-lives (6 weeks for amiodarone) before the electrophysiological study. Programmed ventricular stimulation protocol included 3 drive-cycle lengths (600, 500, and 400 ms) and 3 ventricular extrastimuli while pacing from 2 RV sites (apex and outflow tract).

The site of origin of the ventricular arrhythmia was established by activation mapping and/or pace mapping. The activation map was created by mapping several points within the RVOT during ventricular arrhythmias while using a surface ECG lead as a reference. Activation times were assigned on the basis of the onset of bipolar electrograms and displayed as colour gradients on a 3-dimensional activation map. A suitable target for ablation was selected based on the earliest endocardial activation times during arrhythmia (or during episodes of frequent premature ventricular beats with QRS morphology identical to the clinical tachycardia) and confirmed by the pace mapping that provided ≥11 of 12 matches between paced and spontaneous QRS complexes. Sustained VTs inducible by programmed ventricular stimulation were entrained at

cycle lengths of 20 to 40 ms below the cycle length of the tachycardia to guide the site of ablation. Substrate-based catheter ablation at sinus rhythm was accomplished by creating linear ablation lesions encircling and/or connecting RVOT electroanatomical scars, according to a previously reported method (99,100). Ablation was performed with a 4-mm tip ablation catheter using radiofrequency energy (target temperature 60°C, maximal power 50 W) delivered for up to 60 s. The procedure was considered acutely successful if ventricular arrhythmia was abolished during ablation, remained absent for at least 30 min after ablation, and was not re-induced by either programmed ventricular stimulation or isoproterenol infusion.

Coronary Angiography and Right Side Cathetherization

All patients with DCM underwent to coronary angiography. Selected patients of ARVC group underwent to coronary angiography.

The coronary angiography was obtained in the right anterior oblique -30°/cranial 30° projections for the assessment of the left descending anterior coronary artery (LAD), right anterior oblique -40°/ caudal 30° projections for the left circumflex artery (LCX) and left anterior oblique 30°/ cranial 15° or right anterior 30°/ cranial 0° projections for the right coronary artery (RCA). A final left ventriculogram in a 30° right anterior oblique projection was obtained in all cases, with the exclusion of patients with renal failure or on dialysis. Or previous demonstration of LV thrombous. Angiographic parameters (presence, number and location of major epicardial coronary artery stenosis >75% narrowing), interpreted by the consensus of two experts blinded to patient name and CMR results, were collected.

Right heart catheterization had been performer to assess RV and pulmonary vascular hemodynamics. Pressures were recorded in the wedge position (WP), pulmonary artery (PA), RV and right atrium. Cardiac output was measured by modified Fick's method. Pulmonary hypertension were defined as a mean PA pressure ≥ 25 mmHg accordingly with current guidelines (110). Pre- and post-capillary pulmonary hypertension was defined on the basis of mean value of WP.

In the ARVC group patients who underwent to invasive protocol, a selective RV angiography was performed. A 30° PAO projection was aquired during a deep inspiration and breath-hold (37).

Endomyocardial Biopsy

Endomyocardial Biopsy of the RV was obtained via the femoral vein with the use of the long sheath technique (disposable Cordis bioptome) in all patients. The samples were obtained from the RV septum in patients with DCM and at the junction between the ventricular septum and the anterior RV free wall in patients with a clinical suspicion of ARVC. Three to 5 biopsy specimens (mean, 3.4) were obtained from each patient, fixed in 10% phosphate-buffered formalin (pH 7.35), and then processed for histological examination. Seven-micrometer-thick paraffin-embedded sections were serially cut and stained according to the hematoxylin-eosin and Heidenhain trichrome techniques. Histopathological diagnosis of DCM and ARVC was made independently by 2 observers blinded to clinical information, EVM and CMR results. The ARVC diagnosis was done accordingly with recently modified Task Force criteria (36), as evaluated by histomorphometric analysis (47). Dallas criteria were used for histological diagnosis of myocarditis (111). To characterize cellular infiltrates, additional paraffin-embedded tissue sections were stained with a panel of monoclonal antibodies according to the avidin-biotin peroxidase complex method (Vector). Agreement of interobserver analysis was 94%, and discrepancies were resolved by consensus. Dilated cardiomyopathy was diagnosed on the basis of typical findings on histology of interstitial plus/minus replacement-type fibrosis and abnormalities of myocytes consisting of cytoplasm vacuolization, dysmetric/dysmorphic nuclei, perinuclear halo, with or without inflammatory infiltrates. One or two frozen EMB specimens per patient were used for polymerase chain reaction (PCR) and reverse transcriptase PCR analysis and for detection of cardiotropic viruses genome. (112,113, 114).

Clinical Follow-up

All patients were followed-up by either direct communication (follow-up visit or telephone interview) for the occurrence of (cardiac) death, ICD implantation, ICD discharge, hospitalisation for decompensated congestive heart failure, or heart transplantation. In both groups an echocardiographic follow-up was also obtained. No patient was lost to follow-up.

Events were adjudicated by an independent committee blinded to the CMR results. Appropriate ICD firing was defined as a shock for sustained VT above the programmed rate cut-off of the ICD (generally 180 beats/min) or VF. For outcome analysis, the end point was defined as cardiac death/ heart transplantation, documented ventricular arrhythmias (sustained VT or VF) or appropriate ICD discharge for VF/VT or both, and hospitalisation for heart failure. In the ARVC group was also considered an event a syncope and ICD implantation. If patients underwent heart transplantation, the follow-up data were censored at the time of transplantation.

STATISTICAL ANALYSIS

Data are expressed as mean value ± standard deviation for continuous variables, and as frequency with percentage for categorical variables. Student's t test and chi-square test were used as appropriate.

Sensitivity, specificity, positive and negative predictive values were determined according to standard definitions. Endomyocardial biopsy was taken as the positive reference standard for DCM. Receiver operating characteristics (ROC) curve analysis was generated to test the predictive discrimination of non-ischemic DCM patients with and without ventricular arrhythmias and heart failure.

Stepwise logistic regression analysis was used to model LV dilatation, RV dilatation, LV fatty infiltration, RV fatty infiltration, LV LGE, RV LGE and biventricular LGE versus traditional ECG abnormalities of ARVC disease (duration of PQ interval > 200 ms; duration of QRS interval > 110 ms, epsilon wave, complete RBBB, ST-segment elevation, reduced R wave progression in V1-V2, QT dispersion, voltage amplitude, T wave inversion in V1-V3; T wave inversion beyond V3; T wave inversion in inferior leads, T wave inversion in lateral leads, Q waves in inferior leads, SAECG) and gender. Variables considered for inclusion in the models were chosen on the basis of their discrimination LV dilatation, RV dilatation, LV fatty infiltration, RV fatty infiltration, LV LGE, RV LGE and biventricular LGE as well as on univariate association with ECG parameters of $p<0.1$. In order to exclude possible modulator effects, we then forced all other variables into the models, one at the time.

Evidence of major events was taken as the positive reference standard and receiver-operating characteristics (ROC) curve analysis was generated. Event-free survival curves were traced by use of the Kaplan-Meier method and compared by log-rank test. Manual Cox regression model with backward elimination was performed on blocks of variables until regression models with only significant or marginally significant ($P<0.1$) variables were obtained; then, we evaluated the independent predictive value of selected covariates.

Intraobserver and interobserver reproducibilities of LGE assessment were evaluated by linear regression analysis and expressed as correlation of coefficients (r) and standard error of estimates (SEE), and by the intraclass correlation coefficient. Reproducibility is considered satisfactory if the intraclass correlation coefficient is between 0.81 and 1.0. Intraobserver and interobserver reproducibility measurements were calculated in 50 patients.

Statistical significance was accepted if the null hypothesis could be rejected at $p<0.05$.

Data were analysed by SPSS 17 for Windows (SPSS Inc., Chicago, Illinois).

RESULTS

Group A, Dilated Cardiomyopathy

Patients with LV dilatation were divided in two groups, accordingly to the presence of coronary artery disease (CAD) on angiography: patients with “ischemic” DCM (n= 150), “non-ischemic”

DCM (n= 111). Among the latter, four patients showed a single-vessel CAD not involving the left main or proximal left anterior descending coronary artery: only one of these patients had LGE, not correlated to a specific coronary artery, but as subepicardial stria. All of them had a reduced ejection fraction < 35%: for these reason they were considered as affected by a cardiomyopathy "out-of-proportion" to CAD.

In our global population, the presence of non-ischemic LGE pattern (including the absence of LGE) demonstrated a sensitivity of 100%, a specificity of 91.8%, a positive predictive value of 94.3%, a negative predictive value of 100% with a global accuracy of 96.5% for the identification of non-ischemic DCM.

DCM population

Demographic characteristics of 111 DCM patients enrolled are summarized in Table 1. Fifty-eight (52%) of patients had a previous history of heart failure (HF) (with a median of the time to first episode of HF to CMR of 2.5 years); 53 (48%) had a first acute onset of HF in the hospitalization in which CMR was performed. Positive family history for DCM was found in 17/111 patients (15.3%). The majority of patients were symptomatic as shown by NYHA Class II and III; two patients had an advanced HF during the hospitalization and at time of CMR were completing the check-list for heart transplantation (in those cases patients underwent to CMR with infusion of inotropic drugs). Patients were divided according to the presence (n=67, 60.4%) or the absence of LGE (n=44; 39.6%). No differences in functional class neither in medical treatments were found between the two groups. In the subset of patients in which were collected the data about right side heart catheterization for invasive measurement of pulmonary hemodynamic (34/111; 31%), an increased mean pulmonary artery pressure (PAPm) resulted associated with the presence of LGE, with atypical "junctional" LGE pattern: PAPm 30 ± 9 mmHg (with junctional LGE) vs 23 ± 4 mmHg (without junctional LGE) ($p<0.05$); mean wedge pressure (WPm) 22 ± 9 mmHg (with junctional LGE) vs 16 ± 2 mmHg (without junctional LGE) ($p<0.05$).

Table 1. Study Population Characteristics

Variable	Overall Population (111 patients)	Negative LGE (44 patients)	Positive LGE (67 patients)	P
Age (years)	49.9±15.7	49±17	49±16	0.784
Male gender, n (%)	90 (81.1)	33 (75)	57 (85.1)	0.06
Caucasian race, n (%)	108 (97.3)	43 (97.7)	65 (97)	1

Chronic HF (> 6 months) , n (%)	58 (52)	26 (59.1)	32 (47.8)	0.241
Subacute HF (1 month-6 months) , n (%)	53 (48)	13	40	0.01
EF (mean± SD)	31±8	31.9±8.5	30.6±8	0.784
EF ≤ 35% (non-CMR method) , n (%)	81 (73)	31 (70.5)	50 (74.6)	0.06
EDV (ml/m2) (non-CMR method)	118±33	117.1±34.1	118.8±34.1	0.799
Single vessel CAD >50% ("out-of-proportion") , n (%)	4 (3.6)	3 (6.8)	1 (1.5)	0.05
NYHA functional class, n (%)				
I	27 (24.3)	11 (25)	16 (23.9)	1
II	39 (35.1)	18 (40.9)	21 (31.3)	0.317
III	43 (38.7)	13 (29.5)	30 (44.8)	0.117
IV	2 (1.8)	2 (4.5)	0 (0)	0.155
Medications, n (%)				
ACEI or ARB	98 (88)	38 (86)	60 (89)	0.65
β-blocker	86 (77.5)	32 (72.7)	54 (80.1)	0.08
Spironolactone	50 (45)	23 (52.3)	27 (40.3)	0.07
Diuretics	86 (77.5)	30 (68.1)	56 (83.6)	0.058
Amiodarone	19 (17)	8 (18)	11 (16.4)	0.9
Lipid-lowering	30 (27)	12 (27.3)	18 (26.9)	1
Q wave, n (%)	1 (0.9)	0 (0)	1 (1.5)	1
LBBB, n (%)	37 (33.3)	15 (24.1)	22 (32.8)	1

Table 1 Legend: HF= heart failure; EF = ejection fraction; EDV = end-diastolic volume; CAD = coronary artery disease; NYHA = New York Heart Association; SD = standard deviation; ACEI = angiotensin-converting enzyme inhibitor; ARB = angiotensin receptor blocker; PAPm = mean Pulmonary Artery Preassure; WPm = mean Wedge pressure; LBBB= left bundle branch block.

CMR findings

On functional CMR assessment, no differences between RV and LV volumes and EF were found in two subgroups (Table 2). Out of 67 (60.4%) patients with positive LGE, the following pattern were observed: a "gray" pattern in 12 patients (17.9%); a midwall/subepicardial stria in 49

(73.1%); an isolated septal junction (anterior and/or posterior) in 4 (5.9%) or associated with other patterns in 25 (37.3%); and finally a spot (patchy) pattern in 2 cases (2.9%). In the subset of patients with midwall/subepicardial LGE stria, an isolated involvement of septum was found in 31 patients (63.3%), an isolated LV lateral wall involvement in 5 patients (10.2%) and a multiregional involvement as septum+lateral wall in 10 (20.4%) and septum+lateral+anterior walls in 3 patients (6.1%). An example for each LGE pattern is shown in Figure 6.

Figure 6. Examples of LGE patterns.

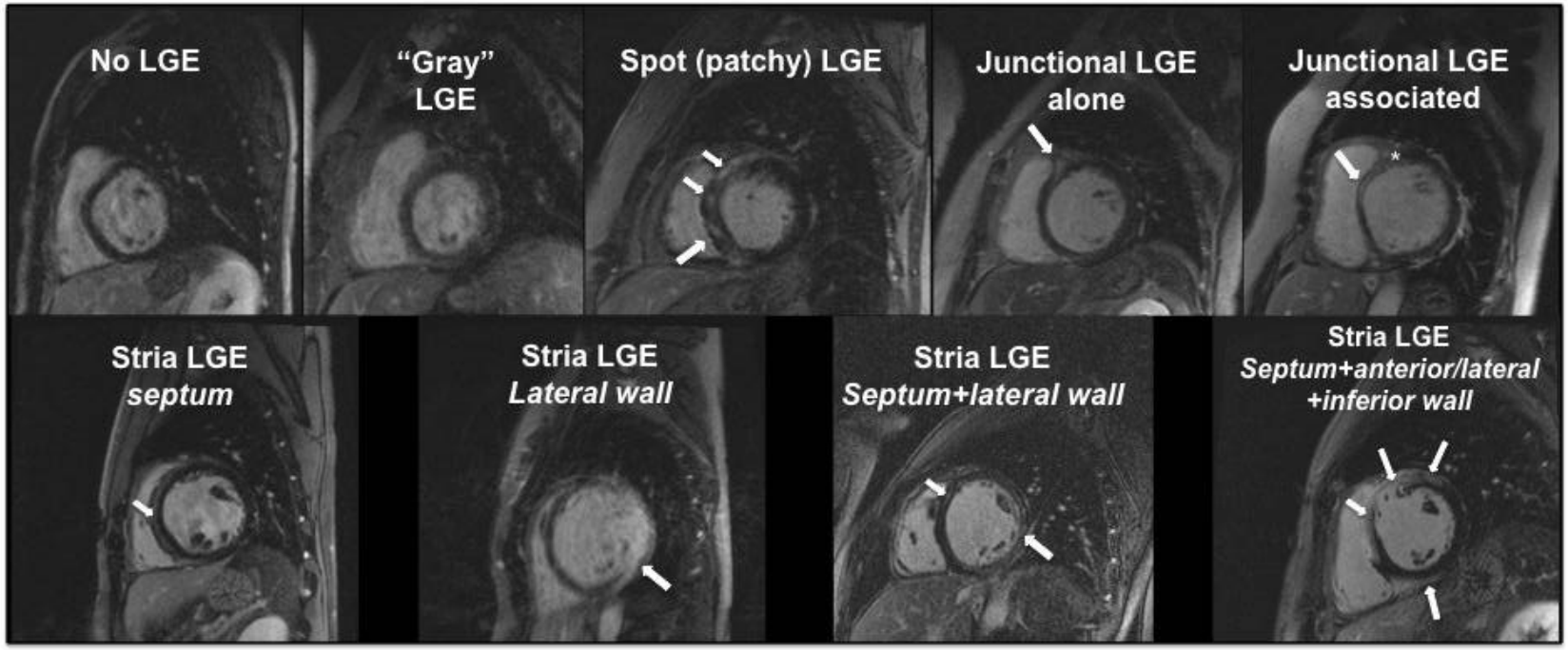
No LGE
"Gray" LGE
Spot (patchy) LGE
Junctional LGE alone
Junctional LGE associated
Stria LGE septum
Stria LGE Lateral wall
Stria LGE Septum+lateral wall
Stria LGE Septum+anterior/lateral +inferior wall

Among patients with LGE, the extent of LGE was 6.3%±8.8% (median 2) of LV mass. With regard to the dichotomous presence of LGE, there was agreement between the two observers in all but 2 patients. Those patients were assigned to the LGE-negative group after a reading by a third blinded observer. With regard to quantification of LGE, linear regression analysis showed good interobserver and intraobserver reliability (R^2 = 0.91 and R^2= 0.97, respectively). No LGE of RV wall was found.

Table 2. Cardiac Magnetic Resonance Characteristics according to presence or absence of LGE.

Variable	Overall	Negative	Positive	P

	Population (111 patients)	LGE (44 patients)	LGE (67 patients)	
LV EDVi (ml/mq), (mean± SD)	127±33	125±30	130±38	0.1
LV ESVi (ml(mq), (mean± SD)	95±25	90±20	97±23	0.085
LV mass (g/mq), (mean± SD)	80±20	83±18	78±20	0.1
LV EF (%) (mean± SD)	30±5	31±4	28±6	1
LGE pattern				-
Gray, n (%)		-	12 (17.9)	-
Stria (overall) • **IVS , n (%)** • **L , n (%)** • **IVS+L , n (%)** • **IVS+L+A, n (%)**		- - - - -	49 (73.1) 31 (63.3) 5 (10.2) 10 (20.4) 3 (6.1)	- - - - -
Septal Junctions • **Alone, n (%)** • **Associated, n(%)**		- -	4 (5.9) 25 (37.3)	- -
Spot, n (%)		-	2 (2.9)	-
Amount of LGE (% of LV mass)		-	11.3±9 (median 9)	- -
Total volume (mean± SD)		-	19.9 ±15.3	-

LGE = Late Gadolinium Enhancement; LV = left ventricle; EDVi = End-diastolic volume index; ESVi= end-systolic volume index; IVS =interventricular septum; L = lateral wall; A = anterior-wall; SD= standard deviation.

Endomyocardial biopsy results

Endomyocardial biopsy (EMB) was obtained in 60 patients: in two cases the samples were inadequate for the analysis. Thus, the patients eventually enrolled for the comparison between CMR and EMB were 58 (Table 3). On EMB, 33/58 patients (56.9%) showed replacement-type fibrosis, of this subgroup 23 patients (69.7%) showed LGE on CMR.

Out of 13/58 patients (22%) without replacement-type fibrosis on EMB, LGE was present in 9/13 (69.2%) patients: in this subgroup the most frequent LGE pattern was midwall/subepicardial stria (n=8/9; 89%) and one patient (11%) showed a “patchy” LGE pattern.

Out of 35 patients with DCM histopatologic findings associated with inflammation on EMB (61.4%), 13 patients (37%) did not show LGE on CMR: in this subgroup of 13 patients, 6 showed also fibrosis on EMB, not seen as LGE on CMR. Two examples of comparison between EMB and CMR findings are showed on Figure 7 and 8.

Figure 7. Comparison between endomyocardial biopsy and CMR. A: panoramic view of RV endomyocardial biopsy samples. B: cardiomyocyte hypertrophy with dysmetric and dysmorphic nuclei and cytoplasmatic vacuolization due to sarcolysis. C: post-contrast CMR sequences without LGE.

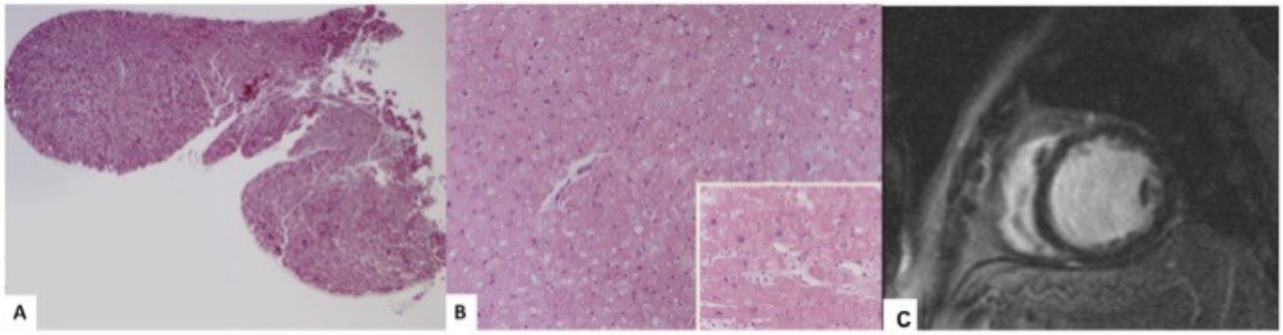

Figure 8. Comparison between endomyocardial biopsy and CMR. A: panoramic view of RV endomyocardial biopsy samples. B: replacement-type and interstitial endo-perymisial fibrosis. C: post-contrast CMR sequences with LGE as mid-wall stria in the septum and in the infero-lateral wall.

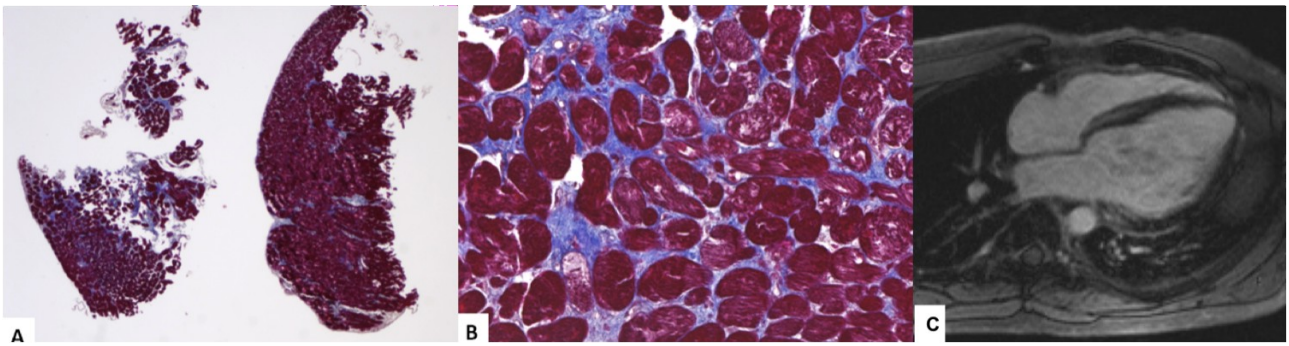

Viral genome analysis by PCR was performer in 39 cases: the analysis was negative in 34 patients. Positive PCR and RT-PCR was found in 5 patients: 3 were positive for Parvovirus B19, 1 was positive for Adenovirus and 1 for Enterovirus. Acute myocarditis was excluded.

Table 3. Characteristics of EMB according with CMR findings.

	Fibrosis (33 patients)	**Myocarditis (35 patients)**	**Fibro-fatty replacement (2 patients)**	**Not conclusive (13 patients)**
LGE presence, n (%)	23 (69.7)	20 (57.1)	2 (100)	9 (69.2)
LGE "gray", n (%)	8 (24.4)	7 (20)	0	0
LGE stria, n (%)	3 (39.4)	12 (34.3)	2 (100)	8 (61.5)
• **IVS**	5 (38.4)	4 (33.3)	0	8 (100)
• **L**	1 (7.7)	2(16.7)	0	0
• **IVS+L**	5 (38.5)	4 (33.3)	2 (100)	0
• **IVS+L+A**	2 (15.4)	2 (16.7)	0	0
LGE junctional, n (%)	5 (15.1)	6 (17.1)	0	4 (30.8)
LGE spot, n (%)	0	0	0	0

LGE = Late Gadolinium Enhancement; IVS = interventricular septum; L = lateral wall; A = anterior-wall.

In two cases, a fibro-fatty replacement was demonstrated on EMB, compatible with ARVC LV involvement. Comparing the accuracy of CMR against EMB (Table 4-5-6) the better values were found for LGE versus fibrosis on EMB: sensitivity 69.7%, specificity 44%, positive predictive value 62.1%, negative predictive value 52.3% and accuracy 58.6% (Table 4).

Table 4. Accuracy of CMR LGE findings against Fibrosis on EMB.

	SENSIBILITY (%)	**SPECIFICITY (%)**	**PPV (%)**	**NPV (%)**	**ACCURACY (%)**
LGE presence	69.7	44	62.1	52.3	58.6
LGE "gray"	24	0	24	0	13.7
LGE stria	39.4	48	50	37.5	43.1
• **IVS**	15	56	31	33.3	32.8
• **L**	3	96	50	42.9	43.1
• **IVS+ L**	15	96	83.3	46.2	50
• **IVS+ L+A**	6	100	100	44.6	46.6
LGE junctional	15	72	42	39.1	39.7
LGE spot	0	96	0	42	41

LGE = Late Gadolinium Enhancement; IVS =interventricular septum; L = lateral wall; A = anterior-wall; PPV = positive predictive value; NPV = negative predictive value.

Table 5. Accuracy of CMR LGE findings against Inflammation on EMB.

	SENSIBILITY (%)	SPECIFICITY (%)	PPV (%)	NPV (%)	ACCURACY (%)
LGE presence	57.1	22.7	54	25	43.9
LGE "gray"	20	95.5	87.5	42.9	49
LGE stria	34.3	36.4	46.1	25.8	35.1
• **IVS**	11	45	25	24	24
• **L**	5	100	100	40	42
• **IVS+ L**	11	90	66.7	39	42
• **IVS+ L+A**	5	100	100	4	42
LGE junctional	17	72.7	50	35.6	38.9
LGE spot	0	95	0	37.5	36.8

LGE = Late Gadolinium Enhancement; IVS =interventricular septum; L = lateral wall; A = anterior-wall; PPV = positive predictive value; NPV = negative predictive value.

Follow-up

The follow-up ranged from 8 years to 1 month (70 months). During the follow-up period, 14 patients suffered cardiac death/heart transplantation; 23 were hospitalized for HF and 25 showed a documented ventricular arrhythmias (sustained VT or VF) (Table 6). Kaplan-Meier curves for composite end-point (Figure 11) and ventricular arrhythmias (Figure 9) showed a significant differences between patients with and without LGE on CMR (Wilcoxon-Breslow: $p< 0.05$).
While a trend towards higher hospitalization for HF among LGE patients could be observed, this failed to reach statistical significance (Figure 10).

By univariate analysis (Table 7), the presence of LGE was strongly associated with ventricular arrhythmias (hazard ratio [HR] 2.194, 95% CI 1.23 to 3.91; $p<0.008$). This association was unchanged in multivariate analysis: in model 2 CMR LGE had a HR of 2.34 (95% CI 1.27 to 4.19; $p <0.006$); in model 3 CMR LGE had HR ratio of 2.5 (95% CI 1.36 to 4.73; $p <0.003$).
The amount of LGE% by univariate analysis (Table 7), was strongly associated with ventricular arrhythmias (HR 1.05, 95% CI 1.02 to 1.08; $p<0.0001$). This association was unchanged in multivariate analysis adjusted for a EF<30% (model 5): HR 1.067, 95% CI 1.034 to 1.1; $p<0.0001$.
With an associated HR of 2.5, the presence of LGE was among the strongest multivariate predictors for the combined end point, surpassed only by age < 49 years (median).
The EF, both as a continuous variable and dichotomous as < 30%, was not found associated with arrhythmic events.
The incidence of ventricular arrhythmic events was associated with “gray” LGE pattern (HR 4.2, 95% CI 1.21 to 14.7; $p=0.02$).
ROC curve analysis revealed a LGE percentage of 3.5 as optimal discriminator for the occurrence of ventricular arrhythmic events with an associated HR of 4.11 (95% CI 1.3 to 12.7; $p<0.001$).

Table 6. Number of Events on the basis of the Positive/Negative LGE.

Events	Overall Population (111 patients)	Negative LGE (44 patients)	Positive LGE (67 patients)
Total Events, n	49	15	34
Cardiac death/Cardiac Transplantation, n	14	5	9
Hospitalization for HF, n	23	7	16
Ventricular Arrhythmias, n	25	4	21

LGE = Late Gadolinium Enhancement; HF = heart failure.

Figure 9. Kaplan-Meier event-free survival curve for the occurrence of Ventricular Arrhythmias.

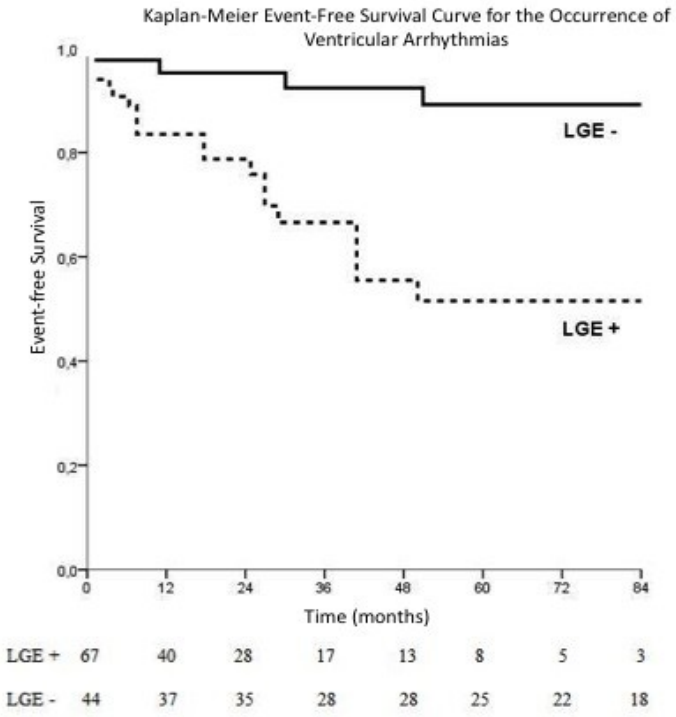

Figure 10. Kaplan-Meier event-free survival curve for the occurrence of Heart Failure.

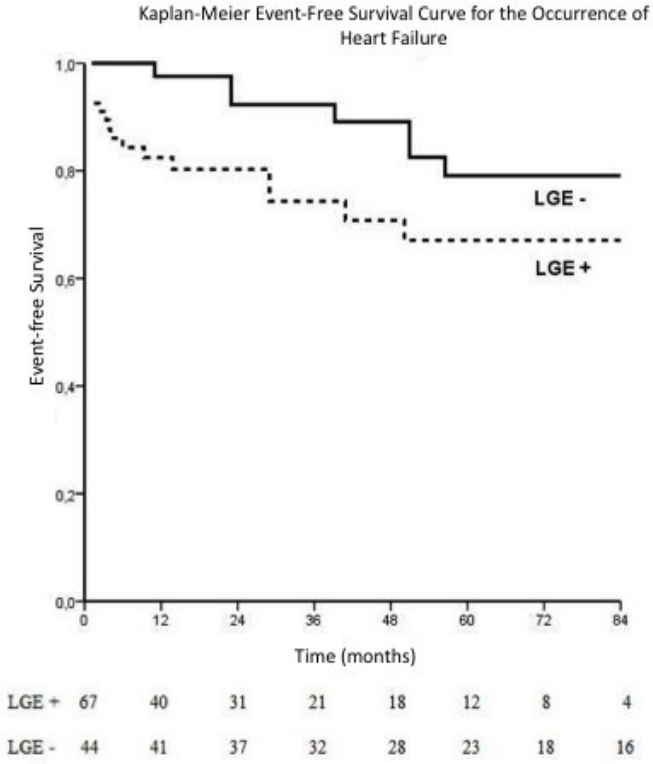

Figure 11. Kaplan-Meier event-free survival curve for the occurrence of cumulative Events.

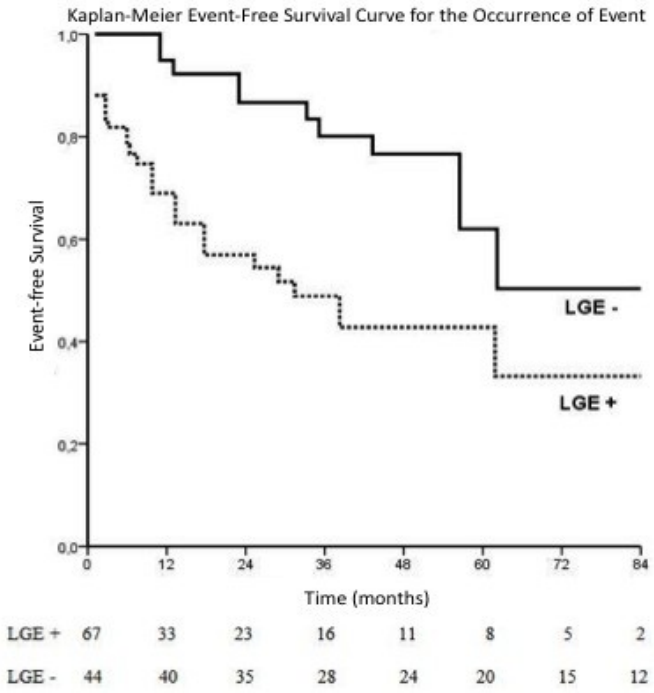

Table 7. Univariate and Multivariable analysis for Ventricular Arrhythmias.

Variables	Univariate Analysis		Multivariate Analysis									
			Model 1		Model 2		Model 3		Model 4		Model 5	
	Unadjusted HR (95% CI)	p Value	Adjusted HR (95% CI)	p Value	Adjusted HR (95% CI)	p Value	Adjusted HR (95% CI)	p Value	Adjusted HR (95% CI)	p Value	Adjusted HR (95% CI)	p Value
LGE presence /absence	2.194 (1.23-3.91)	<0.008	-	-	2.34 (1.27-4.29)	<0.006	2.5 (1.36-4.73)	<0.0003	-	-	-	-
Age	1.029 (1.010-1.048)	< 0.003	1.04 (1.020-1.062)	<0.0001	-	-	-	-	1.04 (1.02-1.06)	<0.0001	1.048 (1.026-1.070)	<0.0001
Age (median < 49 yrs)	2.97 (1.17-3.67)	0.01	-	-	2.62 (1.41-4.87)	<0.002	2.95 (1.57-5.55)	<0.001	-	-	-	-
Gender	0.64 (0.347-1.191)	0.2	-	-	-	-	-	-	-	-	-	-
EF	0.98 (0.95-1.01)	0.38	-	-	-	-	-	-	-	-	-	-
LGE "gray" pattern	4.2 (1.21-14.7)	0.02	-	-	-	-	-	-	-	-	-	-
NYHA class I-II vs III-IV	1.58 (1.1-2.77)	0.109	-	-	-	-	2.02 (1.08-3.78)	0.02	1.96 (1.06-3.6)	<0.03	2.82 (1.38-5.7)	< 0.004
EF < 30%	1.01 (0.58-1.75)	0.9	-	-	-	-	-	-	-	-	-	-
% LGE	1.05 (1.02-1.08)	<0.0001	1.058 (1.028-1.089)	<0.0001	-	-	-	-	1.06 (1.03-1.09)	<0.0001	1.067 (1.034-1.1)	<0.0001
% LGE median	2.12 (1.17-3.8)	0.013	-	-	-	-	-	-	-	-	-	-
EDV	1 (0.9-1.01)	0.2	-	-	-	-	-	-	-	-	-	-
EDV categorized	1.44 (1.19-2.49)	0.1	-	-	-	-	-	-	-	-	-	-

Legend of Table 7: LGE = Late Gadolinium Enhancement; HR = hazard ratio; EF = ejection fraction; NYHA = New York Heart Association functional class; EDV = end-diastolic volume.

Model 1 (with continuous variables): $\chi 2 = 30$; $p < 0.0001$

Model 2 (with categorized variables): $\chi 2 = 16.523$; $p < 0.0001$

Model 3 (with categorized variables and marginal variables): $\chi 2 = 20.830$; $p < 0.0001$

Model 4 (with continuous variables and marginal variables): $\chi 2 = 36.428$; $p < 0.0001$

Model 5 (for variables adjusted by ejection fraction): $\chi 2 = 39.286$; $p < 0.0001$

Study Population

The patients of ARVC group enrolled for the ARVC study and follow-up were 52 (34 males; mean age 33±15 years) (Table 8). The mean Fractional Area Change (FAC) of RV was 39±10% and the mean LV EF was 57±8%.

Table 8. Clinical characteristics of patients enrolled in the ARVC follow-up.

	Patients (n. 52)
Sex (males), n(%)	34 (64)
Mean age (yrs), mean±standard deviation	33 ± 15
Family History, n(%)	29 (56)
Syncope, n(%)	7 (13)
Sustained VT, n(%)	10 (19)
Aborted sudden death, n(%)	1 (2)
Mean baseline LV EF, %	57 ± 8
Mean baseline RV FAC, %	39 ± 10

VT = ventricular tachycardia; LV = Left ventricle; EF = ejection fraction; RV = right ventricle; FAC = Fractional Area Change.

On the basis of clinical and CMR evaluation, 24 patients (46%) were defined as “classic ARVC phenotype”; 14 (27%) as “left dominant phenotype”, and finally 14 (27%) as “biventricular ARVC phenotype” (Table 9).

Table 9. CMR Classification of ARVC patients

	Frequencies
LGE	
RV LGE, n (%)	27 (52%)
LV LGE, n (%)	33 (63%)
Phenotype	
Classic ARVC, n (%)	24 (46%)
Left dominant ARVC, n (%)	14 (27%)
Biventricular ARVC, n (%)	14 (27%)

LGE = late gadolinium enhancement; RV = right ventricle; LV = left ventricle; ARVC = arrhythmogenic right ventricular cardiomyopathy.

Prognostic significance of LGE in ARVC

The ARVC follow-up was conducted either by physician examination, ECG and echocardiography (30 patients, 58%) or with an interview without a complete clinical work-up (22 patients, 42%). In the outpatients group, the mean follow-up was 25.6 months; in the interview group the mean follow-up was longer (35 months). An echocardiographic follow-up was globally available in 40/52 patients (77%).

In the morfo-functional follow-up by echocardiography (Table 10), looking to the overall population, the patients with LGE on CMR showed a trend ($p = 0.07$) of a progression toward LV systolic dysfunction. This trend was not demonstrated for classical ARVC phenotype.

Table 10. Echocardiographic Follow-up.

Overall Population (n. 40/52)			
	Negative LV LGE n = 12 (30%)	Positive LV LGE n = 28 (70%)	P
ΔLV EF %/yr	+ 0.1 (-2.8;+3.0)	- 2.9 (-5.3;-0.4)	0,07
ΔRV FAC %/yr	+ 0.0 (3.8;+3.8)	- 1.8 (-4.3;+0.6)	0,21
Only classical phenotype (n. 16/24)			
	Negative LV LGE N =7 (44%)	Positive LV LGE N = 9 (56%)	P
ΔLV EF %/yr	+ 0.1 (-2.8;+3.0)	-2.6 (-11.6;+6.4)	0.29
ΔRV SF %/yr	+0.0 (-3.8;+3.8)	+0.6 (-4.4;+5.5)	1.00

ΔLV EF%/yr =percentage of left ventricle ejection fraction change per year; ΔRV FAC %/yr = percentage of right ventricle fractional area change per year. LGE = late gadolinium enhancement.

During the follow-up, in 13 patients an ICD was implanted (11 in the LGE group, 2 in the non-LGE group) (Table 11). Total events (excluding ICD implantation that was not considered an end-point) were 12. Only one patient had a syncope and was in the non-LGE group. Considering only the major events (aborted sudden death/VF; sudden death; non sudden death/heart transplantation) they were 12 (7 in the LGE group vs 5 in the non-LGE group).

Table 11. Events on Follow-up.

	Overall **n. 52**	**Negative LV-LGE** **n. 19**	**Positive LV-LGE** **n. 33**

ICD implantation, n (%)	13 (25)	2 (11)	11 (33)
Syncope, n (%)	1 (2)	1 (5)	0
Sustained VT, n (%)	7 (13)	3 (16)	4 (12)
Aborted Sudden death / **VF ICD shock*,n (%)**	**2 (4)**	**1 (5)**	**1 (3)**
Sudden death*,n (%)	**0**	**0**	**0**
Non sudden death/cardiac transplant*, n (%)	**2 (4)**	**0**	**2 (6)**
TOTAL EVENTS	12 (23)	5 (26)	7 (21)
ONLY MAJOR EVENTS, n (%)	**4 (8)**	**1 (5)**	**3 (9)**

* = a major event; ICD = implanted automatic cardioverter; LV = left ventricle; LGE = late gadolinium enhancement; VT = ventricular tachycardia; SD = sudden death; VF = ventricular fibrillation.

On the basis of CMR findings, the clinical events were described for the three different ARVC phenotypes (Table 12). Out of the 12 total events, 7 were referred in the classical phenotype, 2 in the left dominant phenotype an 3 in the biventricular phenotype. Evaluating only the major events (4), one patient showed a VF (classical phenotype) and 2 (both heart transplantation) in the biventricular phenotype.

Table 12. Events on Follow-up divided by CMR ARVC classification.

	Overall n.52	Classic n.24	Left-dominant n.14	Biventricular n.14
ICD implantation, n (%)	13 (25)	5 (21%)	1 (7%)	7 (50%)
Syncope, n (%)	1 (2)	1 (4%)	0	0
Sustained VT, n (%)	7 (13)	5 (21%)	2 (14%)	0
Aborted sudden death / VF ICD shock*, n (%)	2 (4)	1 (4%)	0	1 (7%)
Sudden death*, n (%)	0	0	0	0
Non sudden death/cardiac transplant*, n (%)	2 (4)	0	0	2 (14%)
TOTAL EVENTS, n (%)	12 (23)	7 (29%)	2 (14%)	3 (21%)
ONLY MAJOR EVENTS*, n (%)	4 (8)	1 (4%)	0	2 (14%)

* = a major event; ICD = implanted automatic cardioverter; LV = left ventricle; LGE = late gadolinium enhancement; VT = ventricular tachycardia; SD = sudden death; VF = ventricular fibrillation.

Kaplan-Meier curves (Figure 12) did not show difference between LGE presence/absence for all events and only for major events. Kaplan-Meier curves did not show difference between three phenotypes detected by CMR both for all events and major events.

Figure 12. Kaplan-Meier curves: Prognostic significance of LGE in ARVC.

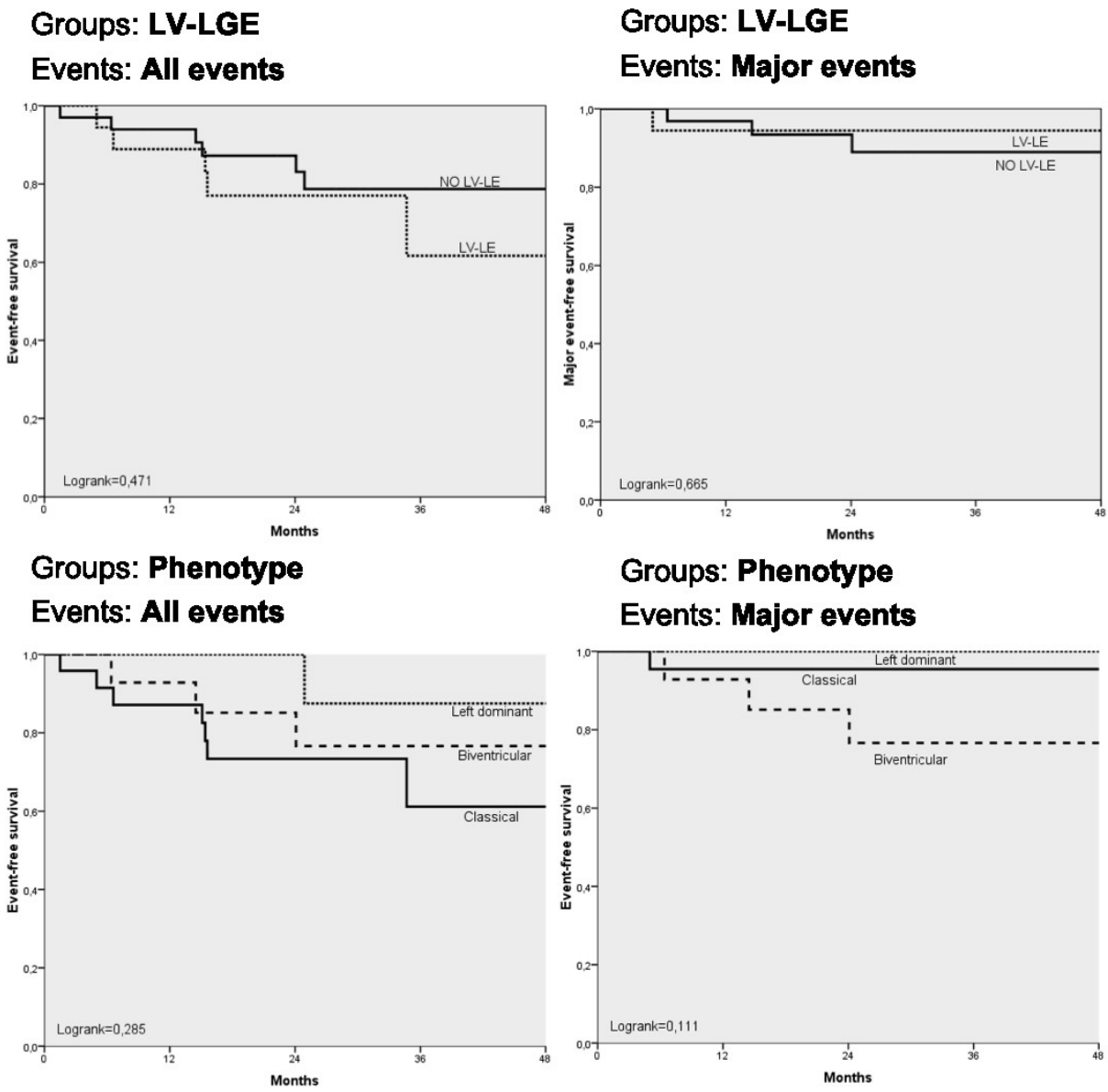

During the follow-up, one patient (G.A.) affected by a biventricular ARVC since the first diagnosis was transplanted and the heart was available for clinic-pathologic correlations.

A 17-year-old boy was referred to the local Emergency Department for abdominal pain, mild irradiated to the chest, and associated with diarrhoea and fever. There was no medical history of cardiac disease or family history of sudden cardiac death. On biochemical test VES and PCR

were increased. A 12-lead ECG showed a sinus rhythm associated with mils ST-segment elevation (Figure 13).

Figure 13. An acute 12-lead ECG showing ST-segment elevation on V1-V4.

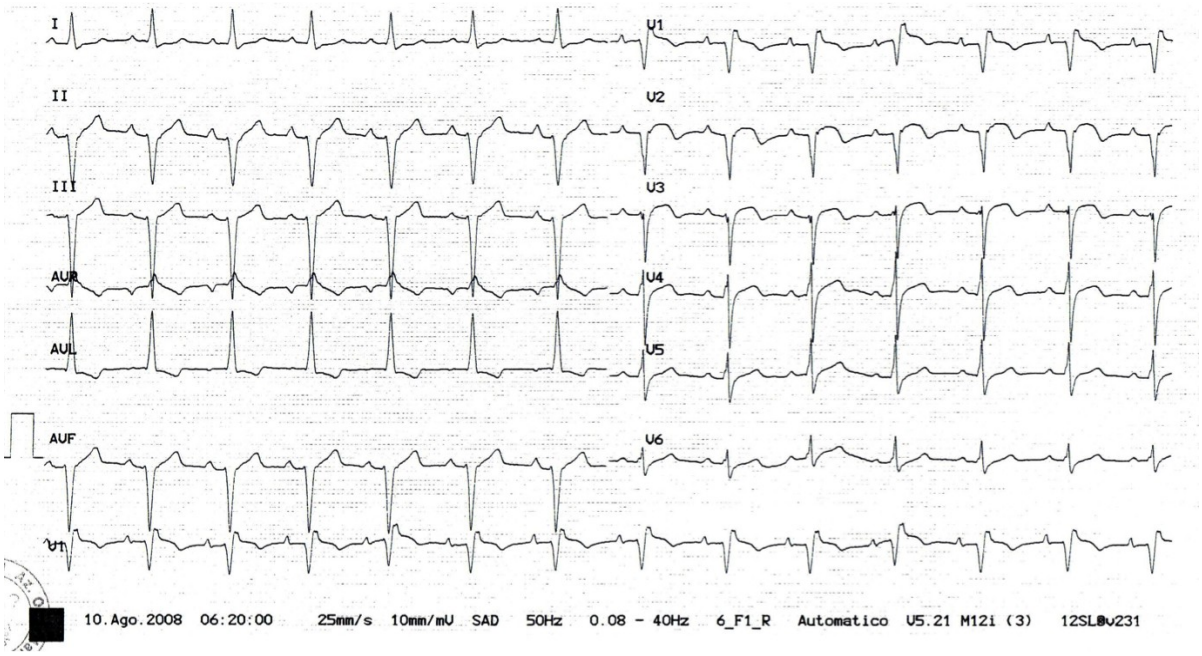

The patient was discharged with the diagnosis of gastro-intestinal infection. Two days later for the persistence of abdominal pain, he was again referred to the Emergency Department: the ECG showed persistence of ST-segment elevation and laboratory test revealed increased values of myocardial necrosis enzymes: Troponin I (TnI) was 4.48 ug/L and CK-MB 6.6 ug/L. A trans-thoracic echocardiogram was immediately performed and showed a sever RV dilatation with moderate systolic dysfunction; LV showed normal dimension with preserved EF, but ipokinesia of inferior and infero-septal wall was detected. On trans-esophageous echocardiography a septal atrial defect was excluded. The TnI increased the following day (39.5 ug/L the second day) and on third day 64.95 ug/l: for a suspected myocarditis the patient was referred to out Tertiary Centre to perform an EMB.

After admission in our Intensive Care Unit a new echo cardiogram was performed, confirming the RV dilatation and dysfunction (Figure 14).

Figure 14. Two-dimensional echocardiogram: an apical 4-chamber view demonstrating the RV dilatation.

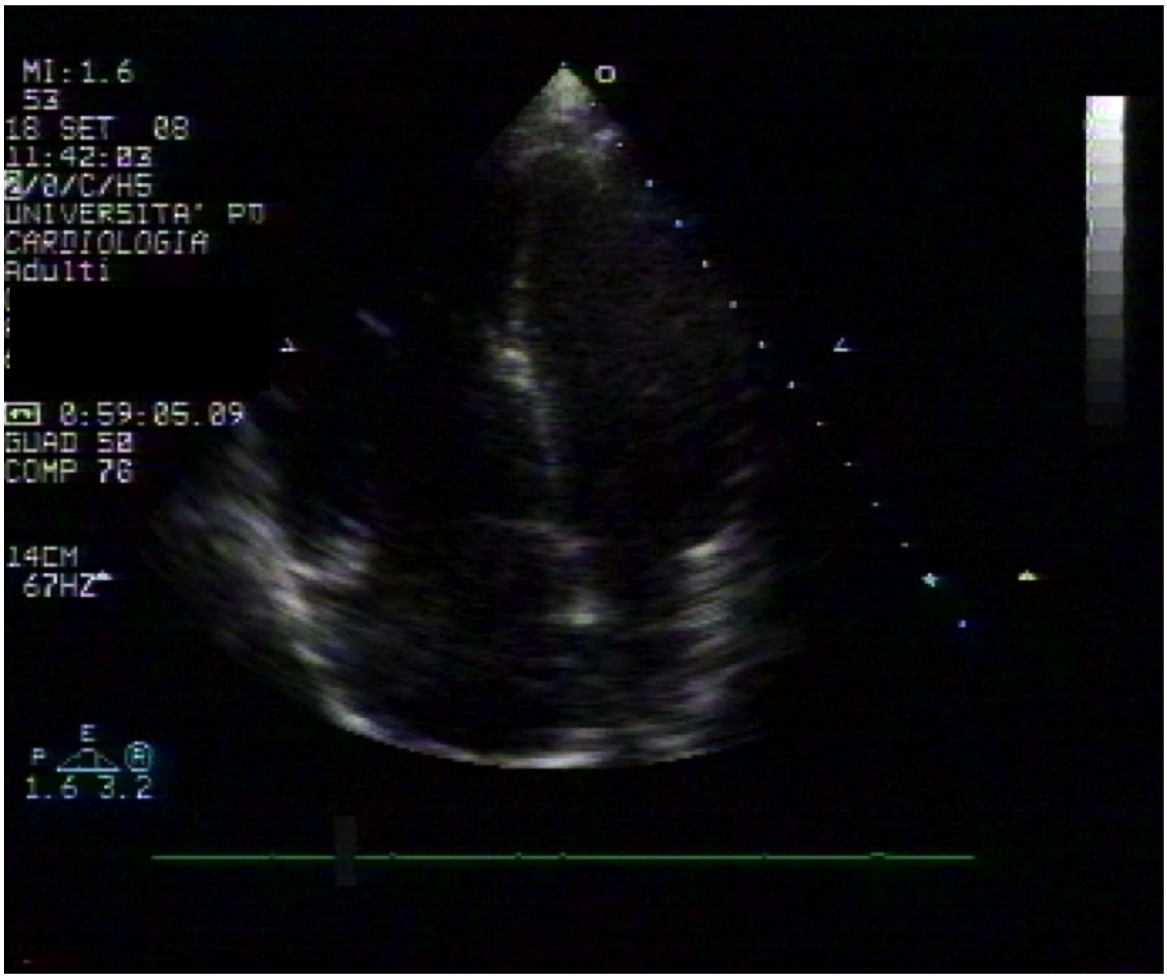

On ECG, ST-segment elevation was present, associated with a prolongation of final portion of QRS compatible with epsilon wave (Figure 15).

Figure 15. A sub-acute 12-lead ECG showing the persistence of ST-segment elevation, associated with epsilon wave on V1 and V2.

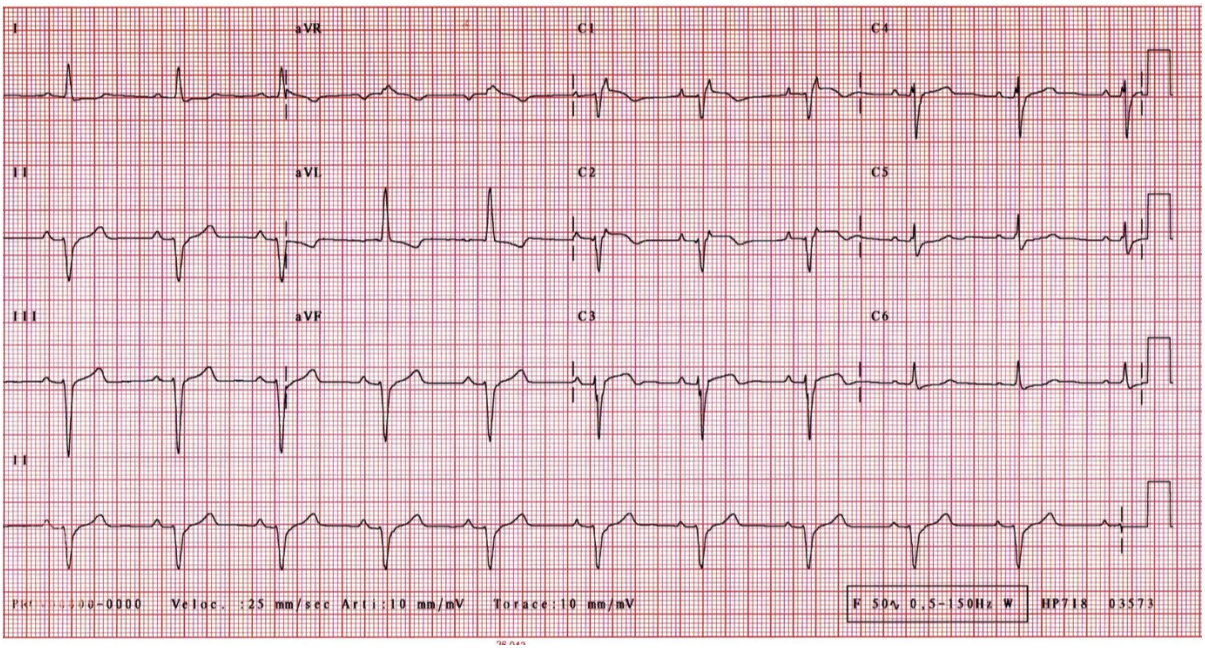

Before performing angiography and EMB, a CMR with contrast injection was done. On cine images a severe RV dilatation was confirmed, associated with severe systolic dysfunction due to diffuse ipokinesia and akinesia of the apex anf subtricuspidal region; LV systolic function was mild reduced for the cine abnormalities in the inferior and infero-septal walls, but without dilatation. On T2-weighted sequences for edema, no myocardial edema was showed. Moreover, on spin-echo sequences (with and without fat saturation) no fatty infiltration was found (Figures 16 and 17).

Figure 16. CMR findings. Top: short axis views of T2 weighted fat-sat images without findings of myocardial edema. Bottom: the same short axis views on T1 black-blood images without fat-saturation without signal of fatty infiltration.

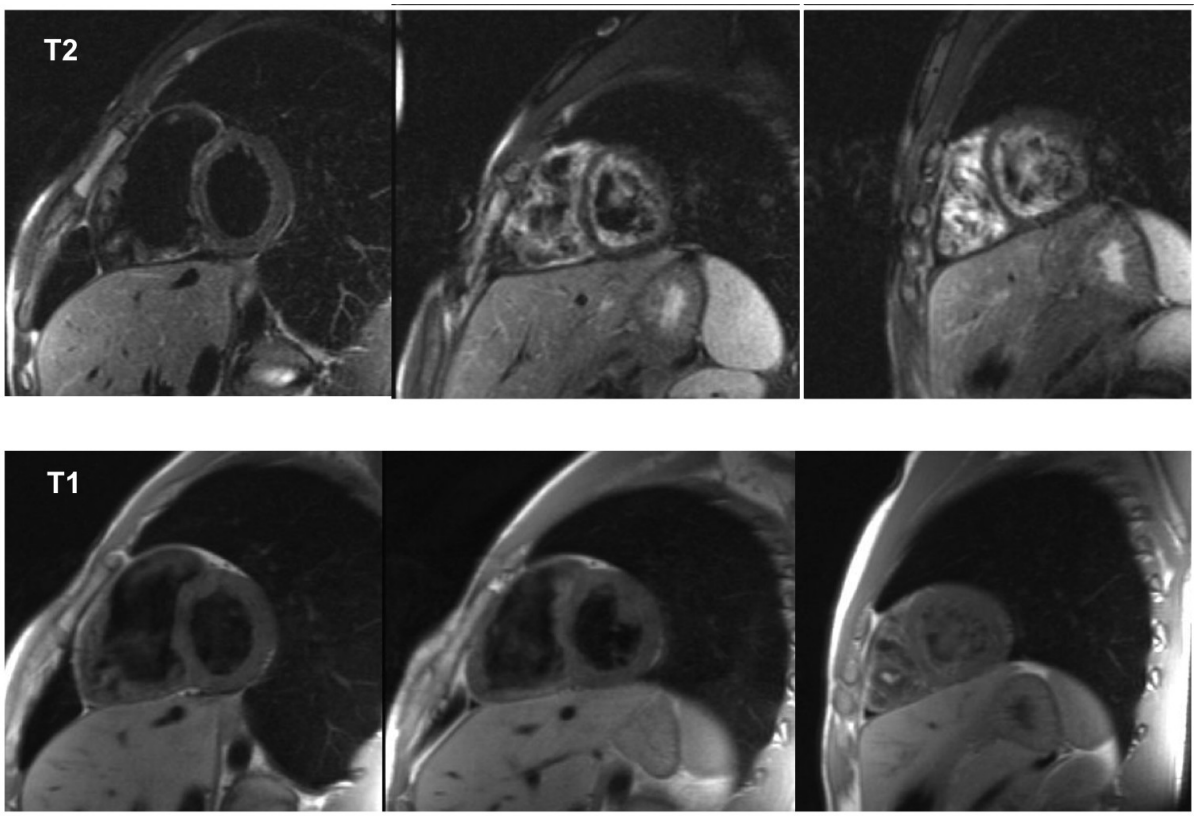

Figure 17. CMR findings. Top: long axis views (3-chamber view on the right; 4 chamber view on the left) of T2 weighted fat-sat images without findings of myocardial edema. Bottom: the same long axis views on T1 black-blood images without fat-saturation without signal of fatty infiltration. Note the RV dilatation.

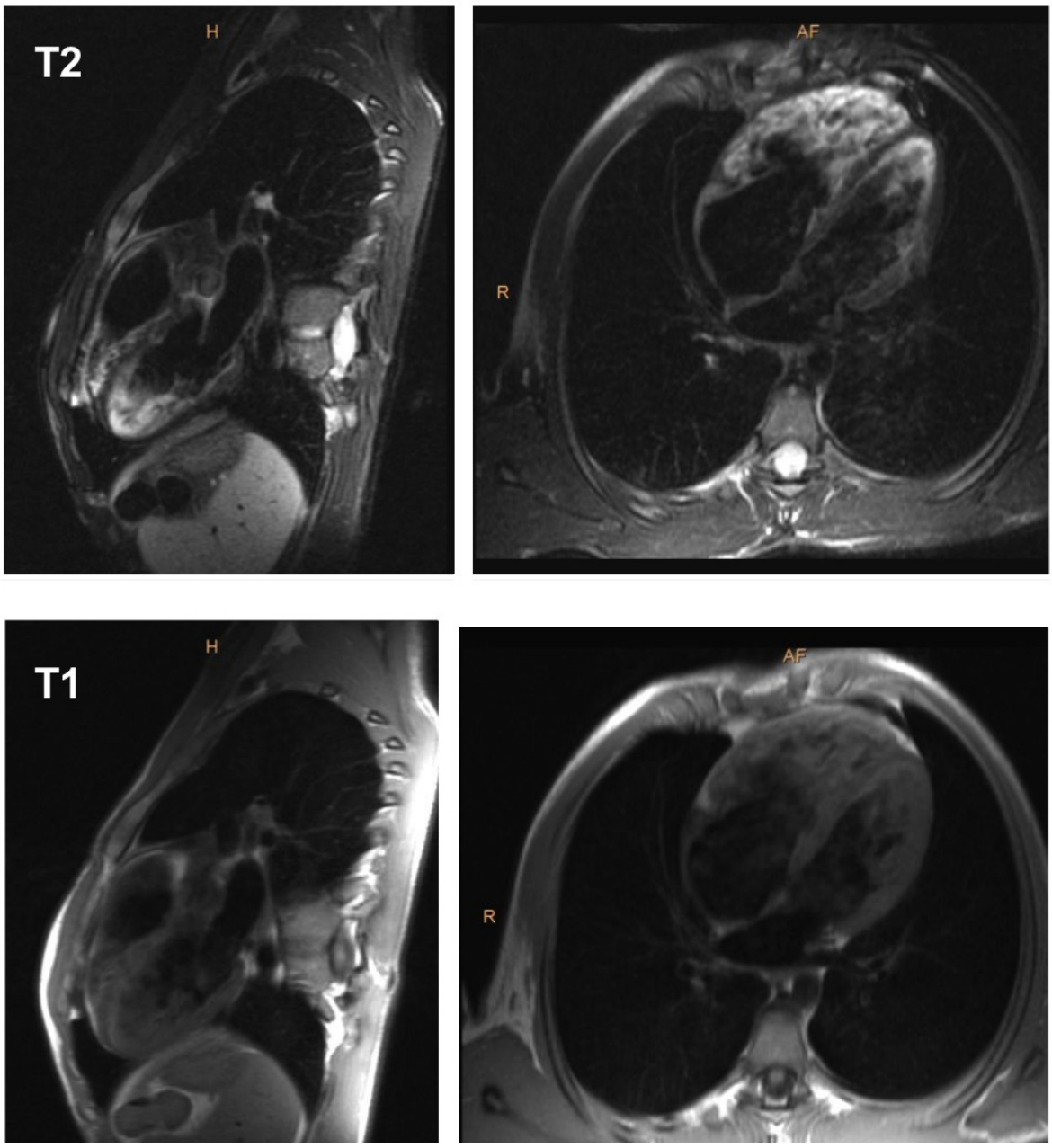

After contrast-injection, a diffuse LGE was showed on the RV wall, involving also the right side of interventricular septum; also LV LGE in the inferior wall was detected (Figure 18).

Figure 18. Post-contrast sequences. A: long axis views (2-chamber view on the right; 3-chamber view on the left) showing LGE (bright white signal) with epicardial distribution in the inferior wall, becoming transmural in the infero-lateral wall. B) In the short axis views is detectable the presence of massive LGE on RV (white wall); note the involvement of the right side of interventricular septum.

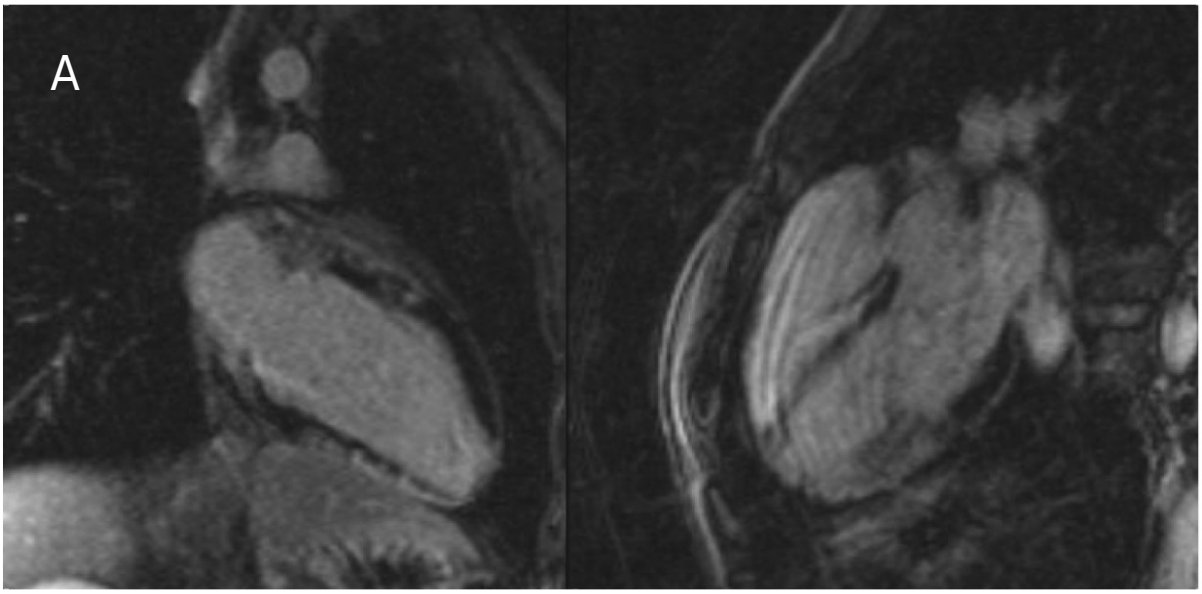

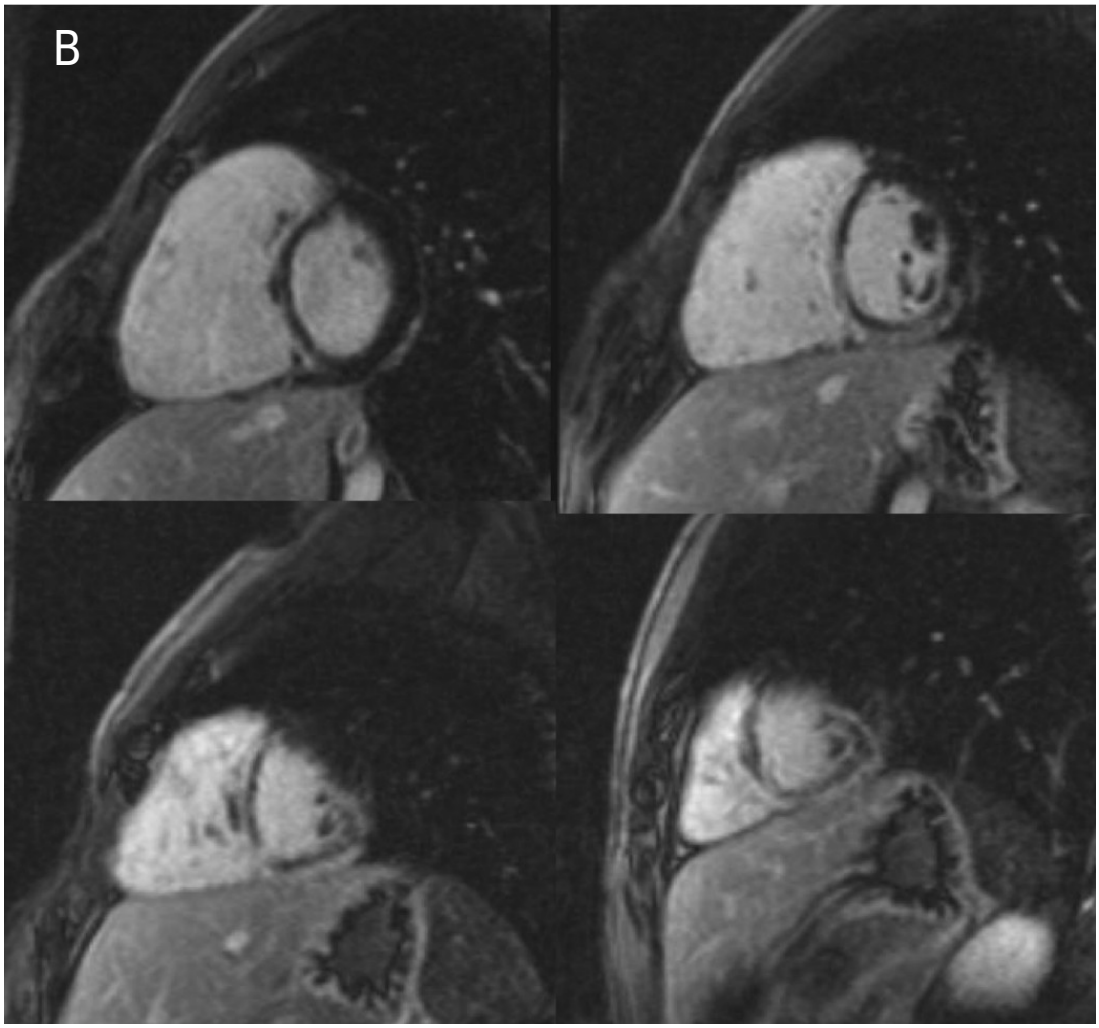

The morpho-functional and LGE findings compatible with a diagnosis of biventricular ARVC, or previous myocarditis. After CMR; LV and RV angiography was performed; no coronary lesions were found. A RV side EMB was also obtained. During the monitoring, ventricular arrhythmias with LBBB morphology were documented (Figure 19).

Figure 19. An ECG obtained by the continuous monitoring: ventricular arrhythmias with LBBB morphology.

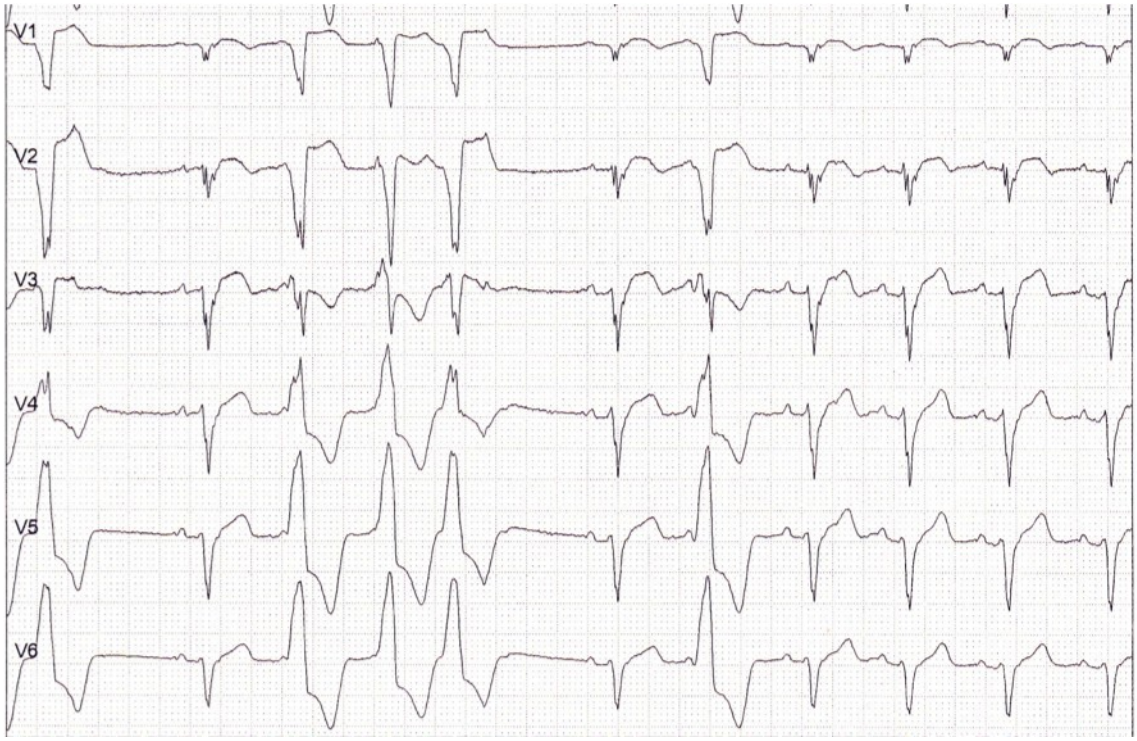

The EMB showed marked myocardial atrophy (residual myocites 60%) with fibrosis and without fatty replacement (Figure 20).

Figure 20. A) Panoramic view of RV endomyocardial biopsy samples. B) extensive cardyomyocyte injury with myocytolysis and vacuolization (insert), and early fibrous tissue repair.

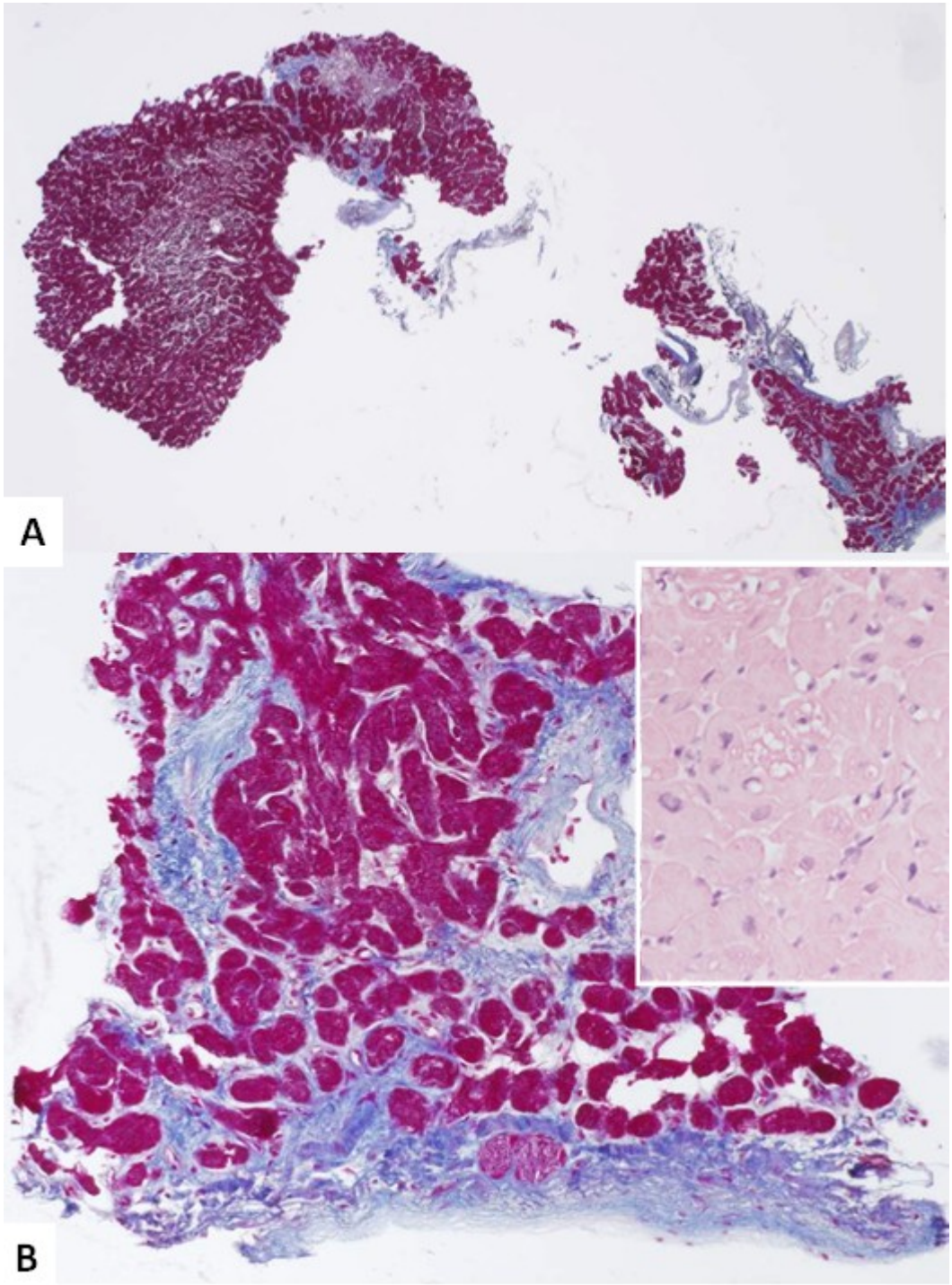

During the follow-up the patient was implanted with ICD and eight months later was underwent cardiac transplantation due to biventricular HF. Explanted heart examination confirmed CMR findings and extensive replacement-type fibrosis corresponding to RV LGE scar areas.

Study Population

In order to evaluate the relationship between ECG abnormalities and CMR 30 consecutive patients with diagnosis of ARVC fulfilling 1994 Task Force Criteria and recently modified 2010 criteria (20 males; 10 females; mean age 36 ± 15 years) findings were prospectively enrolled. On ECG evaluation, only 4 (13.3%) patients had a completely normal ECG; the majority of patients showed a pathological ECG (86.7%) including any ECG abnormalities (Table 13). By including only ECG abnormalities recognized in the current modified Task Force criteria, half of patients showed a positive ECG.

Repolarization abnormalities were described in 15/26 (57.6%): 8/26 (30.7%) showed ST segment elevation in right precordial leads; 8/26 (30.7%) T wave inversion in V1-V3 and the same proportion beyond V3. The minority of patients showed T wave inversion in lateral leads (2/26; 7.7%) and inferior leads (5/26; 19.2%).

Depolarization and conduction abnormalities were described in 13/26 (50%) of patients. The most important abnormalities in this group were low QRS voltage (12/26; 46.1%) and prolonged QRS duration (10/26; 38.5%).

Half of patient population showed positive SAECG (13/26).

Table 13. ECG Characteristics.

ECG Variable	N (%)
Normal ECG	**4 (13.3)**
ECG Abnormalities included in 2010 Modified Task Force Criteria	**15 (50)**
Abnormal ECG	**26 (86,7)**
Repolarization Abnormalities	15 (57.6)
➢ ST-segment elevation	8 (30.7)
➢ T wave inversion V1-V3	8 (30.7)
➢ T wave inversion beyond V3	8 (30.7)
➢ T wave inversion in lateral leads	2 (7.7)
➢ T wave inversion in inferior leads	5 (19.2)
➢ QTc Interval (ms)	424.0.3±23
Depolarization/Conduction Abnormalities	13 (50)
➢ Duration of QRS interval > 110 msec	10 (38.5)
➢ Epsilon wave	3 (11.5)
➢ RBBB	3 (11.5)
➢ Pathological Q wave in inferior leads	5 (7.7)
➢ Low QRS Voltage	12 (46.1)
➢ Poor R-wave progression	9 (34.6)
➢ Positive SAECG	13 (50)

ECG =electrocardiographic; RBBB = Right Bundle Branch Block; SAECG= signal averaged ECG.

The CMR findings were separately evaluated for morpho-functional abnormalities on cine images and tissue characterization findings on T1 spin-echo sequences with fat saturation and T1 inversion recovery post-contrast sequences.

Globally evaluated CMR scan was positive in all patients (30/30; 100%). Accordingly to cut-off defined in the Methods Section, an RV dilatation was found in 8/30 (30.7) patients; all patients showed cine abnormalities (in more than one region) mostly on the apex (90%), and inferior RV wall (83.3%). An RV thinning was found in 31/30 (70%). An LV morpho-functional involvement was found in 56.7% of subjects as for dilatation and dysfunction.

On T1 spin echo sequences after fat-saturation, a fatty infiltration of RV wall was detected in 20 (66.7%) patients, mostly in inferior (55.5%) and antero-lateral wall (44.4%). Epicardial fatty infiltration of LV walls was showed in 13/30 (43.3%) in more than two ventricular region, always including lateral wall.

Globally evaluated, ventricular LGE was detected in 22/30 (73.3%) of patients. A positive RV LGE was showed in 18/30 (60%) of patients, mostly on the apex (55.5%) and antero-lateral wall (38.8%). In all positive RV LGE regions, cine abnormalities such as akinesia or bulging were found.

A LV LGE involvement was found in 19/30 (63.3) subjects.

An exclusive RV LGE involvement was showed in only 2 patients (6.6%); 4/30 patients (13.3%) showed an isolated LV involvement. A biventricular LGE was detected in 16/30 (53.3%) of subjects.

The LV distribution was quite different from fatty infiltration (that was only epicardial): in the lateral and inferior wall LGE was present as an epicardial pattern, but in the other regions (septum, and anterior walls) LGE was showed in the half of cases as “mid-mural” location.

.

Table 14. CMR Characteristics.

CMR Variable	**N (%)**
Abnormal CMR	**30 (100)**
Morpho-functional CMR findings	
➢ RV dilatation	8 (30.7)
➢ RV cine abnormalities: - inflow - inferior - antero-lateral - outflow - apex	30 (100) 9 (30) 25 (83.3) 20 (66.7) 18 (60) 27 (90)
➢ RV thinning	21 (70)
➢ LV dilatation	17 (56.7)
➢ LV dysfunction	17 (56.7)
Fat infiltration	20 (66.7)
➢ RV fatty infiltration - inflow - inferior - antero-lateral - outflow - apex	18 (60) 4 (22) 10 (55.5) 8 (44.4) 3 (16.7) 9 (11.1)
➢ LV fatty infiltration - anterior - lateral - inferior - septum	13 (43.3) 2 (15.4) 13 (100) 1 (7.7) 1 (7.7)
LGE	22 (73.3)
➢ RV LGE - inflow - inferior - antero-lateral - out flow - apex	18 (60) 1 (5.5) 9 (50) 7 (38.8) 1 (5.5) 10 (55.5)
➢ LV LGE - anterior - lateral - inferior - septum	19 (63.3) 8 (42.1) 17 (89.5) 10 (52.6) 3 (15.8)
Only RV LGE	2 (6.6)
Only LV LGE	4 (13.3)
Biventricular LGE	16 (53.3)

CMR = cardiac magnetic resonance; RV = right ventricle; LV = left ventricle; LGE =late gadolinium enhancement.

Univariate Analysis

On univariate analysis by logistic regression the ECG determinants of LV dilatation on CMR were ST-segment elevation (p=0.047), T wave inversion on V1-V3 (p=0.047) and beyond V3 (p=0.014). On Univariate analysis by $\chi 2$ analysis even the presence of pathological Q waves in inferior leads was associate with LV dilatation (p=0.032).

Table 15. Determinants of **Left Ventricular Dilatation** on CMR.

Univariate Predictors				**Multivariate Predictors**		
Covariate	**HR**	**95% CI**	**p**	**HR**	**95% CI**	**p**
Gender	1.5	0.325-6.918	0.603	-	-	-
ST-segment elevation	6.429	1.026-40.261	**0.047**	23.197	1.699-316.655	**0.018**
T wave inversion V1-V3	0.156	0.025-0.974	**0.047**	0.087	1.2-111	**0.032**
T wave inversion beyond V3	17.2	1.794-166.6	**0.014**	-		
T wave inversion in inferior leads	3.00	0.616-14.617	0.174	-		
T wave inversion in lateral leads	1.615	-	1	-	-	-
Corrected QT interval	1.313	-	1	-	-	-
Duration of QRS interval > 110 msec	4.889	0.822-29.060	0.081	-	-	-
Epsilon wave	1.600	0.129-19.838	0.714	-	-	-
Complete RBBB	5.000	0.506-49.438	0.169	-	-	-
Pathological Q wave in inferior leads	1.740	-	1	-	-	-
Poor R-wave progression	0.938	0.194-4.522	0.936	-	-	-
Parietal block	6.545	0.677-63.330	0.105	-	-	-
Low QRS Voltage	6.545	0.677-63.330	0.105	-	-	-
SAECG	3.375	0.705-16.168	0.128	-	-	-

CMR: Cardiac Magnetic Resonance; RBBB: Right Bundle Branch Block; SAECG: Signal Average ECG; HR = hazard ratio.

On univariate analysis by logistic regression any ECG determinants of RV dilatation (p>0.05) were found.

Table 16. Determinants of **Right Ventricular Dilatation** on CMR.

Univariate Predictors				Multivariate Predictors		
Covariate	**HR**	**95% CI**	**p**	**HR**	**95% CI**	**p**
Gender	0.265	0.045-1.543	0.139	-	-	-
ST-segment elevation	2.7	0.448-16.255	0.278	-	-	-
T wave inversion V1-V3	2.7	0.448-16.255	0.278	-	-	-
T wave inversion beyond V3	0.622	0.099-3.923	0.614	-	-	-
T wave inversion in inferior leads	0.550	0.082-3.682	0.583	-	-	-
T wave inversion in lateral leads	4.846	-	0.999	-	-	-
Corrected QT interval	5.140	-	1	-	-	-
Duration of QRS interval > 110 msec	0.750	0.118-4.773	0.761	-	-	-
Epsilon wave	0	-	1	-	-	-
Complete RBBB	1.9	0.267-13.523	0.522	-	-	-
Pathological Q wave in inferior leads	0.792	0.074-8.518	0.847	-	-	-
Poor R-wave progression	0.313	0.032-3.068	0.318	-	-	-
Parietal block	0	-	1	-	-	-
Low QRS Voltage	0	-	1	-	-	-
SAECG	0.5	0.075-3.316	0.473	-	-	-

CMR: Cardiac Magnetic Resonance; RBBB: Right Bundle Branch Block; SAECG: Signal Average ECG; HR = hazard ratio.

On univariate analysis by logistic regression any ECG determinant of LV fatty infiltration (p>0.05) was found. On Univariate analysis by $\chi 2$ analysis ST segment elevation was associated with LV fatty infiltration (p=0.031). Other ECG abnormalities associated with LV fatty infiltration were epsilon wave (p=0.042) and low QRS voltage (p=0.002). (examples on Figure 21 and 22).

Table 17. Determinants of **Left Ventricular Fat Infiltration** on CMR.

Univariate Predictors				Multivariate Predictors		
Covariate	**HR**	**95% CI**	**p**	**HR**	**95% CI**	**p**
Gender	5.056	0.959-26.664	0.056	-	-	-
ST-segment elevation	9.333	0.968-90.029	**0.053**	-	-	-
T wave inversion V1-V3	1.515	0.286-8.032	0.625	-	-	-
T wave inversion beyond V3	0.286	0.059-1.375	0.118	-	-	-
T wave inversion in inferior leads	0.778	0.159-3.795	0.756	-	-	-
T wave inversion in lateral leads	0	-	0.999	-	-	-
Corrected QT interval	0	-	0.999	-	-	-
Duration of QRS interval > 110 msec	0.269	0.051-1.420	0.122	-	-	-
Epsilon wave	0	-	0.999	-	-	-
Complete RBBB	0.150	0.014-1.560	0.112	-	-	-
Pathological Q wave in inferior leads	0.222	0.020-2.451	0.219	-	-	-
Poor R-wave progression	0.122	0.019-0.771	0.025	-	-	-
Parietal block	0.321	0.048-2.133	0.240	-	-	-
Low QRS Voltage	0	-	0.999	-	-	-
SAECG	0.260	0.51-1-313	0.103	-	-	-

CMR: Cardiac Magnetic Resonance; RBBB: Right Bundle Branch Block; SAECG: Signal Average ECG; HR = hazard ratio.

On univariate analysis by logistic regression any ECG determinant of RV fatty infiltration ($p>0.05$) was found. By $\chi 2$ analysis Univariate analysis no ECG abnormalities were associated with RV fatty infiltration.

Table 18. Determinants of **Right Ventricular Fat Infiltration** on CMR.

Univariate Predictors				Multivariate Predictors		
Covariate	**HR**	**95% CI**	**p**	**HR**	**95% CI**	**p**
Gender	0.875	0.182-4.212	0.868	-	-	-
ST-segment elevation	0.975	0.182-5.235	0.976	-	-	-
T wave inversion V1-V3	0.975	0.182-5.235	0.976	-	-	-
T wave inversion beyond V3	0.469	0.093-2.369	0.359	-	-	-
T wave inversion in inferior leads	0.333	0.062-1.779	0.199	-	-	-
T wave inversion in lateral leads	1.5	0.084-26.855	0.783	-	-	-
Corrected QT interval	0	-	1	-	-	-
Duration of QRS interval > 110 msec	0.750	0.144-3.903	0.732	-	-	-
Epsilon wave	0.8	0.064-10.014	0.863	-	-	-
Complete RBBB	1.111	0.155-7.974	0.917	-	-	-
Pathological Q wave in inferior leads	0.5	0.045-5.514	0.571	-	-	-
Poor R-wave progression	1.486	0.299-7.389	0.629	-	-	-
Parietal block	1.875	0.305-11.524	0.497	-	-	-
Low QRS Voltage	0.260	0.026-2.593	0.251	-	-	-
SAECG	0.292	0.056-1.525	0.144	-	-	-

CMR: Cardiac Magnetic Resonance; RBBB: Right Bundle Branch Block; SAECG: Signal Average ECG; HR = hazard ratio.

On univariate analysis by logistic regression the only ECG determinant of LV LGE on CMR was the ST-segment elevation (p=0.035).

Table 19. Determinants of **Left Ventricular LGE** on CMR.

Univariate Predictors				Multivariate Predictors		
Covariate	**HR**	**95% CI**	**p**	**HR**	**95% CI**	**p**
Gender	1.750	0.151-20.231	0.654	-	-	-
ST-segment elevation	16	1.216-210.587	**0.035**	18	1.194-271.461	**0.037**
T wave inversion V1-V3	0.933	0.078-11.177	0.957	-	-	-
T wave inversion beyond V3	0.458	0.040-5.256	0.531	-	-	-
T wave inversion in inferior leads	1.429	0.161-12.701	0.749	-	-	-
T wave inversion in lateral leads	4.039	-	0.999	-	-	-
Corrected QT interval	-	-	-	-	-	-
Duration of QRS interval > 110 msec	0.571	0.049-6.606	0.654	-	-	-
Epsilon wave	0	-	0.999	-	-	-
Complete RBBB	0	-	0.999	-	-	-
Pathological Q wave in inferior leads	1.429	0.161-12.701	0.749	-	-	-
Poor R-wave progression	0.722	0.062-8.464	0.796	-	-	-
Parietal block	0	-	0.999	-	-	-
Low QRS Voltage	0	-	0.999	-	-	-
SAECG	0.8	0.091-7.002	0.840	-	-	-

CMR= Cardiac Magnetic Resonance; RBBB= Right Bundle Branch Block; SAECG= Signal Average ECG; LGE= Late Gadolinium Enhancement; HR = hazard ratio.

On univariate analysis by logistic regression, any ECG determinant of RV LGE ($p>0.05$) was found.

Table 20. Determinants of **Right Ventricular LGE** on CMR.

Univariate Predictors				Multivariate Predictors		
Covariate	**HR**	**95% CI**	**p**	**HR**	**95% CI**	**p**
Gender	0.256	0.033-2.022	0.196	-	-	-

ST-segment elevation	2.333	0.284-19.72	0.430	-	-	-
T wave inversion V1-V3	0	-	0.999	-	-	-
T wave inversion beyond V3	3	0.39-23.072	0.291	-	-	-
T wave inversion in inferior leads	0.250	0.023-2.757	0.258	-	-	-
T wave inversion in lateral leads	0	-	0.999	-	-	-
Corrected QT interval	-	-	-	-	-	-
Duration of QRS interval > 110 msec	0.393	0.036-4.276	0.443	-	-	-
Epsilon wave	0	-	0.999	-	-	-
Complete RBBB	1.250	0.101-15.499	0.862	-	-	-
Pathological Q wave in inferior leads	0	-	0.999	-	-	-
Poor R-wave progression	5.250	0.639-43.138	0.123	-	-	-
Parietal block	0	-	0.999	-	-	-
Low QRS Voltage	0.875	0.75-10.210	0.915	-	-	-
SAECG	1.333	0.176-10.120	0.781	-	-	-

CMR: Cardiac Magnetic Resonance; RBBB: Right Bundle Branch Block; SAECG: Signal Average ECG; LGE: Late Gadolinium Enhancement; HR = hazard ratio.

On univariate analysis by logistic regression, the only ECG determinant of Biventricular LGE on CMR was ST-segment elevation (p=0.038).

Table 21. Determinants of **Biventricular LGE** on CMR.

Univariate Predictors				**Multivariate Predictors**		
Covariate	**HR**	**95% CI**	**p**	**HR**	**95% CI**	**p**
Gender	0.606	0.097-3.788	0.592	-	-	-

ST-segment elevation	9.333	76.690	**0.038**	9.33	1.136-76.690	**0.038**
T wave inversion V1-V3	0.367	0.034-3.908	0.406	-	-	-
T wave inversion beyond V3	1.250	0.205-7.615	0.809	-	-	-
T wave inversion in inferior leads	1	0.160-6.255	1	-	-	-
T wave inversion in lateral leads	0	-	0.999	-	-	-
Corrected QT interval	-	-	-	-	-	-
Duration of QRS interval > 110 msec	0.667	0.097-4.579	0.680	-	-	-
Epsilon wave	0	-	0.999	-	-	-
Complete RBBB	-	-	-	-	-	-
Pathological Q wave in inferior leads	0	-	0.999	-	-	-
Poor R-wave progression	2.250	0.345-14.694	0.397	-	-	-
Parietal block	0	-	0.999	-	-	-
Low QRS Voltage	0.5	0.045-5.514	0.571	-	-	-
SAECG	1.167	0.191-7.116	0.867	-	-	-

CMR: Cardiac Magnetic Resonance; RBBB: Right Bundle Branch Block; SAECG: Signal Average ECG; LGE: Late Gadolinium Enhancement; HR = hazard ratio.

Multivariable Analysis

On multivariable logistic regression, the ECG variables independently related to LV dilatation remains ST segment elevation (p=0.018; OR 23.197; 95% IC 1.699-316.655) and T wave inversion in V1-V3 (p=**0.032**; OR 0.087; 95% IC 1.2-111).

On multivariable logistic regression, the only ECG variable independently related to LV LGE remains ST segment elevation (p=**0.037**; OR 18; 95% IC 1.194-271.46).

On multivariable logistic regression, the only ECG variable independently related to Biventricular LGE remains ST segment elevation (p=**0.038**; OR 9.33; 95% IC 1.136-76.690).

Figure 21. A case of a 26-year-old male with an episode of ventricular tachycardia with LBBB morphology and subsequent diagnosis of ARVC. On the ECG an inversion T-wave beyond V3 and in inferior leads is present. CMR (T1 IR post contrast) shows a biventricular ARVC with epicardial LGE on LV antero-lateral wall. SAECG was also positive.

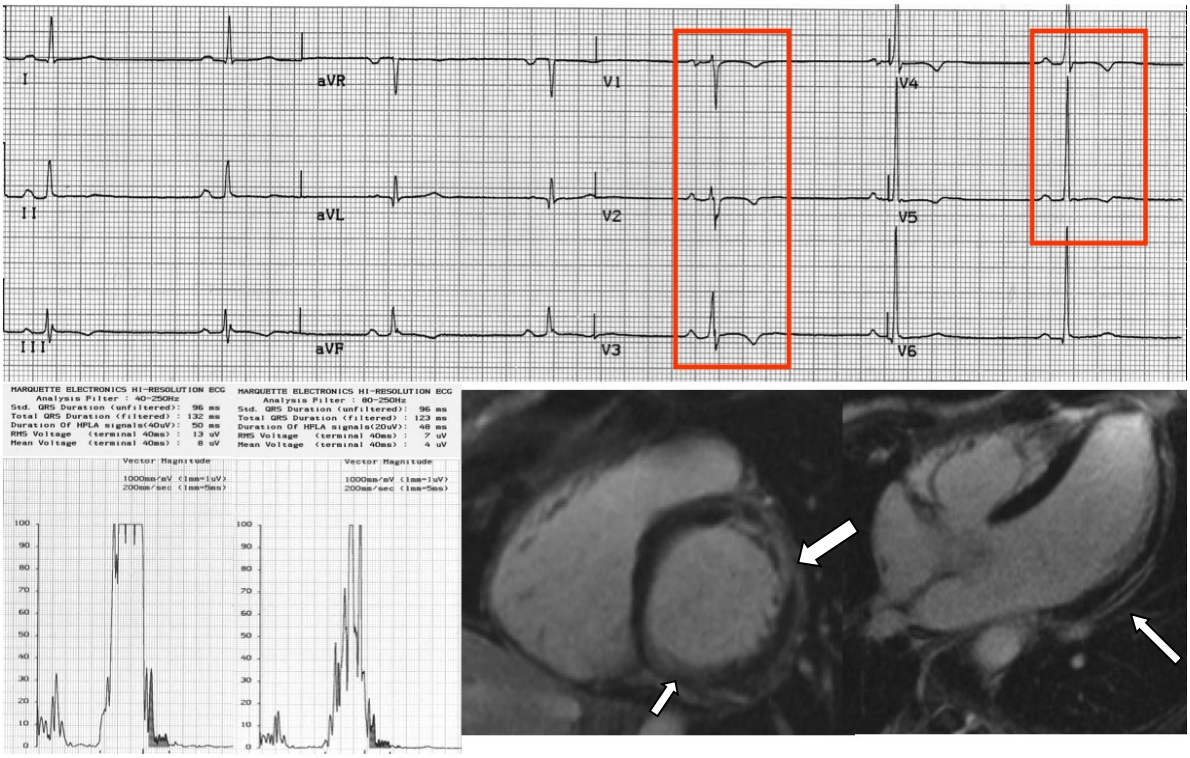

Figure 22. A case of a 32-year-old female with family history for sudden death and final diagnosis of ARVC. At ECG, an epsilon wave is present (red circle). CMR shows a fibro-fatty scar on the lateral free-wall (High T1 signal on spin-echo on the left; T1 IR post contrast image on the right.

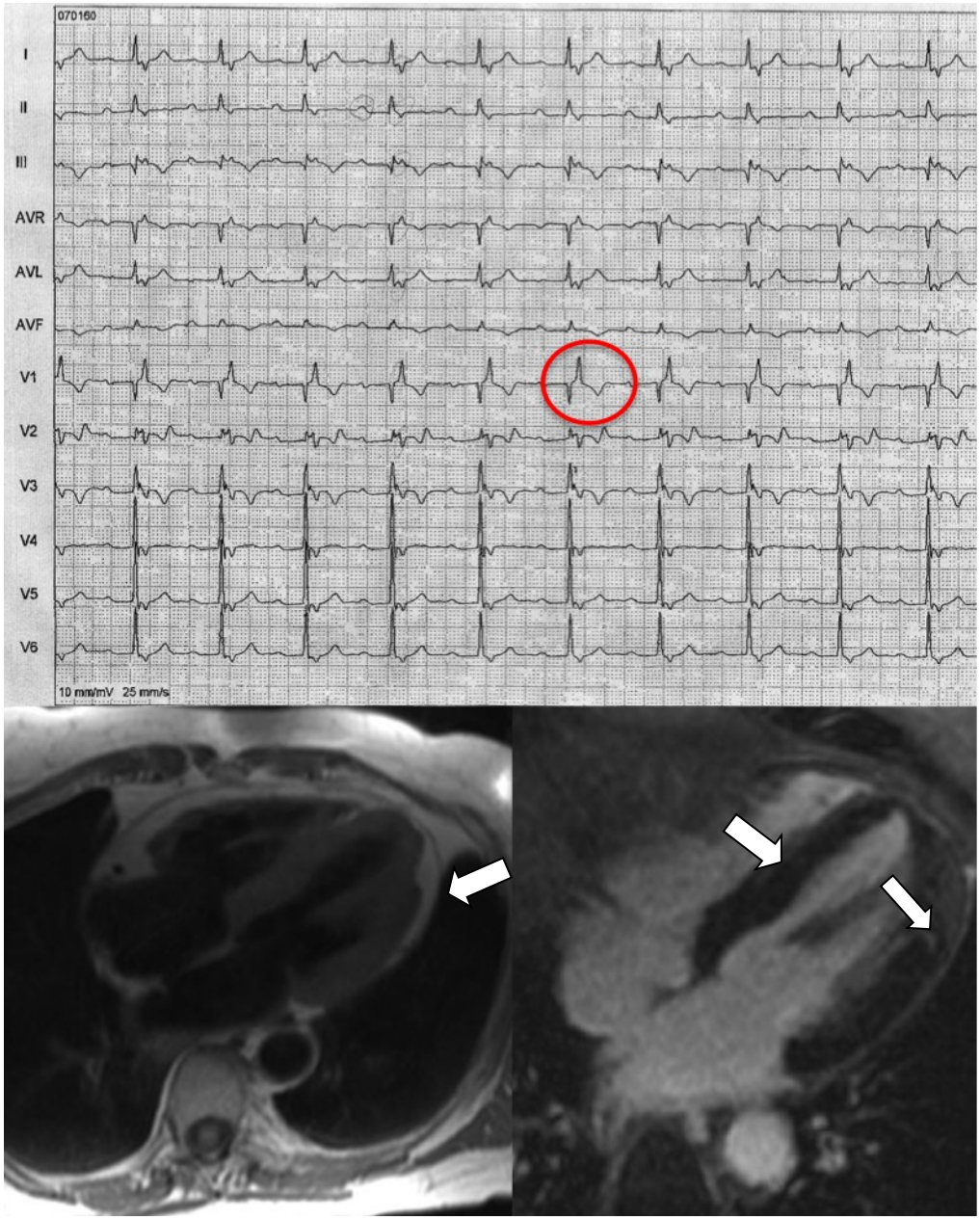

Comparison between electroanatomic scar detected by endocardial voltage mapping and LGE scars on CMR examination

Study Population

The study population included 23 consecutive patients (16 males and 7 females; mean age 38±12 yrs), whose the clinical characteristics are summarized in Table 22. Eight patients had a family history of premature (age<40 years) sudden death. Fourteen patients experienced symptoms such as palpitations (10 patients), syncope (2 patients) and pre- syncope (2 patients). On basal ECG, 7 (30%) patients showed a QRS complex prolongation (≥ 110 ms), 15 patients (65%) T wave inversion in the precordial leads and 9 (39%) patients showed T waves inversion in inferior leads. Late potentials on SAECG were detected in 13 (57%) patients. All patients had ≥ 1 episode of VT with a LBBB, either sustained (22%) or non- sustained (78%). Morpho-functional RV abnormalities, either global or regional, were observed at echocardiography/angiography in all patients (Table 18). None had evidence of pulmonary hypertension, congenital heart disease or CAD.

Table 22. Demographics and Instrumental Characteristics of 23 ARVC patients.

Variables	**N**
Age (yrs)	38±12
Males, n (%)	16 (70)

Family history for SD, n (%)	8 (35)
Clinical Symptoms	
Cardiac arrest, n (%)	0
Palpitations, n (%)	10 (43)
Syncope, n (%)	2 (9)
Pre-syncope, n (%)	2 (9)
ECG	
QRS duration≥110ms (V1 to V2), n (%)	7 (30)
TWI V1 to V2/V3, n (%)	15 (65)
TWI beyond V3, n (%)	11 (48)
TWI inferior leads, n (%)	9 (39)
SAECG	
Late potentials, n (%)	13 (57)
Ventricular Arrhythmias	
Sustained VT, n (%)	5 (22)
Non-sustained VT, n (%)	18 (78)
Electrophysiological Findings	
EPS VT inducibility	13 (56)
VT cycle length (mean) (ms)	353±68 ms
Acute success of catheter ablation	9/13 (69)
Angiography	
RV dilatation/dysfunction, n (%)	16 (70)
RV wall motion abnormalities, n (%)	14 (61)

Values are expressed as n (%). ARVC = Arrhythmogenic Right Ventricular Cardiomyopathy; SD = sudden death; ECG = electrocardiogram; TWI = T wave inversion; SAECG = signal-averaged electrocardiogram; VT = ventricular tachycardia; RV = right ventricular.

Endocardial Voltage Mapping

The mean number of RV sites sampled by EVM was 172±19. Twenty-one of 23 (91.3%) ARVC patients had an abnormal RV EVM showing ≥1 (mean, 2.29±0.6) low voltage area (electroanatomic scars; "EAS"). Low-voltage areas were sharply demarcated and typically surrounded by a border zone with reduced signal amplitudes (0.5 to 1.5 mV), which merged into normal myocardium (>1.5 mV) (Figure 13). A total of 45 RV EAS were identified in these patients, which involved the following region (Table 23): 17 (38%) in the infero-basal region, 12 (26.6%) in the antero-lateral region, 8 (17.7%) in the RVOT and 8 (17.7%) in the apex. The RV side of septum was spared in all patients.

No patients from control group showed RV EAS by EVM analysis.

Table 23. Regional analysis of RV Scars: comparison between EVM and CMR.

RV Region	EAS (n=45)	LGE scars (n=23)	Mismatch
Infero-basal, n (%)	17 (38)	4 (17.4)	13
Antero-lateral, n (%)	12 (26.6)	9 (39.1)	3
RVOT, n (%)	8 (17.7)	4 (17.4)	6*
Apex, n (%)	8 (17.7)	6 (26.1)	2

RV = right ventricular; EAS = electroanatomic scar; RVOT = right ventricular outflow tract; CMR = contrast-enhanced cardiac magnetic resonance; LGE = late gadolinium enhancement.

* On Contrast CMR, 2 RV LGE scars localized on RVOT were not confirmed by EVM with corresponding EAS.

Cardiac Magnetic Resonance

Findings of cine CMR and tissue characterization study are reported in Table 24. All patients had global and/or segmental RV dilatation/dysfunction, which was associated with wall thinning in 15 (65%) patients. A LV dilatation/dysfunction was demonstrated in 13 (57%)

patients. Spin-echo sequences, with and without fat suppression, showed fatty infiltration of the RV wall in 11 (47.8%) patients and of the LV free wall in 2 patients (8.7%).

Right ventricular LGE scars. RV LGE was found in 9 of 23 (39%) patients (Table 23 and Table 25). A total of 23 RV LGE scars were identified: 4 (17.4%) in the infero-basal region, 9 (39.1%) in the antero-lateral region, 4 (17.4%) in the RVOT region and 6 (26.1%) in the apex. Affected regions showed an abnormal motion on cine images in all patients. The 6 patients with diffuse RV involvement (>2 RV DCE scar regions) had a significantly lower RV ejection fraction (36±3% vs 39±2%; p= 0.03), compared to those with segmental RV disease (≤ 2 RV DCE scar regions). The interobserver and intraobserver reproducibility for RV LGE was 95% and 90%, respectively.

Left ventricular LGE scars. LV LGE was found in 14 of 23 patients (61%), either in the form of isolated-LV involvement (9 patients) or in combination with RV involvement (5 patients). LV LGE involved the subepicardial and/or mid-wall layers of the anterolateral (10 patients), inferolateral (9 patients), anteroseptal (2 patients), and posteroseptal (1 patient) regions. Overall, any ventricular LGE scar was detected in 78% of ARVC patients.

Control Group. Controls did not show evidence of LGE on the RV, LV, and septal myocardium.

Correlation of results. RV scars were detected in 21 patients (91%) by EVM versus 9 (39%) by CMR (p = 0.001), with a total of 45 EAS versus 23 LGE scars. Topographic comparison between EVM and CMR findings showed a mismatch in 24 RV scar regions, with 22 EAS not confirmed by LGE (3 in antero-lateral region, 2 on apex, 4 in RVOT and 13 in the infero-basal walls), and 2 LGE scars (both in the RVOT) undetectable by EVM (see an example of concordance on Figure 23 and a case of mismatch on Figure 24). These latter RVOT scars were evidenced in one patient with isolated RVOT LGE and another patient with multiregional RV lesions, which also involved the lateral and the apical wall by both CMR and EVM.

Left ventricular LGE was observed in 9 of the 12 (75%) patients who showed an abnormal RV EVM, but normal RV CMR.

Table 24. Morpho-functional CMR characteristics of 23 patients.

RV findings	
RVEDV, (ml/m^2), mean ± SD	125 ± 8
RVEF, %, mean ± SD	37 ± 7
RV aneurysms, n (%)	15 (65.2)
Akinesia/dyskinesia, n (%)	23 (100)
Intramyocardial fat	11 (47.8)
LV findings	
LVEDV, (ml/m^2), mean ± SD	87 ± 8
LVEF, %, mean ± SD	50 ± 8
LV aneurysms, n (%)	1 (4.3)
Akinesia/dyskinesia, n (%)	1 (4.3)
Intramyocardial fat	2 (8.7)

Values are expressed as n (%) or mean ± SD. CMR = Cardiac magnetic resonance; RV = right ventricular; RVEDV = right ventricular end-diastolic volume; RVEF = right ventricular ejection fraction; LV = left ventricular; LVEDV = left ventricular end-diastolic volume; LVEF = left ventricular ejection fraction.

Table 25. Contrast CMR: overall LGE scar for 23 ARVC patients.

RV Region	**ARVC (23 subjects)**
RV LGE, n (%)	**9 (39)**
Infero-basal, n (%)	4 (44)
Antero-lateral, n (%)	9 (100)
RVOT, n (%)	4 (44)
Apex, n (%)	6 (67)
Biventricular involvement, n (%)	**5 (22)**
Only LV LGE, n (%)	**9 (39)**
Overall LGE, n (%)	**18 (78)**

RV = right ventricular; LV = left ventricular; RVOT = right ventricular outflow tract; LGE = late gadolinium enhancement

The k agreement test demonstrated a low concordance between EVM and CMR (k = 0,026), either overall or specific, for detection of RV scar regions, with the exception of the apical region for which there was a moderate agreement (k = 0,444) (Table 25). P value was not significant for all k square test.

Table 26. Agreement analysis for detection of RV scars by EVM versus LGE.

RV Regions	**k values**
Overall	k = 0.026 SE for k=0 0.118; SE for k≠0 0.115
RVOT region	k = 0.021 SE for k=0 0.206; SE for k≠0 0.208
Apical region	k = 0.444 SE for k=0 0.217; SE for k≠0 0.209
Antero-lateral region	k = 0.054 SE for k=0 0.214; SE for k≠0 0.214
Infero-basal region	k = - 0.121 SE for k=0 0.124; SE for k≠0 0.145

EAS = electroanatomic scar; RV = right ventricular; RVOT = right ventricular outflow tract; LGE = late gadolinium enhancement.

Endomyocardial Biopsy

Endomyocardial biopsy was obtained in 16 cases (16/23; 70%), including all patients with LV LGE involvement for differential diagnosis with myocarditis and sarcoidosis. In all 16 patients, EMB demonstrated a diagnostic amount of residual myocites (<60%) and fibrofatty replacement, in the absence of histological features of non caseous granulomatous and/or giant cell myocarditis (a case of correlation between EVM scars and EMB is showed in Figure 25).

Figure 23. Representative cases of concordance between EVM and CMR.

Top: (A) Antero-posterior view the RV endocardial voltage mapping (EVM) showing a large electro-anatomic scar (EAS) involving almost completely the RV free wall. (B) Four-chamber view of contrast-enhanced CMR confirms the widespread RV delayed contrast enhancement (LGE) with septal involvement. Bottom: (C) Right anterior oblique view of EVM showing EASs (red indicates < 0.5 mV) in the RV infero-basal region and outflow tract. (D) Basal short axis view of CMR showing LGE in the RV infero-basal wall and outflow tract (white arrows); note that LGE also involves the subepicardial layer of the inferior LV free wall (white asterisk).

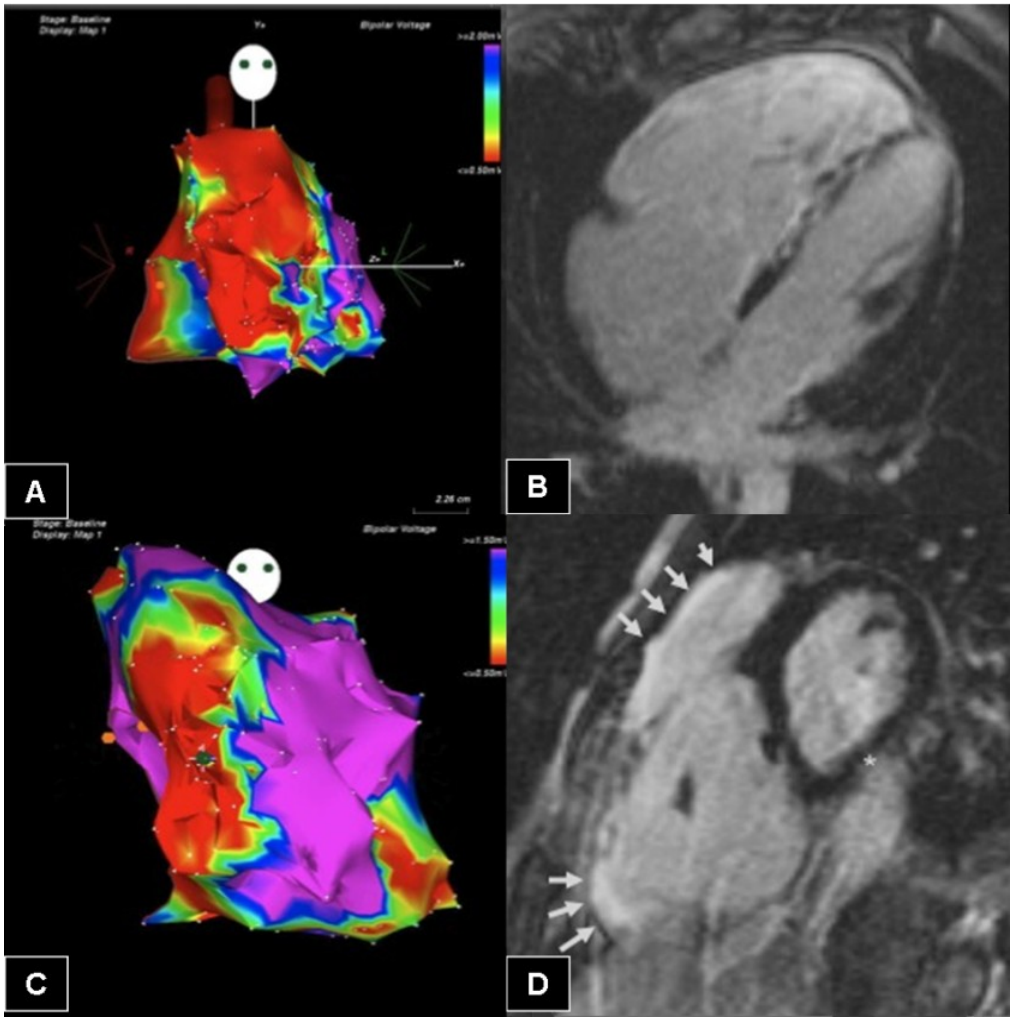

Figure 24. Representative cases of mismatch between EVM and CMR

Top: (A) Lateral view of the RV endocardial voltage mapping (EVM) showing electro-anatomic scar (EAS) in the RV infero-basal region and outflow tract. (B) Basal short axis view of CMR shows no RV delayed contrast enhancement (LGE), whereas a gadolinium scar is visible in the LV infero-septal region (white arrows). Bottom: (C) Lateral view of EVM showing a large EAS affecting the infero-basal, antero-lateral and, part of, the RV outflow tract region. (D) Basal short axis view of CMR shows neither RV nor LV LGE.

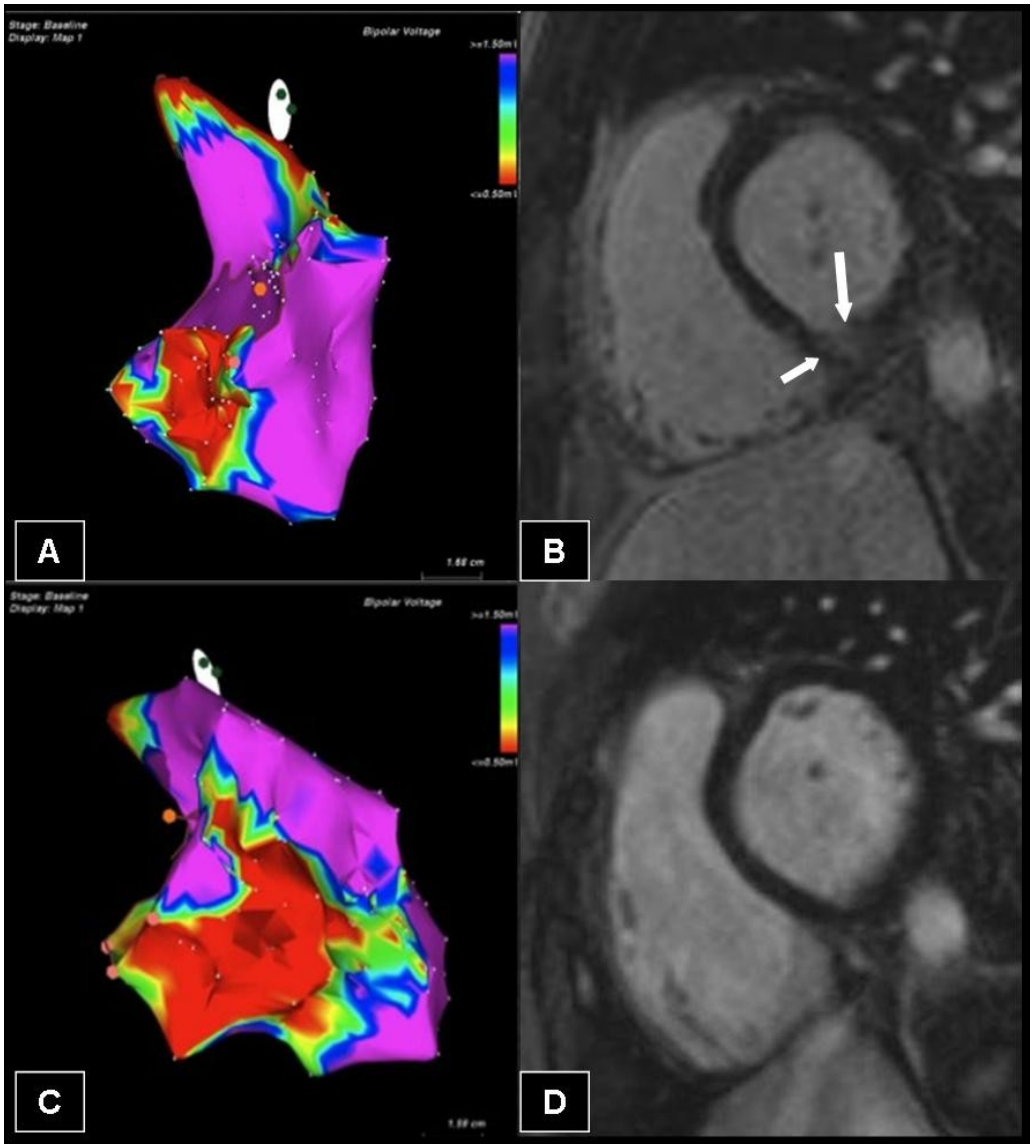

Figure 25. Comparison between EVM and EMB. A) an antero-posterior EVM view with low voltage areas in the infero-basal, antero-lateral walls and RVOT (red regions). B) EMB demonstrated a diagnostic amount of residual myocites (<60%) and fibrofatty replacement, in the absence of histological features of non caseous granulomatous and/or giant cell myocarditis.

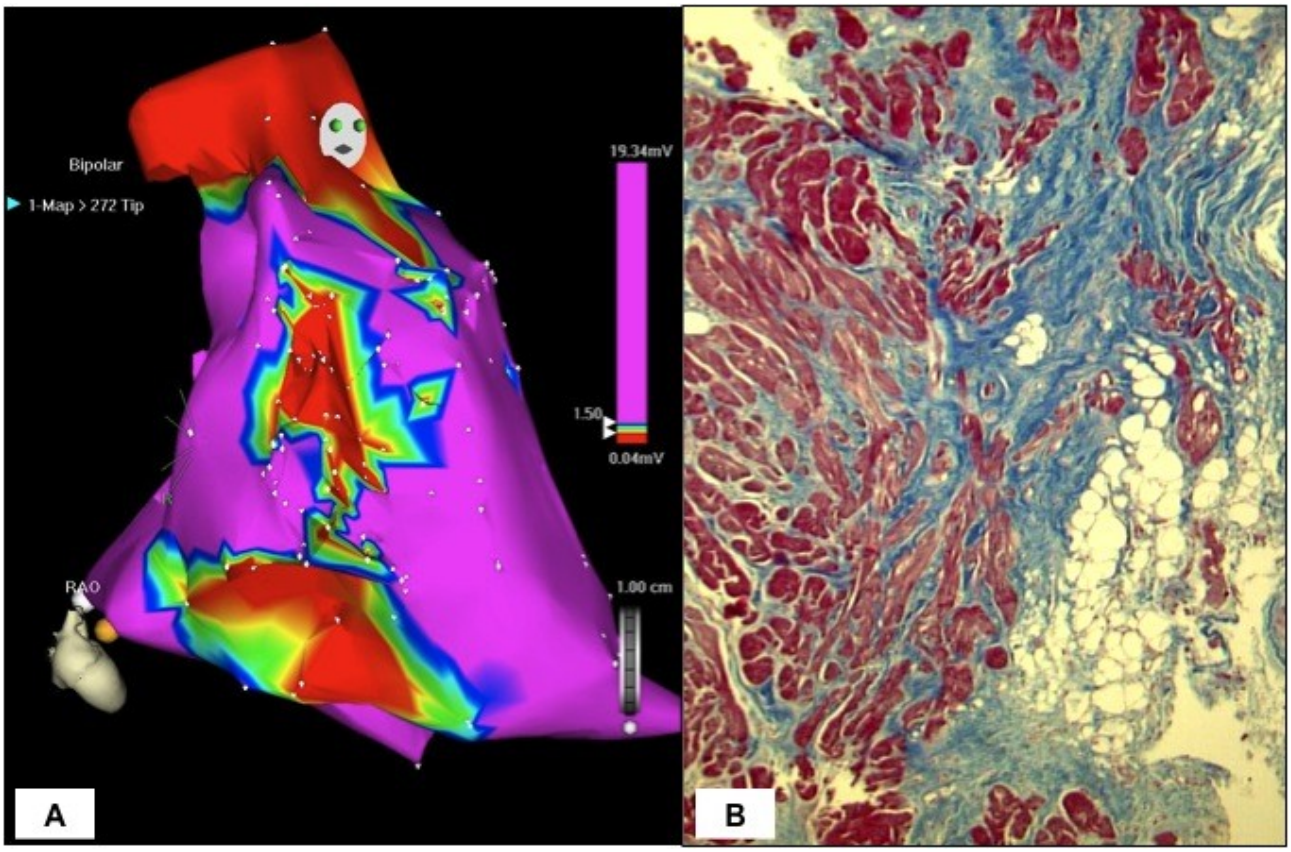

DISCUSSION

The major findings of this PhD thesis is the demonstration of the possibility to assess the full spectrum of morpho-functional abnormalities, including tissue characterization, in non-ischemic cardiomyopathies such as DCM and ARVC.

Moreover, LGE CMR is useful for prognostic arrhythmic stratification both in DCM and ARVC. The comparison of LGE CMR with clinical, ECG, endocardial voltage mapping and biopsy/cardiac specimens offers the possibility to better understand the real significance of LGE so far defined only “tout court” as fibrosis on the basis of post-infarction scar studies.

Clinical and prognostic significance of late enhancement in dilated cardiomyopathy

The structural and functional abnormalities in DCM are well shown by CMR, and changes over time, during follow-up with or with treatment, can be monitored serially. However, in patients presenting with LV dilatation, as the cohort of patients here reported, the main issue is to differentiate the DCM from the ischemic aetiology. The results of our series patients with DCM demonstrate that CMR with LGE analysis allows us to distinguish between patients with “non-ischemic” true DCM, in whom LGE is absent or atypical, and those with ischemic “DCM” due to previous myocardial infarction, in whom LGE is always present. However, in patients with CAD, but without previous infarction, LGE is not systematically detected, thus making the differentiation from DCM potentially difficult.

A study of patients labelled as having “DCM” who had normal coronary angiography showed no LGE in 59% and patchy or circumferential LGE in the midwall in 28%, thus excluding myocardial infarction as the cause of ventricular dysfunction (71). The final group of 13% had LGE compatibly with extensive myocardial infarction, which suggested that these patients had been incorrectly assigned to DCM after “normal” coronary angiography, but they were probably cases with coronary recanalization after myocardial infarction and untreated ventricular remodelling.

The major finding of our Research in DCM, relates to the prognostic significance of LGE and its total amount, beyond the classical EF, as an independent predictor for adverse events and mostly for ventricular arrhythmic events. Recent study investigated partially the role of LGE as a predictor of events, but without a specific differentiation against potential lethal ventricular arrhythmias. In 2008 Wu et al. (115) studied 65 patients with DCM referred to ICD implantation, with an EF $\leq$ 35%, and demonstrated that the presence of LGE on CMR, irrespective of extent or segmental pattern, was independently associated with an adverse cardiac prognosis (even after controlling for LV volume, mass, or EF as well as NYHA functional class), for an index

composite of cardiac event compared with those without LGE. In this group of patients referred for ICD the prevalence of LGE in DCM was 42%. A similar proportion was found by Assomull et al (80) who reported an incidence of 35%. More recently, Lehrke et al (116) in 184 patients with chronic heart failure found the presence of LGE in 39% of the patients. In our study the prevalence of LGE was 60.3%. This higher proportion can be explained by the fact that our population includes patients with LV dilatation detected by echo, with/without severe systolic dysfunction, and patients referred to a Tertiary Centre with special interest to heart transplantation.

Moreover, we included in the analysis a “gray” pattern, a pattern defined by the presence of an intermediate signal intensity. This pattern was present in 22 patients. By excluding those from the global LGE analysis, the prevalence of LGE decreases to 49.5%, but it is still higher than previously reported in smaller and selected patients population.

The most important findings of our study, remains the additional value of LGE detection in the arrhythmic risk stratification, moreover, the multivariable analysis showed that the presence of LGE and its extent were the strongest predictors of ventricular arrhythmic events. This observation is important since the few studies previously cited on the prognostic significance of LGE so far, used combined end-point, and not different single end point in a similar unselected population, as in our study protocol. Lehrke et al (116) found that a LGE percentage of 4.4% of LV mass was the optimal discriminator for composite end point. In our series, the value of 3.5% was the best predictor of ventricular arrhythmic events.

The reason why the presence of LGE an independent predictor for adverse arrhythmic outcome, (besides others such as EF), may be the promotion of re-entry mechanisms by replacement-type fibrosis, causing malignant arrhythmias. Areas of fibrosis detected by CMR have been identified as substrates for inducible VT in patients with ischemic heart disease (117) and, more recently, in patients with DCM (118). In addition to the impact on the electrophysiological properties of the heart, increasing amounts of fibrosis also lead to elasto-mechanical alterations, with a loss of ventricular compliance and subsequent increases in filling pressure, promoting the development of pulmonary and peripheral oedema.

As reported by previous studies, there is not a typical LGE pattern as a predictor of clinical

events. In our series, only the “gray” pattern was associated with ventricular arrhythmias, but was not confirmed on multivariable analysis. At this point, it is not clear whether the various LGE patterns have different underlying causes or even represent different aetiologies of DCM. Of note, the majority of patients in which a pulmonary hypertension on invasive measurement by right side catheterization was documented, showed a LGE on RV-LV junctions. This finding supports the hypothesis that LGE at this level represents the hemodynamic adaptation of ventricles to increased pressures in pulmonary circulation. In fact, it has been demonstrated that patients with pulmonary idiopathic hypertension also show this LGE junctional pattern on CMR (119). So far, this finding has been described only in pre-capillary hypertension: the presence of LGE junctional pattern associated with other typical LGE DCM pattern in post-capillary hypertension (as documented in our series) makes this pattern not specific for idiopathic hypertension, but for all conditions of pulmonary hypertension.

Future studies focused on the relationship between genotype and phenotype in DCM patients are needed to better define the prognostic role of CMR.

Clinical and prognostic significance of late enhancement in Arrhythmogenic Right Ventricular Cardiomyopathy

Tissue abnormalities underling ECG pattern

Arrhythmogenic right ventricular cardiomyopathy (ARVC) is predominantly a genetically determined heart muscle disorder that is characterized pathologically by fibrofatty replacement of the RV myocardium (48). Even if ECG abnormalities are present in the majority of cases, the presence of a normal 12-lead ECG should not preclude the diagnosis of ARVC.

Traditional ECG findings associated with ARVC include repolarization and depolarization/conduction abnormalities. In our research we found that globally evaluation of ECG, in this selected population able to perform a complete CMR protocol, showed pathological findings in the majority of patients (86.7%). However, looking at the ECG abnormalities included in the Task Force criteria only half of patients showed a pathological ECG. This discrepancy may be explained by the different phase and severity of forms, but its may be due

even to other tissue abnormalities unrecognized by traditional instrumental examination. Regarding tissue characterization, CMR offers the possibility to detect fibro-fatty infiltration not only in the RV, but even in the LV where the typical mid-mural and epicardial distribution does not affect the contractility thus explaining its supporting to 2-D echo assessment of the LV involvement. Of note the ECG determinants, on univariate analysis, of LV LGE and LV fatty infiltration is the ST-segment elevation, but after multivariable analysis the only determinants remains the LGE, interpreted as replacement fibrosis. The ST segment observed in our patients is very different form the coved-type S elevation typical for Brugada syndrome and has been described in a cohort of ARVC patients. Nava ad co-workers (120) described this ST segment elevation similar to acute myocardial infarction in 34/136 patients affected. Five subjects had an ST segment elevation greater than 2 mm while an ST elevation less than 2 mm was present in the other 29 patients. Thereafter, Peters et al (121) observed a prevalence of ST segment elevation of 18%, but without negative arrhythmogenic prognostic significance. Even Turrini et al (43) demonstrated that an ST segment elevation equal to 0.5 mm without "coved" or "saddle back" was not associated with poor prognosis, even if the patients with this pattern showed a greater frequency of arrhythmias (40% versus 15%).

Moreover, the Author specified that this finding was not constant in the same patient, as this feature modifies over time. From a electrophysiological point of view, the substrate of ST segment elevation may be due to the progression of fibro-fatty replacement from epicardium to endocardium, creating an electrical gradient such as the repolarization abnormalities during acute myocardial infarction. The demonstration in vivo that ST segment elevation is determined by epicardial LV LGE supports this hypothesis. However, currently T1 inversion recovery sequecences used to visualize LGE are not able to differentiate fibrosis from other fatty infiltration since are not fat-satured. Future sequences may be able to differentiate these two different tissue. The fact that on multivariable analysis only LGE is confirmed as determinant of ST segment elevation and not LV fatty infiltration, supports the idea that the fibrous variants are characterized by this ECG findings.

Beyond ECG abnormalities included in the Task Force criteria, the only pattern associated to a specific CMR findings was the T-wave inversion in V1-V3 related to LV dilatation. Regarding T-wave inversion in V1-V3 and beyond lead V3, it has been described to range from 19% to 81% (120); in our series, we found that nearly 40% of patients had a normal T-wave

pattern, whereas T-wave inversion beyond V3 was seen in only 30.7%. Noteworthy, the high prevalence of T-wave inversion beyond V3 described in other studies was predominantly found in patients with severe forms of disease. The extent of T-wave inversion toward the left precordial leads increases according to disease severity, confirming the direct relationship between T-wave negativity and RV enlargement (38). Comparison with patients with isolated severe RV enlargement showed that the presence of T-wave inversion beyond V3 was more specific for RV dilatation than LV involvement, whereas lateral T-wave inversion in the precordial leads seemed to be a clinical marker of left ventricular involvement (46). In our series T-wave inversion was associated with RV dilatation, but after multivariable analysis the major determinant of RV enlargement was the T-wave inversion beyond V3. This result is important since this repolarization abnormality has been defined a major criterion in the current Modified 2010 Task Force criteria (36).

Electroanatomic scar compared with late gadolinium enhancement scar

The results of this Thesis confirm that ventricular scar is identified in the majority of patients fulfilling Task Force criteria for diagnosis of ARVC either by EVM or by LGE CMR. However, there was a mismatch between the two techniques with regard to the visualization of RV lesion with fewer RV scars detected by RV-LGE as compared with RV-EVM. In ARVC patients with abnormal RV-EVM/normal RV-LGE, a high prevalence of LV LGE was found demonstrating the frequent biventricular involvement and pointing out the diagnostic relevance of LV scar detection by LGE CMR.

RV electroanatomic scar

Electroanatomical voltage mapping has been proven to identify areas of myocardial loss by recording and spatially associating low amplitude electrograms to generate a 3-D electroanatomic ventricular map (101,102,106,108). In ARVC patients, RV EAS have been demonstrated to correlate with the histopathologic finding of myocardial atrophy and fibrofatty replacement at EMB (101). EVM assesses the electrical consequences of loss of RV

myocardium, rather than the mechanical dysfunction, either regional or global, traditionally seen by echocardiography and angiography. EVM was reported to enhance the accuracy of differential diagnosis between ARVC and acquired inflammatory cardiomyopathy (101) or idiopathic RVOT tachycardia (102). Ventricular tachycardia in ARVC is the result of a scar-related macro-reentry circuit, similar to that observed in the post-myocardial infarction setting. Hence, RV EVM-guided catheter ablation has been used as a successful therapeutic strategy for VT in ARVC (105,106).

In the present study, RV EAS were identified by EVM in the majority of ARVC patients. The high prevalence of RV low voltage areas in our study population may be explained by the clinical and electrophysiologic characteristics of patients who were probands with an overt disease phenotype, including VT, either sustained or non-sustained. Regional distribution of RV scars, with predominant involvement of the antero-lateral and infero-basal RV regions, resembled that observed in autopsy hearts of patients who died suddenly from ARVC in whom the most severe atrophy and wall aneurysms were characteristically localized in the antero-infundibular wall and underneath the tricuspid valve, being the so called “triangle of dysplasia”(31).

Right ventricular delayed contrast enhancement

Typical ARVC features on CMR consist of RV dilatation/dysfunction, wall motion abnormalities, diastolic bulging, and thinning of the RV free wall. Moreover, CMR has the unique ability to detect intramyocardial fatty deposition, which may be differentiated by the adjacent myocardium due to its brighter signal with the spin-echo technique (50,81,83,94). Although CMR provides an accurate quantitative analysis of RV volumes (97), a significant interobserver variability in the interpretation of segmental contraction analysis of the RV free wall has been reported. A CMR study demonstrated a 93.1% prevalence of RV wall motion abnormalities in normal subjects, including areas of apparent dyskinesia (75.9%) and bulging (27.6%) (122). CMR has been implicated in over-diagnosis of ARVC based on the low specificity of qualitative findings such as increased intramyocardial fat and wall thinning. All these data indicate that conventional CMR may lead to misdiagnosis of ARVC by showing equivocal morpho-functional RV abnormalities. A significant step forward in the imaging of

ARVC has been the introduction of CE-CMR, which is based on the ability of gadolinium to identify areas of intramyocardial fibrosis.

Previous studies demonstrated that fibrofatty ventricular scar can be non invasively visualized in patients with ARVC using CMR. Tandri et al. (88) first reported RV LGE in 8 of 12 (67%) of patients with ARVC and demonstrated its relation to inducibility of sustained monomorphic VT at electrophysiological testing and fibrofatty myocardial changes at EMB. Hunold et al. (89) found RV LGE in 5 of 7 (71%) of patients with an ARVC diagnosis based on the Task Force criteria. Sen-Chowdhry et al. (94) reported unequivocal RV LGE in 13 of 20 (65%) patients who fulfilled Task Force diagnostic criteria for ARVC and were desmosomal-gene mutation carriers. It is noteworthy that all studies failed to show RV LGE in approximately one third of ARVC patients. The lack of RV LGE in a significant proportion of patients fulfilling diagnostic criteria of ARVC was explained by early disease variants with small amount of fibro-fatty tissue or even by pure fatty variants of the disease undetectable by LGE techniques.

Our study showed a low prevalence (39%) of RV LGE in patients with clinical ARVC. Moreover, by specifically comparing EVM and LGE CMR for RV scar visualization, we found a significant mismatch between the two techniques (for imaging RV lesions), with fewer RV scars detected by RV- LGE as compared to RV-EVM. The 19 EAS not confirmed by the LGE were mostly located in the anterolateral and inferobasal RV regions. Previous reports comparing EVM and CMR findings in ARVC found a topographic relationship between low voltages areas and RV diskinesia/dilation (69,102), but no information was obtained regarding relationship with LGE scars since contrast images were not performed. Because all our patients had clinically overt disease with significant RV dilatation/dysfunction, the low yield of RV LGE can not be ascribed to early/minor disease forms but, more probably, can be explained by the low resolution of current CMR for the RV free wall as well as by the protocol design with inversion time set to null LV myocardium and inversion recovery sequence not-fat suppressed. The RV free wall is up to 4 mm and the motion artefacts often result in poor quality/spectral resolution to quantify RV wall thickness accurately. Additionally, transmural myocardial atrophy and fibrofatty replacement in ARVC patients may lead to further RV free wall thinning (<2 mm) with suboptimal contrast-to-noise ratio between normal and scar tissue (123). Of note, the inversion time required for optimal nulling of the myocardium probably differ between RV and LV, making inaccurate simultaneous examination of both ventricles with LGE imaging (123).

Finally, while the kinetic of gadolinium in the fibrous tissue of chronic ischemic heart disease has been well established, the real mechanisms underlying gadolinium enhancement in fibro-fatty scar of ARVC is not well known and might account for a proportion of false negative findings.

The RVOT scars identified by LGE CMR and undetected by EVM in two patients, may suggest a limited EVM power for detection of scar lesions in this area. As alternative explanation, this LGE finding may be interpreted as a false positive. Even if the LGE findings may be interpreted as a false positive, the possible alternative explanation may related to the pathophysiology underlying the proportion of fibrofatty replacement in ARVC. In autopsy series and experimental studies (124) it has been demonstrated that the epicardial substrate of ARVC lesions and arrhythmias may be more extensive than in the endocardial layers (31), since the fibro-fatty replacement proceeds from the epicardium as a “wavefront phenomenon” opposite to the one observed in ischemic heart disease. The histologic pattern of ARVC may be sometimes transmural, but can also consists of replacement of midmural or external layers of myocardium, leaving endocardium spared. For this reason, endocardial mapping may underrepresent the magnitude of the substrate compared to epicardial mapping, as recently demonstrated applying the epicardial voltage mapping to ARVC patients (125, 126). In this context, according to partial volume effects, the LGE of midmural or epicardial layer may be addressed as transmural in particular thinned myocardial segments, mostly in the fibro-fatty variant.

Left ventricle late gadolinium enhancement

The results of our study are in agreement with previous data suggesting a key role of LGE for detection and morphologic characterization of LV myocardial fibrofatty scar in ARVC (94,86). Sen-Chowdhry et al. found LV involvement in the majority of ARVC patients, mostly thanks to LGE which was the most sensitive marker of LV lesions (94). In the present study, we observed a comparable prevalence of LV-LGE (78%), with a similar predominant involvement of inferolateral and inferoseptal LV regions and with subepicardial/midmural locations. Noteworthy, in both studies there is a significantly lower prevalence of RV- LGE than LV- LGE, a finding that substantiates the current limited ability of LGE -CMR to visualize fibro-fatty RV scars. On the contrary, Dalal et al. (87) reported no LV LGE involvement in a ARVC population

characterized by high prevalence of plakophilin-2 gene- mutations. Left ventricular involvement was originally considered an end-stage complication of ARVC, occurring after the onset of global RV dysfunction, and leading ultimately to biventricular pump failure (31,46). Several clinico-imaging studies confirmed, both by invasive and non invasive techniques (49,127-131), the high prevalence of LV abnormalities in ARVC patients. More recently, genotype/phenotype correlations have shown early and greater LV involvement in desmoplakin-gene mutations carriers (49,50). These findings support the modern concept of ARVC as a genetically-determined biventricular cardiomyopathy (5,48,49).

Left ventricular involvement in ARVC was initially reported by pathologic studies (31,30). Fibrofatty replacement of LV myocardium was found to be a common histologic finding in autopsy series of ARVC, with a reported prevalence up to 76% (46). Fibro-fatty changes affect both the septum and free wall, either diffusely or regionally, with a predilection for postero-septal and postero-lateral regions. Like RV lesions, the wavefront of fibrofatty myocardial replacement in the LV progresses from the epicardium to the endocardium, with scar tissue frequently confined to subepicardial/midmural layers (31, 46).

The incidence of LV involvement in this patient population is 61%, in agreement with previous observation of Padua series indicating LV fibro-fatty pattern in nearly half of cases (31). The LGE is observed in the same LV regions and with the same distribution pattern as in the cohort of patients previously reported by Sen-Chowdhry et al (86). Not surprisingly, extensive LV LGE might precede the onset of global LV systolic dysfunction, since ARVC is a progressive disease and the LV dysfunction is consequent to the transmural extent of fibro-fatty replacement. In fact, by conventional 2D echocardiography LV involvement might be under-detected since, as previously described (76), LV LGE is commonly observed in the absence of coincident wall motion abnormalities and can be extensive without global LV dilatation/dysfunction until even the subendocardium is involved, accordingly with demonstration of contribute of subendocardial layers to contractility (132). Moreover, the reliability of results of LV LGE is proven by EMB since the it was obtained (3 or 5 specimens) both at the junction between the ventricular septum (pertinence of LV) and at the anterior RV free wall. Furthermore, in all cases EMB excluded sarcoidosis, thus onfirming the final diagnosis of ARVC.

Cardiac magnetic resonance and left-dominant variant of Arrhythmogenic Right Ventricular Cardiomyopathy.

Left ventricular involvement in ARVC assessed by CMR, has been fundamental for the delineation of 3 distinct patterns of ARVC disease expression. In the well recognized "classic" form of the disease, LV LGE is observed in the setting of global RV dysfunction, with a predilection for the infero-lateral wall and the inferior wall-septal junction, consistent with reports of pathological series (31,46). Differently from the classic form, LV dominant phenotype may include prominent LV LGE, often involving the septum, with preserved RV volumes and function. This recent new classification made by CMR findings has to be tested against the significance in terms of prognostic index. The hypothesis that we tested was that the LV dominant pattern had a worse prognostic significance as compared to other forms, in particular with the classic ARVC. During our follow-up, we found that the biventricular phenotype has the worse outcome, but there is not a significant different prognosis for the three phenotypes globally evaluated. The reasons can be substantially two. First of all, a period of mean follow-up of 35 months may be too short for a disease with a known low mortality. Second, the inclusion of one patient into one of the three different patterns is not definitive, since it is a progressive disease, and so, for a real stratification, repetitive CMR scans are needed and probably many forms labelled as isolated "LV" are concealed biventricular.

Futures studies in genotyped ARVC patients for longer period of follow-up are needed to better define the prognostic role of CMR findings well as quantitative analysis of LV LGE.

Histological basis of late enhancement in Dilated Cardiomyopathy and Arrhythmogenic Right Ventricular Cardiomyopathy.

Fibrosis in the myocardium of patients with DCM have been recognised at histopathology evaluation, both on EMB and on heart specimen, for decades and can be classified into either interstitial or replacement-type fibrosis (19,133). While its limited spatial resolution does not permit the visualisation of interstitial fibrosis, macroscopic areas of replacement fibrosis can reliably be detected by LGE CMR in patients with DCM. Our experience in the subset of 58

patients who underwent to both CMR and EMB showed a low accuracy of LGE for identification of fibrosis. This result may be due to the lower power resolution to detect diffuse microscopic (< 2-3 mm) fibrosis compared to EMB. Our observation is similar to previously reported comparison analysis performerd by Schalla et al (16). The Authors described the patterns of “focal fibrosis” in a group of patients with DCM and correlated “focal fibrosis” at CMR with interstitial fibrosis, myocardial viral load, and inflammation on EMB: in the 56 patients analyzed, 22 (39%) showed LGE. No differences were found between patients with or without focal fibrosis detected with LGE and the amount of collagen volume fraction of interstitial fibrosis (area under the curve = 0.51, 95% CI: 0.35–0.67). The amount of focal fibrosis measured with LGE as percentage of LV was also not correlated with of collagen volume fraction amount. Although LGE imaging for the detection of focal fibrosis, such as in the context of myocardial infarction, is robust, fast, and implemented into standard clinical CMR imaging protocols and the images are easily analysed by viewing, future technical advances are needed to increase the accuracy of LGE for both focal replacement-type and interstitial fibrosis detection. One promising approach for the evaluation of microscopic fibrosis is the implementation of post-contrast T1 mapping sequences, which use the concept that gadolinium accumulation in interstitial fibrosis leads to shortening of T1 relaxation times (134).

In our series, the prevalence of LGE is ~60%, higher than previously reported in CMR studies and in clinico-pathologic studies. Interstitial and replacement fibrosis (15) have been described in as many as 57% of patients (17), and grossly visible scars have been noted in 23% (18). On histology, also the prevalence of replacement-type fibrosis (33/58 patients; 56.8%) is higher than previously reports. This result on EMB makes reliable the prevalence of LGE found in our population, probably due to selection of patients in a Tertiary Transplantation Centre. Moreover, our result are in line with the total amount detected of LGE as percentage of LV mass, mild higher than other CMR studies.

Noteworthy, two patients with DCM phenotype had fibro-fatty replacement detected on pathologic evaluation on EMB. None of the patients showed CMR on RV findings compatible with ARVC, but both showed an infero-lateral LGE of LV wall. Similar EMB patterns have been demonstrated in patients affected by muscolar dystrophy with a myocardial involvement (135,136). Interestingly, in patients with muscolar dystrophy, the typical LGE shows the same infero-lateral deposition jet described in the myocarditis, or sarcoidosis, Chagas disease, Anderson-Fabry. An explanation for this LGE in the setting of muscolar dystrophye that the

genetically determined dystrophin damage is not diffusely distributed but accentuated in the posterolateral wall (136). The other possibility is that a diffuse (genetically determined) disease process with ubiquitous alterations in cell metabolism and signal transduction precedes functional impairment leading to myocardial damage preferentially in the posterolateral wall. Based on this observation, the LGE findings showed even in the left dominant ARVC phenotype in the posterolateral wall, represent a non-specific CMR phenotype in response to exaggerated mechanical stress in this region. Different pathophysiologies (such as myocardial inflammation or intracellular accumulation of storage products) may predispose the human heart to myocardial damage, which is amplified by increased mechanical stress and characterised by necrosis and/or fibrosis beginning in the inferolateral wall. Whether the inferolateral wall constitutes the "weakest cadet" of LV segments due to metabolic, structural or functional characteristics or otherwise has to withstand the highest mechanical stress during LV contraction and relaxation still has to be explored.

The observation of fibrofatty replacement in two patients referred for DCM supports the link between DCM and ARVC, and support the need to recognize imaging phenotypic features that can suggest a genetic cause (85).

Finally, the comparison between the EMB and the explanted heart of the young ARVC patient who underwent cardiac transplantation and performed in vivo a CMR, without neither demonstration of fatty infiltration nor myocardial edema, but with a clinical suspicion of myocarditis underlies the age-related penetrance of ARVC with different stages of myocardial injury, ranging from acute necrosis to replacement-type fibrosis, and open some controversies related to mechanism of LGE in ARVC. In fact, the myocardial kinetic of gadolinium, and so of the LGE, is well understood only in the setting of myocardial infarction where experimental studies demonstrated the correspondence between LGE scar and histological scar. In ARVC, there is a variable mixture of myocardial atrophy, sometimes with myocardial necrosis in the acute phase, fibrosis and fatty tissue, with a segmental distribution. Taking into account all these factors, it seems probably too simple to translate the “scar” on CMR as a scar on “histology”.

CONCLUSIONS

Cardiac magnetic resonance can provide a wide range of information on both DCM and ARVC, beyond traditional imaging modalities.

In the setting of DCM, the CMR interpreted by angiography provides with high accuracy the information on aetiology underlying LV dysfunction either “ischemic” DCM or “non-ischemic” DCM. Moreover, the LGE detection in DCM improves arrhythmic risk stratification over traditional parameters. In fact, LGE may identify in patients with not severe LV systolic dysfunction those at high risk, currently non recognized by non-invasive imaging tools. Although LGE imaging for the detection of replacement fibrosis (such as post-infarction scar), is robust, CMR imaging by LGE in DCM is not yet able to define the diffuse interstitial spotty-

replacement fibrosis as compared to EMB. So, a normal LGE CMR study does not exclude fibrosis.

In the setting of 3 forms of ARVC (RV, LV dominant and biventricular), the preliminary results in a subgroup of patient, showed that ECG indexes able to identify LV dilatation are ST-segment elevation and T-wave inversion beyond V3; on tissue characterization parameters, only LV LGE has an identificable ECG abnormality defined by ST segment elevation, that may be due to electrical gradient betwenn endocardium and epicardium replaced by fibro-fatty tissue.

The short follow-up on ARVC patients divided into the three groups newly defined by the CMR ("Classic ARVC", "Biventricular phenotype", and "Left dominant phenotype") not allowed us to a definitive conclusion on the prognostic significance of this classification.

The results of the correlation between EVM and CMR confirm that EVM allows an accurate identification of RV EAS in patients with a clinical diagnosis of ARVC and support its clinical use for substrate-based mapping and catheter ablation of RV tachycardias as well as for imaging-guided EMB. Currently available LGE CMR appears to visualize RV scars unsatisfactorily and this limits its usefulness in ARVC diagnosis and for guiding interventional RV procedures. The high prevalence of LV involvement in ARVC patients is in keeping with the current perspective of biventricular cardiomyopathy and points out the diagnostic relevance of LV scar detection by LGE CMR.

REFERENCES

1. Maron B, Towbin A, Thiene G et al. Contemporary Definitions and Classification of the Cardiomyopathies. An American Heart Association Scientific Statement From the Council on Clinical Cardiology, Heart Failure and Transplantation Committee; Quality of Care and Outcomes Research and Functional Genomics and Translational Biology Interdisciplinary Working Groups; and Council on Epidemiology and Prevention Circulation 2006;113:1807-1816.

2. Report of the WHO/ISFC Task Force on the Definition and Classification of Cardiomyopathies. Br Heart J 1980;44:672– 673.

3. Richardson P, McKenna W, Bristow M, et al. Report of the 1995 World Health Organization/International Society and Federation of Cardiology Task Force on the Definition and Classification of Cardiomyopathies. Circulation. 1996;93:841–842.

4. Thiene G, Corrado D, Basso C. Cardiomyopathies: is it time for a molecular classification? Eur Heart J. 2004; 25: 1772–1775.

5. Elliott P, Andersson B, Arbustini E, et al. Classification of the cardiomyopathies: a position statement from the european society of cardiology working group on myocardial and pericardial diseases. Eur Heart J 2008;29:270–276.

6. Thiene G, Corrado D, Basso C. Revisiting definition and classification of cardiomyopathies in the era of molecular medicine. Eur Heart J. 2008;29:144-6

7. Codd MB, Sugrue DD, Gersh BJ, et al. Epidemiology of idiopathic dilated and hypertrophic cardiomyopathy: a population-based study in Olmsted County, Minnesota, 1975–1984. Circulation. 1989; 80:564 –572

8. Mestroni L, Maisch B, McKenna WJ, et al. Guidelines for the study of familial dilated cardiomyopathies. Eur Heart J. 1999;20:93–102.

9. Wood MJ, Picard MH. Utility of echocardiography in the evaluation of individuals with cardiomyopathy. Heart. 2004;90:707–712.

10. Baroldi G, Thiene G. Biopsia Endomiocardica ed Piccin 1996.

11. Schwarz F, Mall G, Zebe H, et al. Quantitative morphologic findings of the myocardium in idiopathic dilated cardiomyopathy. Am J Cardiol 1983;51:501–506.

12. Brooks A, Schinde V, Bateman AC, et al. Interstitial fibrosis in the dilated non-ischaemic myocardium. Heart 2003;89:1255–1256.

13. Baig MK, Mahon N, McKenna WJ, et al. The pathophysiology of advanced heart failure. Am Heart J 1998;135:216-30.

14. De Leeuw N, Ruiter DJ, Balk AHMM, et al. Histopathologic findings in explanted heart tissue from patients with end-stage idiopathic dilated cardiomyopathy. Transpl Int 2001;14:299-306.

15. Beltrami CA, Finato N, Rocco M, et al. The cellular basis of dilated cardiomyopathy in humans. J Mol Cell Cardiol 1995;27: 291–305.

16. Schalla S, Bekkers SC, Dennert R, et al. Replacement and reactive myocardial fibrosis in idiopathic dilated cardiomyopathy: comparison of magnetic resonance imaging with right ventricular biopsy. Eur J Heart Fail 2010;12:227-31.

17. Roberts WC, Siegel RJ, McManus BM. Idiopathic dilated cardiomyopathy: analysis of 152 necropsy patients. Am J Cardiol 1987;60:1340–55.

18. Waller TA, Hiser WL, Capehart JE, et al. Comparison of clinical and morphologic cardiac findings in patients having cardiac transplantation for ischemic cardiomyopathy, idiopathic dilated car- diomyopathy, and dilated hypertrophic cardiomyopathy. Am J Cardiol 1998;81:884 –94.

19. Unverferth DV, BakerPB, Swift SE, et al. Extent of myocardial fibrosis and cellular hypertrophy in dilated cardiomyopathy. Am J Cardiol 1986;57;816-820.

20. Drozdz J, Krzeminska-Pakula M, Plewka Met al. Prognostic value of low-dose dobutamine echocardiography in patients with idiopathic dilated cardiomyopathy. Chest 2002;121:1216-22.

21. Investigators of MERIT-HF. Effect of metoprolol CR/XL in chronic heart failure: Metoprolol CR/XL Randomised Intervention Trial in Congestive Heart Failure (MERIT-HF). Lancet 1999;353:2001-7.

22. Tomaselli GF BD, Calkins HG, Berger RD, et l. Sudden cardiac death in heart failure. The role of abnormal repolarization Circulation 1994;90:2534-2539.

23. Moss AJ HW, Cannom DS, Daubert JP, et al. for the Multicenter Automatic Defibrillator Implantation Trial Investigators: N Engl J Med 1996;335:1933-1940.

24. Moss AJ ZW, Hall J, Klein H, et al for the Multicenter Automatic Defibrillator Implantation Trial II Investigators: Prophylactic Implantation of a Defibrillator in Patients with Myocardial Infarction and Reduced Ejection Fraction. N Engl J Med 2002;346:877-883.

25. Bristow MR SL, Boehmer J, Krueger S, et al. for the Comparison of the Medical Therapy, Pacing, and Defibrillation in Heart Failure (COMPANION). Investigators Cardiac Resynchronization Therapy with or without an Implantable Defibrillator in Advanced Chronic Heart Failure. N Engl J Med 2004. 350 2140-2150.

26. ESC Guidelines for the diagnosis and treatment of acute and chronic heart failure 2008.The Task Force for the Diagnosis and Treatment of Acute and Chronic Heart Failure 2008 of the European Society of Cardiology. Developed in collaboration with the Heart Failure Association of the ESC (HFA) and endorsed by the European Society of Intensive Care Medicine (ESICM). Eur Heart J 2008;29, 2388–2442.

27. Bardy GH, Lee KL, Mark DB, et al. Amiodarone or an implantable cardioverter–defibrillator for congestive heart failure. N Engl J Med 2005;352:225–237.

28. Desai AS, Fang JC, Maisel WH, et al. Implantable defibrillators for the prevention of mortality in patients with nonischemic cardiomyopathy: a meta-analysis of randomized controlled trials. JAMA 2004;292:2874–2879.

29. Marcus FI, Fontaine GH, Guiraudon G, et al. Right Ventricular dysplasia: a report of 24 adult cases. Circulation 1982; 65:384-398

30. Thiene G, Nava A, Corrado D, Rossi L, et al. Right ventricularcardiomyopathy and sudden death in young people. N Engl J Med 1988; 318: 129–33.

31. Basso C, Thiene G, Corrado D, et al. Arrhythmogenic right ventricular cardiomyopathy: dysplasia, dystrophy or myocarditis? Circulation 1996; 94: 983–91.

32. Nava A, Thiene G, Canciani B, et al. Familial occurrence of right ventricular dysplasia: a study involving nine families. J Am Coll Cardiol 1989;12:1222–28.

33. Corrado D, Basso C, Thiene G. Arrhythmogenic right ventricular cardiomyopathy: an update. Heart 2009;95;766-73.

34. Thiene G, Corrado D, Basso C. Arrhythmogenic right ventricular cardiomyopathy/dysplasia. Orphanet Journal of Rare Disease 2007;2:45.

35. McKenna WJ, Thiene G, Nava A, et al. Diagnosis of arrhythmogenic right ventricular dysplasia/cardiomyopathy. Task Force of the Working Group Myocardial and Pericardial Disease of the European Society of Cardiology and of the Scientific Council on Cardiomyopathies of the International Society and Federation of Cardiology. Br Heart J. 1994;71:215–218.

36. Marcus FI, McKenna WJ, Sherrill D, et al. Diagnosis of arrhythmogenic right ventricular cardiomyopathy/dysplasia: proposed modification of the task force criteria. Circulation. 2010;121:1533–1541.

37. Daliento L, Rizzoli G, Thiene G, et al. Diagnostic accuracy of right ventriculography in arrhythmogenic right ventricular cardiomyopathy. Am J Cardiol 1990; 66: 741–45.

38. Nava A, Canciani B, Buja G, et al. Electrovectorcardiographic study of negative T waves on precordial leads in arrhythmogenic right ventricular dysplasia: relationship with right ventricular volumes. J Electrocardiol 1988; 21: 239–45.

39. Zareba W, Piotrowicz K, Turrini P. Electrocardiographic manifestations. In: Marcus FI, Nava A, Thiene G. Arrhythmogenic right ventricular cardiomyopathy/dysplasia: recent advances. Milano: Springer Verlag 2007: 121–28.

40. Nava A, Folino AF, Bauce B, et al. Signal-averaged electrocardiogram in patients with arrhythmogenic right ventricular cardiomyopathy and ventricular arrhythmias. Eur Heart J 2000;21:58–65

41. Turrini P, Angelini A, Thiene G, et al. Late potentials and ventricular arrhythmias in arrhythmogenic right ventricular cardiomyopathy. Am J Cardiol 1999;83:1214–1219

42. Folino AF, Bauce B, Frigo G, et al. Long term follow-up of the signal-averaged ECG in arrhythmogenic right ventricular cardiomyopathy: correlation with arrhythmic events and echocardiographic findings. Europace 2006;8:423–429

43. Turrini P, Corrado D, Basso C, et al. Dispersion of ventricular depolarization-repolarization: a noninvasive marker for risk stratification in arrhythmogenic right ventricular cardiomyopathy. Circulation. 2001;25:3075-80

44. Nasir K, Bomma C, Tandri H, et al. Electrocardiographic features of arrhythmogenic right ventricular dysplasia/cardiomyopathy according to disease severity: a need to broaden diagnostic criteria. Circulation 2004;110:1527–3.

45. Cox MG, Nelen MR, Wilde AA, et al. Activation Delay and VT Parameters in Arrhythmogenic Right Ventricular Dysplasia/ Cardiomyopathy: Toward Improvement of Diagnostic ECG Criteria. J Cardiovasc Electrophysiol 2008; 19: 775–81.

46. Corrado D, Basso C, Thiene G, et al. Spectrum of clinicopathologic manifestations of arrhythmogenic right ventricular cardiomyopathy/dysplasia: a multicenter study. J Am Coll Cardiol 1997; 30: 1512–20.

47. Basso C, Ronco F, Marcus F et al. Quantitative assessment of endomyocardial biopsy in arrhythmogenic right ventricular cardiomyopathy/dysplasia: an in vitro validation of diagnostic criteria. Eur Heart J 2008;29:2760-71.

48. Basso C, Corrado D, Marcus FI, et al. Arrhythmogenic right ventricular cardiomyopathy Lancet 2009;373:1289–1300.

49. Bauce B, Basso C, Rampazzo A, et al. Clinical profile of four families with arrhythmogenic right ventricular cardiomyopathy caused by dominant desmoplakin mutations. Eur Heart J. 2005;26: 1666 –1675.

50. Sen-Chowdhry S, Syrris P, Ward D, et al. Clinical and genetic characterization of families with arrhythmogenic right ventricular dysplasia/cardiomyopathy provides novel insights into patterns of disease expression. Circulation 2007; 115: 1710–20.

51. Lombardi M, Bartolozzi C. Risonanza Magnetica del cuore e dei vasi, Ed. Springer 2006.

52. Selvanayagam JB, Robson MD, Francis JM & Neubauer S. Cardiac CT, PET and MR. Chapter 2. Ed. Blackwell Futura 2006.

53. Wesbey G, Higgins C, McNamara M et al. Effect of gadolinium-DTPA on the magnetic relaxation times of normal and infarcted myocardium. Radiology 1984;153:165–169.

54. Simonetti OP, Kim RJ, Fieno DS et al. An improved MR imaging technique for the visualization of myocardial infarction. Radiology 2001; 218:215–223.

55. Kim RJ, Fieno DS, Parrish TB et al. Relationship of MRI delayed contrast enhancement to irreversible injury, infarct age, and contractile function. Circulation 1999;100:1992–2002.

56. Choi KM, Kim RJ, Gubernikoff G et al. Transmural extent of acute myocardial infarction predicts long- term improvement in contractile function. Circulation 2001;104:1101–1107.

57. Judd RM, Lugo-Olivieri CH, Arai M, et al. Physiological basis of myocardial contrast enhancement in fast magnetic resonance images of a 2-day-old reperfused canine infarcts. Circulation 1995; 92: 1902-10

58. Wu E, Judd RM, Vargas JD et al. Visualisation of pres- ence, location, and transmural extent of healed Q-wave and non-Q-wave myocardial infarction. Lancet 2001;357:21–28.

59. Wagner A, Mahrholdt H, Holly TA et al. Contrast- enhanced MRI and routine single photon emission computed tomography (SPECT) perfusion imaging for detection of subendocardial myocardial infarcts: An imaging study. Lancet 2003;361:374–379.

60. Kim RJ, Wu E, Rafael A. The use of contrast-enhanced magnetic resonance imaging to identify reversible myo- cardial dysfunction. N Engl J Med 2000; 343: 1445–1453.

61. Selvanayagam JB, Porto I, Channon K et al. Troponin elevation following percutaneous coronary intervention directly represents the extent of irreversible myocardial injury: Insights from cardiovascular magnetic resonance imaging. Circulation 2005; 111: 1027–1032.

62. Bucciarelli-Ducci C, Wu E, Lee DC, et al. Contrast-enhanced cardiac magnetic resonance in the evaluation of myocardial infarction and myocardial viability in patients with ischemic heart disease. Curr Probl Cardiol. 2006; 31:128-68.

63. Grobner T. Gadolinium-a specific trigger for the development of nephrogenic fibrosing dermopathy and nephrogenic systemic fibrosis? Nephrol Dial Transplant 2006;21:1104–8.

64. Thomsen HS. ESUR guideline: gadolinium-based contrast media and nephrogenic systemic fibrosis. Eur Radiol 2007;17:2692–6.

65. Grobner T, Prischl FC. Patient characteristics and risk factors for nephrogenic systemic fibrosis following gadolinium exposure. Semin Dial 2008;21:135–9.

66. Pennel DJ. Cardiovascular magnetic resonance. Circulation 2010;121:692 –705.

67. Sarwar A, Shapiro MD, Abbara S, et al. Cardiac magnetic resonance imaging for the evaluation of ventricular function. Semin Roentgenol 2008;43:183–92.

68. Imai H, Kumai T, Selya M et al. Left ventricular trabeculae evaluated with MRI in dilated cardiomyopathy and old myocardial infarction. J Cardiol 1992;22:83-90.

69. Boulos M, Lashevsky I, Reisner S, et al. Electroanatomical mapping of arrhythmogenic right ventricular dysplasia. J Am Coll Cardiol 2001;38:2020 –7.

70. Karamitsos TD, Francis JM, Myerson S et al. The role of cardiovascular magnetic resonance imaging in heart failure. J Am Coll Cardiol 2009;54:1407–24.

71. McCrohon JA, Moon JC, Prasad SK, et al. Differentiation of heart failure related to dilated cardiomyopathy and coronary artery disease using gadolinium-enhanced cardiovascular magnetic resonance. Circulation 2003;108:54–9.

72. Friedrich MG, Sechtem U, Schulz-Menger J et al. Cardiovascular Magnetic Resonance in Myocarditis: A JACC White Paper. J Am Coll Card 2009;53:1475-87.

73. Mahrholdt H, Wagner A, Deluigi CC, et al. Presentation, patterns of myocardial damage, and clinical course of viral myocarditis. Circulation 2006;114:1581–90.

74. Mahrholdt H, Goedecke C, Wagner A, et al. Cardiovascular magnetic resonance assessment of human myocarditis: a comparison to histology and molecular pathology. Circulation 2004;109:1250–8.

75. De Cobelli F, Pieroni M, Esposito A, et al. Delayed gadolinium-enhanced cardiac magnetic resonance in patients with chronic myocarditis presenting with heart failure or recurrent arrhythmias. J Am Coll Cardiol 2006;47:1649–54.

76. Mahrholdt H, Wagner A, Judd RM, et al. Delayed enhancement cardiovascular magnetic resonance assessment of non- ischaemic cardiomyopathies. Eur Heart J 2005;26:1461–74.

77. Yared K, Johri AM, Soni AV, et al. Cardiac sarcoidosis imitating arrhythmogenic right ventricular dysplasia. Circulation 2008;118:113–5.

78. Moon JC, Sheppard M, Reed E, et al. The histological basis of late gadolinium enhancement cardiovascular magnetic resonance in a patient with Anderson-Fabry disease. J Cardiovasc Magn Reson 2006;8:479–82.

79. Rochitte CE, Oliveira PF, Andrade JM, et al. Myocardial delayed enhancement by magnetic resonance imaging in patients with Chagas' disease: a marker of disease severity. J Am Coll Cardiol 2005;46:1553– 8.

80. Assomull RG, Prasad SK, Lyne J, et al. Cardiovascular magnetic resonance, fibrosis, and prognosis in dilated cardiomyopathy. J Am Coll Cardiol 2006;48:1977–85.

81. Menghetti L, Basso C, Nava A et al. Spin-echo nuclear magnetic resonance for tissue characterization in arrhythmogenic right ventricular cardiomyopathy. Heart 1997;76:467-470.

82. Tandri H, Bomma C, Calkins H, et al. Magnetic resonance and computed tomography imaging of arrhythmogenic right ventricular dysplasia. J Magn Reson Imaging. 2004;19:848–858.

83. Tandri H, Castillo E, Ferrari VA, et al. Magnetic resonance imaging of arrhythmogenic right ventricular dysplasia: sensitivity, specificity, and observer variability of fat detection versus functional analysis of the right ventricle. J Am Coll Cardiol 2006; 48:2277-84.

84. Abbara S, Migrino RQ, Sosnovik D et al. Conventional spin echo magnetic resonance imaging is superior to fast spin echo in detection of intramyocardial fatty infiltration J Cardiovasc Magn Reson 2004;6:233-34.

85. Raman SV, Basso C, Tandri H et al. Imaging Phenotype vs Genotype in Nonhypertrophic Heritable Cardiomyopathies: Dilated Cardiomyopathy and Arrhythmogenic Right Ventricular Cardiomyopathy. Circ Cardiovasc Imaging 2010;3;753-765.

86. Sen-Chowdhry S, Syrris P, Prasad SK, et al. Left-dominant arrhythmogenic cardiomyopa- thy: an under-recognized clinical entity. J Am Coll Cardiol. 2008;52: 2175–2187.

87. Dalal D, Tandri H, Judge DP, et al. Morphologic variants of familial arrhythmogenic right ventricular dys- plasia/cardiomyopathy: a genetics-magnetic resonance imaging corre- lation study. J Am Coll Cardiol. 2009;53:1289–1299.

88. Tandri H, Saranathan M, Rodriguez ER, et al. Noninvasive detection of myocardial fibrosis in arrhythmogenic right ventricular cardiomyopathy using delayed-enhancement magnetic resonance imaging. J Am Coll Cardiol. 2005;45:98–103.

89. Hunold P, Wieneke H, Bruder O, et al. Late en- hancement: a new feature in MRI of arrhyth- mogenic right ventricular cardiomyopathy? J Cardiovasc Magn Reson2005; 7:649–655.

90. Felker GM, Shaw LK, O'Connor CM. A standardized definition of ischemic cardiomyopathy for use in clinical research. J Am Coll Cardiol 2002;39:210–8.

91. Blackburn H, Keys A, Simonson E, et al. The electrocardiogram in population studies. A classification system. Circulation 1960; 21:1160-1175.

92. Grimm RH Jr, Tillinghast S, Daniels K, et al. Unrecognized myocardial infarction: experience in the Multiple Risk Factor Intervention Trial (MRFIT). Circulation 1987; 75:116–118.

93. Sheifer SE, Gersh BJ, Yanez ND III, et al. Prevalence, predisposing factors and prognosis of clinically unrecognized myocardial infarction in the elderly. J Am Coll Cardiol 2000; 35:119 – 126.

94. Sen-Chowdhry S, Prasad SK, Syrris P, et al. Cardiovascular magnetic resonance in arrhythmogenic right ventricular cardiomyopathy revisited: comparison with task force criteria and genotype. J Am Coll Cardiol 2006; 48:2132-40.

95. Kim RJ, Chen EL, Lima JA, et al. Myocardial Gd-DPTA kinetics determine MRI contrast enhancement and reflect the extent and severity of myocardial injury after acute reperfused infarction. Circulation 1996; 94:3318–26.

96. Maceira AM, Prasad SK, Khan M, et al. Normalized left ventricular systolic and diastolic function by steady state free precession cardiovascular magnetic resonance. J Cardiovasc Magn Reson 2006; 8:417-26.

97. Maceira AM, Prasad SK, Khan M, et al. Reference right ventricular systolic and diastolic function normalized to age, gender and body surface area from steady-state free precession cardiovascular magnetic resonance. Eur Heart J 2006; 23:2879-88.

98. Schmidt A, Azevedo CF, Cheng A, et al. Infarct tissue heterogeneity by magnetic resonance imaging identifies enhanced cardiac arrhythmia susceptibility in patients with left ventricular dysfunction. Circulation 2007;115:2006 –14.

99. Strauss DG, Selvester RH, Lima JA et al. ECG quantification of myocardial scar in cardiomyopathy patients with or without conduction defects. Correlation with cardiac magnetic resonance and arrhythmogenesis. Circ Arrhythmia Electrophysiol 2008;1:327-336.

100. Cerqueira MD, Weissman NJ, Dilsizian V, et al. American Heart Association Writing Group on Myocardial Segmentation and Registration for Cardiac Imaging. Standardized myocardial segmentation and nomenclature for tomographic imaging of the heart: a statement for healthcare professionals from the Cardiac Imaging Committee of the Council on Clinical Cardiology of the American Heart Association. Circulation 2002; 105:539-42.

101. Corrado D, Basso C, Leoni L, et al. Three-dimensional electroanatomic voltage mapping increases accuracy of diagnosing arrhytmogenic right ventricular cardiomyopathy/dysplasia. Circulation 2005; 111:3042-3050.

102. Corrado D, Basso C, Leoni L, et al. Three-dimensional electroanatomical voltage mapping and histologic evaluation of myocardial substrate in right ventricular outflow tract tachycardia. J Am Coll Cardiol 2008;51:731-739.

103. Klein H, Karp RB, Kouchoukos NT, et al. Intraoperative electrophysiologic mapping of the ventricles durino sinus rhythm in patients with a previous myocardial infarction. Identification of the electrophysiologic substrate of ventricular arrhythmia.Circulation 1982;66:847–54.

104. Cassidy DM, Vassallo JA, Miller JM, et al. Endocardial catheter mapping in patients in sinus rhythm: relationship to underlying heart disease and ventricular arrhythmias. Circulation 1986;73:645–52.

105. Marchlinski FE, Zado E, Dixit S, et al. Electroanatomic substrate and outcome of catheter ablative therapy for ventricular tachycardia in setting of right ventricular cardiomyopathy. Circulation 2004;110:2293–8.

106. Verma A, Kilicaslan F, Schweikert RA, et al. A. Short- and long-term success of substrate-based mapping and ablation of ventricular tachycardia in arrhythmogenic right ventricular dysplasia. Circulation 2005; 111:3209-16.

107. Yoerger DM, Marcus F, Sherrill D, et al. Multidisciplinary study of right ventricular dysplasia investigators. Echocardiographic findings in patients meeting task force criteria for arrhythmogenic right ventricular dysplasia: new insights from the multidisciplinary study of right ventricular dysplasia. J Am Coll Cardiol 2005;45:860–5.

108. Marchlinski FE, Callans DJ, Gottlieb CD, et al. Linear ablation lesions for control of unmappable ventricular tachycardia in patients with ischemic and nonischemic cardiomyopathy. Circulation 2000;101:1288–96.

109. Hsia HH, Callans DJ, Marchlinski FE. Characterization of endocardial electrophysiologic substrate in patients with nonischemic cardiomyopathy and monomorphic ventricular tachycardia. Circulation 2003;108:704–10.

110. Galiè N et al. ESC Guidelines for diagnosis and treatment of pulmonary hypertension. Eur Heart J 2009;30:2493-2537.

111. Aretz HT, Billingham ME, Edwards WD, et al. Myocarditis: a histopathologic definition and classification. Am J Cardiovasc Pathol. 1987;1:3–14.

112. Gorzer I, Niesters HG, Cornelissen JJ, et al. Characterization of Epstein-Barr virus Type I variants based on linked polymorphism among EBNA3A, -3B, and -3C genes. Virus Res 2006;118:105–114.

113. Monpoeho S, Maul A, Mignotte-Cadiergues B, et al. Best viral elution method available for quantification of enteroviruses in sludge by both cell culture and reverse transcription–PCR. Appl Environ Microbiol 2001;67:2484–248.

114. Caforio ALP, Calabrese A, Angelini A et al. A prospective study of biopsy-proven myocarditis: prognostic relevance of clinical and aetiopathogenetic features at diagnosis. Eur Heart J 2007;28: 1326–1333.

115. Wu KC, Weiss RG, Thiemann DR, et al. Late gadolinium enhancement by cardiovascular magnetic resonance heralds an adverse prognosis in nonischemic cardiomyopathy. J Am Coll Card 2008;51:2414-21.

116. Lehrke S, Lossnitzer D, Schöb M, et al Use of cardiovascular magnetic resonance for risk stratification in chronic heart failure: prognostic value of late gadolinium enhancement in patients with non-ischaemic dilated cardiomyopathy. Heart published online November 20, 2010.

117. Bello D, Fieno DS, Kim RJ, et al. Infarct morphology identifies patients with substrate for sustained ventricular tachycardia. J Am Coll Cardiol 2005;45:1104-08.

118. Nazarian S, Bluemke DA, Lardo AC, et al. Magnetic resonance assessment of the substrate for inducible ventricular tachycardia in nonischemic cardiomyopathy. Circulation 2005;112:2821-2825.

119. Bradlow WM, Assomull R, Kilner PJ, et al. Understanding late gadolinium enhancement in pulmonary hypertension.Circ Cardiovasc Imaging. 2010;4:501-3.

120.Nava A, Rossi L, Thiene G. Arrhythmogenic right ventricular cardiomyopathy-dysplasia, Ed. Elsever 1997.

121. Peters S, Peters H, Thierfelder L. Risk stratification of sudden cardiac death and malignant ventricular arrhythmias in right ventricular dysplasia-cardiomyopathy. Int J Cardiol 1999;71:243-250.

122.Sievers B, Addo M, Franken U, et al. Right ventricular wall motion abnormalities found in healthy subjects by cardiovascular magnetic resonance imaging and characterized with a new segmental model. J Cardiovasc Magn Reson 2004;6:601–8.

123.Grosse-Wortmann L, Macgowan CK, Vidarsson L, et al. Late gadolinium enhancement of the right ventricular myocardium: is it really different from the left? Cardiovasc Magn Reson 2008; 8:10:20.

124. Pilichou K, Remme CA, Basso C et al. Myocyte necrosis underlies progressive myocardial dystrophy in mouse dsg2-related arrhythmogenic right ventricular cardiomyopathy. J Exp Med 2009; Vol. 206 No. 8, 1787-1802

125. Garcia FC, Bazan V, Zado ES et al. Epicardial substrate and out come with epicardial ablation of ventricular tachycardia in arrhythmogenic right ventricular cardiomyopathy/dysplasia Circulation 2009; 120:366-375.

126. Polin GM, Haqqani H, Tzou W, et al. Endocardial unipolar voltage mapping to identify epicardial substrate in arrhythmogenic right ventriculardysplasia/cardiomyopathy. Heart Rhythm 2011;8:76-83.

127. Manyari DE, Klein GJ, Gulamhusein S, et al. Arrhythmogenic right ventricular dysplasia: a generalized cardiomyopathy? Circulation 1983; 68:251-7.

128. Pinamonti B, Sinagra G, Salvi A, et al. Left ventricular involvement in right ventricular dysplasia. Am Heart J 1992; 123:711-24.

129.Peters S, Reil GH. Risk factors of cardiac arrest in arrhythmogenic right ventricular dysplasia. Eur Heart J 1995; 6:77-80.

130. Kullo IJ, Edwards WD, Seward JB. Right ventricular dysplasia: the Mayo Clinic experience.Mayo Clin Proc. 1995;70:541-8.

131. Lindström L, Nylander E, Larsson H, et al. Left ventricular involvement in arrhythmogenic right ventricular cardiomyopathy - a scintigraphic and echocardiographic study. Clin Physiol Funct Imaging 2005; 25:171-7.

132.Myers JH, Stirling MC, Choy M et al. Direct measurement of inner and outer wall thikening dynamis with epicardial echocardiography. Circulation 1986;74:164-172.

133. De Leeuw N, Ruiter DJ, Balk AHMM, et al. Histopathologic findings in explanted heart tissue from patients with end-stage idiopathic dilated cardiomyopathy. Transpl Int 2001;14:299-306.

134.Iles L, Pfluger H, Phrommintikul A, et al. Evaluation of diffuse myocardial fibrosis in heart failure with cardiac magnetic resonance contrast-enhanced T1 mapping. J Am Coll Cardiol 2008;52:1574-80.

135. Frankel KA, Rosser RJ: The pathology of the heart in progressive muscular dystrophy: epimyocardial fibrosis. Hum Pathol 1976, 7:375-386.

136. Yilmaz A, Gdynia Hj, Baccouche H et al. Cardiac involvement in patients with Becker muscular dystrophy: new diagnostic and pathophysiological insights by a CMR approach. Journal of Cardiovascular Magnetic Resonance 2008,10:50-57.